

# **Design, Synthesis and Application of Novel Degradable Materials Based on Polyesters by Radical Ring-Opening Polymerization**

DISSERTATION

Zur Erlangung des akademischen Grades eines

Doktors der Naturwissenschaften (Dr. rer. nat.)

an der Bayreuther Graduiertenschule für Mathematik und

Naturwissenschaften der Universität Bayreuth

vorgelegt von

**Yinfeng Shi**

Geboren in Jiangsu, V. R. China

Bayreuth, 2015



Die vorliegende Arbeit wurde in der Zeit von Mai 2012 bis September 2012 in Marburg am Lehrstuhl Makromolekulare Chemie, Philipps-Universität Marburg und in der Zeit von Oktober 2012 bis Mai 2015 in Bayreuth am Lehrstuhl Makromolekulare Chemie II unter Betreuung von Prof. Dr. Seema. Agarwal angefertigt.

Vollständiger Abdruck der von der Bayreuther Graduiertenschule für Mathematik und Naturwissenschaften (BayNAT) der Universität Bayreuth genehmigten Dissertation zur Erlangung des akademischen Grades eines Doktors der Naturwissenschaften (Dr. rer. nat.).

Dissertation eingereicht am: 21.05.2015

Zulassung durch die Promotionskommission: 01.07.2015

Wissenschaftliches Kolloquium: 19.11.2015

Amtierender Direktor: Prof. Dr. Stephan Kümmel

Prüfungsausschuss:

Prof. Dr. Seema Agarwal (Erstgutachter)

Prof. Dr. Mukundan Thelakkat (Zweitgutachter)

Prof. Dr. Birgit Weber (Vorsitz)

Prof. Dr. Matthias Karg



*Men who are resolved to find a way for themselves will always find opportunities enough; and if they do not find them, they will make them.*

*-- Samuel Smiles*



*To My Wife Yiqun*



---

---

## Table of Contents

<b>Summary</b> .....	1
<b>Zusammenfassung</b> .....	3
<b>Glossary</b> .....	7
<b>Chapter 1 - Introduction</b> .....	9
1.1 Chemistry of Radical Ring-Opening Polymerization (RROP) .....	10
1.1.1 Starting monomers for Radical Ring-Opening Polymerization .....	11
1.1.2 Mechanism of Radical Ring-Opening Polymerization .....	14
1.2 Controlled Radical Ring-Opening Polymerization.....	17
1.2.1 Radical Ring-Opening Polymerization under ATRP Condition .....	17
1.2.2 Radical Ring-Opening Polymerization under RAFT Condition .....	18
1.2.3 Radical Ring-Opening Polymerization under NPM Condition.....	19
1.3 Applications of radical ring-opening polymerization for producing functional polyesters.....	21
1.3.1 Functional polyesters generated by radical ring-opening homopolymerization .....	21
1.3.2 Functional polyesters generated by copolymerization of cyclic ketene acetals (CKAs) and various vinyl monomers.....	25
1.4 Aim of the Thesis.....	32
1.5 References.....	33
<b>Chapter 2 - Overview of Thesis</b> .....	41
2.1 Formation of Polystyrene Grafted Aliphatic Polyester in One-Pot by Radical Polymerization.....	42
2.2 Designed Enzymatically Degradable Amphiphilic Conetworks (APCNs) by RROP .....	45
2.3 Enzymatically Degradable DOPA-containing Polyester Based Adhesives by Radical Polymerization.....	48

2.4	Thermally stable optically transparent copolymers with degradable ester linkages .....	51
2.5	Individual Contributions to Joint Publications .....	55
<b>Chapter 3 - Formation of Polystyrene Grafted Aliphatic Polyester in One-Pot by Radical Polymerization .....</b>		<b>57</b>
3.1	Abstract .....	55
3.2	Introduction .....	61
3.3	Results and Discussion .....	64
3.4	Conclusion .....	79
3.5	Experimental Section .....	80
3.6	References .....	83
3.7	Supporting Information .....	87
<b>Chapter 4 - Designed Enzymatically Degradable Amphiphilic Conetworks by Radical Ring-Opening Polymerization .....</b>		<b>89</b>
4.1	Abstract .....	91
4.2	Introduction .....	93
4.3	Experimental Section .....	95
4.4	Results and Discussion .....	97
4.5	Conclusion .....	107
4.6	References .....	108
4.7	Supporting Information .....	112
<b>Chapter 5 - Enzymatically Degradable DOPA-containing Polyester Based Adhesives by Radical Polymerization .....</b>		<b>117</b>
5.1	Abstract .....	119
5.2	Introduction .....	121
5.3	Experimental Section .....	123
5.4	Results and Discussion .....	127
5.5	Conclusion .....	135

---

5.6	References	136
<b>Chapter 6 - Thermally stable optically transparent copolymers with degradable ester linkages</b>		
	<b>linkages</b>	139
6.1	Abstract	141
6.2	Introduction	143
6.3	Experimental Section	145
6.4	Results and Discussion	147
6.5	Conclusion	162
6.6	References	163
6.7	Supporting Information	165
<b>List of Publications</b>		167
<b>Conference Presentations</b>		169
<b>Acknowledgements</b>		171
<b>Versicherung und Erklärungen</b>		173



## Summary

Design, synthesis and application of novel degradable material based on polyesters by radical ring-opening polymerization (RROP) were described in this thesis. Herein, we studied a rare example of the formation of polystyrene-grafted aliphatic polyester in one-pot by radical polymerization including the reaction mechanism, designed enzymatically degradable amphiphilic conetworks by RROP, developed enzymatically degradable DOPA-containing polyester based adhesives by radical polymerization, and prepared and characterized novel thermally stable optically transparent copolymers with degradable ester linkages.

In the case of formation of a graft copolymer in one-pot by radical polymerization, the cyclic ester  $\beta$ -propiolactone ( $\beta$ -PL) and styrene (St) were copolymerized at 120 °C with various monomer ratios. It is a rare example of a system providing graft copolymers (PSt-g- $\beta$ -PL) with a complete range of monomer ratios in one pot. The structure of the resulting  $\beta$ -PL-St copolymers was proved by using a combination of different characterization techniques, such as 1D and 2D NMR spectroscopy and gel permeation chromatography (GPC), and also the analysis before and after alkaline hydrolysis of polymers. A significant difference in the reactivity of St and  $\beta$ -PL and radical chain transfer reactions at the polystyrene (PSt) backbone, followed by combination with the active growing poly( $\beta$ -PL) chains, led to the formation of graft copolymers by a grafting-onto mechanism.

We designed a different route for the preparation of enzymatically degradable amphiphilic conetworks (APCNs) based on unsaturated polyesters by RROP of vinylcyclopropane (VCP) with cyclic ketene acetal (CKA). In the first step, the unsaturated degradable polyesters with random distribution of cross-linkable double bonds and degradable ester units were prepared by radical ring-opening copolymerization of VCP and 2-methylene-4-phenyl-1,3-dioxolane (MPDO). Very similar reactivity ratios,

unimodal GPC curves and 2D NMR technique (heteronuclear multiple bond correlation, HMBC) showed the formation of random copolymers with unsaturation and ester units. The unsaturated units were used for cross-linking with hydrophilic macromonomer (oligo(ethylene glycol) methacrylate, OEGMA) by radical polymerization in a second step for the formation of enzymatically degradable APCNs. Enzymatic degradability was studied using Lipase from *Pseudomonas cepacia*. Due to the hydrophilic (HI) and hydrophobic (HO) microphase separation, the APCNs showed swelling in both water and organic solvents with different optical properties. This method provides an interesting route for making functional degradable APCNs using radical chemistry in the future.

We developed a 3,4-dihydroxyphenylalanine (DOPA) containing enzymatic degradable non-toxic synthetic adhesive with good adhesion to soft tissue and metals by a simple two-step reaction. This adhesive had degradable polycaprolactone- type repeating units together with glycidyl methacrylate (GMA) and OEGMA in the polymer backbone. Radical initiated copolymerization of 2-methylene-1,3-dioxepane (MDO), GMA and OEGMA followed by immobilization of DOPA on epoxy rings of GMA provided the adhesive material. Fe(acac)<sub>3</sub> was proved to be the most effective cross-linking agent with lap shear strength on soft tissue (porcine skin) and metal (aluminum). The cross-linked adhesive showed good adhesion stability in pH 7 PBS buffer at 37 °C for at least one week. Due to the high adhesive strength, enzymatic degradability and low toxicity, the material is a promising candidate for future studies as medical glue.

Finally, copolymers with high thermal stability, glass transition temperature and optical transparency were produced by radical polymerization of MDO and *N*-phenyl maleimide (NPM). The polymers made under specific reaction conditions, i.e. 120 °C and high amounts of MDO had degradable ester units, which were formed via radical ring-opening polymerization of MDO. Formation of charge-transfer complex between MDO and NPM also led to the formation of high molar mass copolymers by simple mixing and heating of monomers without use of any initiator. The structural characterization of copolymers including mechanistic studies was studied in details.

## Zusammenfassung

Das Design, die Synthese und Anwendung von neuartigen bioabbaubaren Polyestern, welche mittels der radikalischen ringöffnenden Polymerisation (RROP) synthetisiert wurden, werden im Rahmen dieser Arbeit beschrieben. Dabei wurde die Synthese von Polystyrol gepfropften aliphatischen Polyestern mittels eines radikalischen „one-pot“ Verfahrens sowie der Reaktionsmechanismus untersucht. Weiter wurden mittels RROP enzymatisch abbaubare, amphiphile Co-Netzwerke, ein enzymatisch abbaubarer DOPA enthaltender Klebstoff (auf der Basis eines Polyesters), sowie thermisch stabile und optisch transparente Polymere mit abbaubaren Ester Bindungen, entwickelt und charakterisiert.

Im Falle der Herstellung von Pfropfcopolymeren durch ein „one-pot“ Verfahren der radikalischen Polymerisation, konnten Styrol (St) und  $\beta$ -Propiolacton ( $\beta$ -PL) in unterschiedlichen Molverhältnissen bei 120°C copolymerisiert werden. Dies ist ein seltenes Beispiel für ein „one-pot“ System, bei dem (PSt-g- $\beta$ -PL) Pfropfcopolymere mit sehr unterschiedlichen Molverhältnisse der Monomere, hergestellt werden können. Die Struktur der erhaltenen (PSt-g- $\beta$ -PL) Copolymere konnte durch mehrere Charakterisierungsmethoden, wie z.B. der 1D sowie der 2D NMR-Spektroskopie und der Gel-Permeations-Chromatographie (GPC), vor und nach der alkalischen Hydrolyse der Polymere, aufgeklärt werden. Der deutliche Reaktivitätsunterschied von Styrol und  $\beta$ -PL, die radikalische Kettenübertragungsreaktionen am Polyesterrückgrad, sowie die anschließende Reaktion mit den wachsenden aktiven Poly( $\beta$ -PL)-Polymerketten, führte zu einem grafting onto Mechanismus.

Im Rahmen dieser Arbeit wurde außerdem, eine alternative Syntheseroute zur Herstellung von enzymatisch abbaubaren und amphiphilen Co-Netzwerkstrukturen (APCNs) entwickelt. Dies geschah auf der Basis von ungesättigten Polyestern, mittels radikalischer ringöffnenden Polymerisation von Vinylcyclopropan (VCP) und zyklischen

Ketenacetalen (CKA). Im ersten Schritt wurde ein bioabbaubarer, ungesättigter Polyester, der eine statistische Verteilung der Doppelbindungen und der bioabbaubaren Estereinheiten aufweist, durch eine radikalische ringöffnende Polymerisation von VCP und 2-Methyl-4-phenyl-1,3-dioxolan (MPDO) synthetisiert. Eine ähnliche Reaktivitäten von VCP und MPDO, die mittels GPC ermittelte monomodale Molekulargewichtsverteilung, sowie durch Verwendung der 2D NMR Technik heteronuclear multiple bond correlation (HMBC) konnte gezeigt werden, dass Copolymere mit statistisch verteilten Doppelbindungen und Estereinheiten synthetisiert wurden. Die vorhandenen Doppelbindungen mit einem hydrophilen Makromonomer (oligo(ethylen glycol methacrylat, OEGMA) wurde über radikalische Polymerisation quervernetzt. Dies ermöglichte die Herstellung eines enzymatisch abbaubaren Co-Netzwerkes (APCNs). Die enzymatische Abbaubarkeit des APCN wurde durch die Verwendung von Lipase aus *Pseudomonas cepacia* untersucht. Zudem zeigte das APCN, aufgrund seines hydrophilen und seines hydrophoben Anteils, wodurch Mikrophasenseparation auftritt, ein hohes Quellvermögen und unterschiedliche optische Eigenschaften in Wasser sowie in organischen Lösemitteln. Für zukünftige Arbeiten, ermöglicht diese Synthesemethode die Herstellung von anderen funktionalisierten und bioabbaubaren APCNs über radikalische Polymerization.

Ein weiterer Teil dieser Arbeit bestand in der Entwicklung eines ungiftigen, 3,4-Dihydroxyphenylamin (DOPA) enthaltenden, enzymatisch abbaubaren Klebstoffes, welcher sich durch gute Klebfestigkeit auf weichen und metallischen Oberflächen auszeichnet. Der hergestellte Klebstoff besteht sowohl aus abbaubaren Polycaprolacton-Repetiereinheiten, als auch aus Glycidylmethacrylat (GMA)- und OEGMA- Einheiten. Hierfür wurde eine einfache zweistufige Copolymerisation von 2-Methylen-1,3-dioxepan, GMA und OEGMA, gefolgt von der Immobilisierung von DOPA an den Epoxyringen von GMA, durchgeführt. Dabei zeichnete sich  $\text{Fe}(\text{acac})_3$  als geeignetster Quervernetzer mit hoher Zugscherfestigkeit auf weichem Material (Schweinehaut) und Aluminiumoberflächen aus. Der so hergestellte Klebstoff wies weiter eine hohe Klebstabilität in

Pufferlösung (PBS, pH = 7) bei 37°C für mindestens eine Woche auf. Aufgrund der genannten Eigenschaften, ist das Material ein vielversprechender Kandidat für zukünftige Forschungsarbeiten über Klebstoffe für die Medzintechnik.

Außerdem wurde ein optisch klares Copolymer mit hoher thermischer Stabilität und einer hohen Glasübergangstemperatur, über radikalische Polymerisation von MDO und *N*-phenyl Maleinimid (NPM), hergestellt. Die unter bestimmten Reaktionsbedingungen hergestellte Polymere, d.h. 120°C und große Mengen an MDO, zeichneten sich durch abbaubare Estereinheiten aus, welche durch die radikalische ringöffnende Polymerisation von MDO gebildet wurden. Durch einfaches Mischen und Erhitzen von MDO und NPM (ohne die Verwendung eines Initiators) bildete sich ein Charge-Transfer-Complex aus. Dies führt zur Bildung eines Copolymers mit hohem Molekulargewicht. Die Strukturaufklärung des Copolymers sowie mechanische Studien wurden im Detail behandelt.



---

## Glossary

<b>2D</b>	two-dimensional
<b>AIBN</b>	azobisisobutyronitrile
<b>APCN(s)</b>	amphiphilic conetworks(s)
<b>ATRP</b>	atom-transfer radical polymerization
<b><math>\beta</math>-PL</b>	$\beta$ -propiolactone
<b>BA</b>	<i>n</i> -butyl acrylate
<b>BMDO</b>	5,6-benzo-2-methylene-1,3-dioxepane
<b>CKA(s)</b>	cyclic ketene acetal(s)
<b>DOPA</b>	3,4-dihydroxyphenylalanine
<b>DSC</b>	differential scanning calorimetry
<b>DTBP</b>	di- <i>tert</i> -butyl peroxide
<b>GMA</b>	glycidyl methacrylate
<b>GPC</b>	gel permeation chromatography
<b>HI</b>	hydrophilic
<b>HMBC</b>	heteronuclear multiple bond correlation
<b>HO</b>	hydrophobic
<b>MALLS</b>	multi-angle laser light scattering
<b>MDO</b>	2-methylene-1,3-dioxepane
<b>M<sub>n</sub></b>	number-average molecular weight
<b>M<sub>w</sub></b>	weight-average molecular weight
<b>MMA</b>	methyl methacrylate
<b>MPDO</b>	2-methylene-4-phenyl-1,3-dioxolane
<b>MTT</b>	3-(4,5-Dimethylthiazol-2-yl)-2,5-diphenyltetrazolium bromide
<b>NMP</b>	nitroxide mediated polymerization
<b>NPM</b>	<i>N</i> -phenyl maleimide

<b>OEGMA</b>	oligo(ethylene glycol) methacrylate
<b>PBS</b>	phosphate-buffered saline
<b>PCL</b>	poly( $\epsilon$ -caprolactone)
<b>PDI</b>	polydispersity index
<b>PEG</b>	poly(ethylene glycol)
<b>PEO</b>	poly(ethylene oxide)
<b>PSt</b>	polystyrene
<b>RAFT</b>	reversible addition fragmentation chain transfer polymerization
<b>RI</b>	refractive index
<b>ROP</b>	ring-opening polymerization
<b>RROP</b>	radical ring-opening polymerization
<b>St</b>	styrene
<b>T<sub>g</sub></b>	glass transition temperature
<b>TGA</b>	thermogravimetric analysis
<b>TMS</b>	tetramethylsilane
<b>UP</b>	unsaturated polyester
<b>VAc</b>	vinyl acetate
<b>VCP</b>	vinylcyclopropane

## Chapter 1

### Introduction

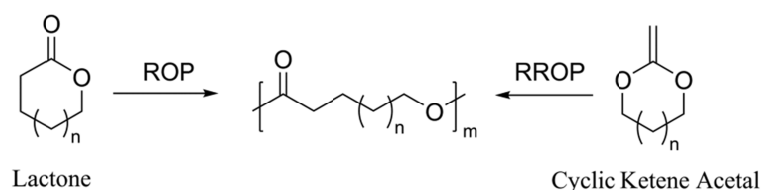
Under the consideration of environmental pollution based on the wasted and stable polymers, biodegradable polymers have been deeply researched and widely applied as environmental friendly materials.<sup>1-3</sup> The design and property studies of synthetic biodegradable polymers are interesting and attractive. Due to the controllable biodegradation profiles and good biocompatibility, aliphatic polyesters are spotlighted as an important class of biodegradable polymers and used in a broad range of applications in different fields.<sup>4</sup>

Conventionally, aliphatic polyesters can be produced by two synthetic routes: polycondensation and ring-opening polymerization of lactones or lactides. Polycondensation is carried out between diols and diacids<sup>5-8</sup> or self-combination of hydroxyacids<sup>9-11</sup> for the formation of polyesters. The polycondensation using enzyme-catalyst was also widely developed in the last 20 years. The limitation of this method is getting very high molar mass polyesters. For getting polyesters with high molar mass by polycondensation, higher reactions temperatures and longer reaction times are required.<sup>2</sup> Besides, the chain-length of the resulting polyesters cannot be controlled using this synthetic method.

Ring-opening polymerization (ROP) of lactones / lactides is the second conventional method for producing biodegradable aliphatic polyesters.<sup>12-15</sup> Polyesters with high molar mass can be produced under mild reaction conditions and short reaction time using this synthetic route. In addition, producing of polyesters with controlled chain length can be realized using ring-opening polymerization. However, ring-opening polymerization has another restriction. The functionalization of polyesters remains synthetic challenges and can only be realized by respective lactones / lactides<sup>16-18</sup> and chain-end modification<sup>19, 20</sup>.

Due to the compatibility with catalysts and reaction process, the methods of functionalization of ROP monomers require protection/deprotection steps.<sup>17</sup> For the approach of chain-end modification, the functional group density on the polyester chains is limited.<sup>19,20</sup>

An alternative synthetic route for producing aliphatic polyesters is by radical ring-opening polymerization of cyclic ketene acetals (CKAs), which has attracted lots of research interest in recent years (Scheme 1-1).<sup>21</sup> Compared with the conventional ROP of lactones / lactides, the polyester formation by RROP of CKAs can be carried out under less stringent reaction conditions.<sup>22</sup> In addition, RROP provides potentially limitless possibilities for introducing ester linkages onto vinyl polymer backbones and forming a broad range of functional polyesters for various applications. This chapter explores the various CKAs for RROP, the chemistry of RROP, and utility of RROP for different applications.



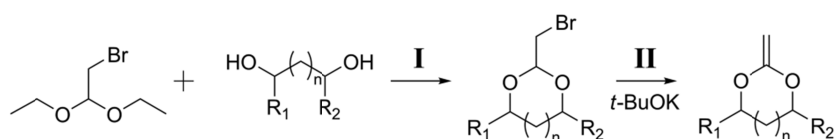
**Scheme 1-1.** Analogy between the formation of aliphatic polyester from the ROP of lactone and RROP of cyclic ketene acetal.

## 1.1 Chemistry of Radical Ring-Opening Polymerization (RROP)

Since the pioneer reports of J. Bailey and his coworkers<sup>23, 24</sup>, the chemistry of radical ring-opening polymerization (RROP) attracted researchers' interests and different CKAs were used for RROP to generate different types of aliphatic polyesters. The study was widely progressed in the last 20 years. In the following, different CKA-monomers for RROP and the mechanism of RROP are described in details.

### 1.1.1 Starting monomer for Radical Ring-Opening Polymerization

Various cyclic ketene acetals (CKAs) with different ring-sizes and substituents were used for radical ring-opening polymerization with aim to prepare polyesters. In general, the CKAs for radical ring-opening polymerization can be prepared with a two-step reaction, the first step is an acetal exchange reaction (**I** in Scheme 1-2) followed by dehydrohalogenation (**II** in Scheme 1-2).<sup>25-28</sup>



**Scheme 1-2.** Synthesis of cyclic ketene acetals (CKAs), R<sub>1</sub>, R<sub>2</sub>: substituents on CKAs' ring.

In addition, some other starting cyclic monomers like  $\beta$ -propiolactone<sup>29</sup> and cyclic allylic sulphide monomers<sup>30</sup> can also lead to a radical ring-opening polymerization and form polyesters. The reported starting cyclic monomers for radical ring-opening polymerization and the corresponding polyester structures are summarized and listed in Table 1-1.

**Table 1-1.** Starting cyclic monomers for radical ring-opening polymerization and corresponding polyester structure.

Starting cyclic monomer	Polyester structure
 2-methylene-4-phenyl-1,3-dioxalane ( <b>1</b> )	
 5,6-benzo-2-methylene-1,3-dioxepane ( <b>2</b> )	
 2-methylene-1,3-dioxepane ( <b>3</b> )	

Table 1-1. (Contd.)

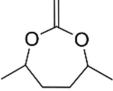
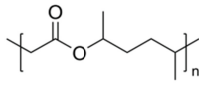
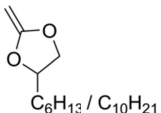
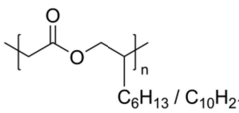
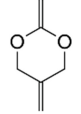
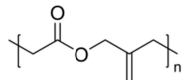
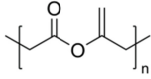
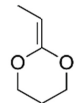
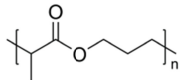
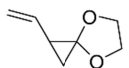
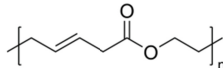
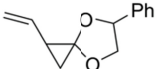
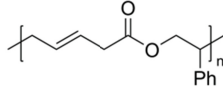
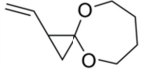
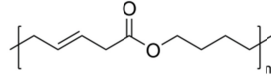
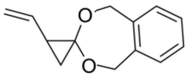
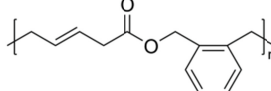
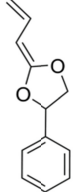
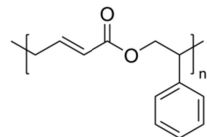
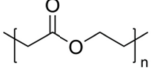
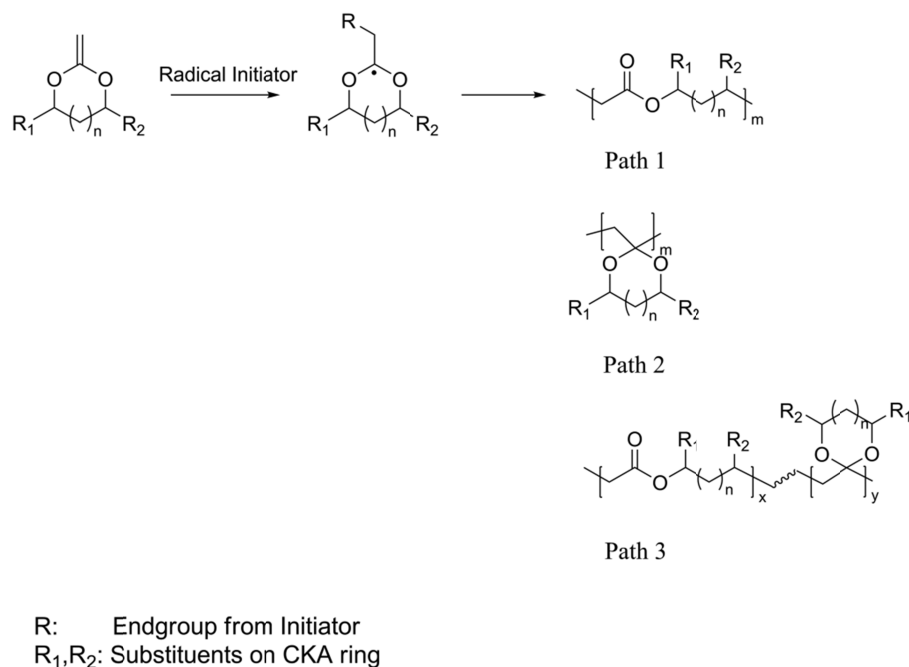
Starting cyclic monomer	Polyester structure
	
	
	
	
	
	
	
	
	
	
	
	

Table 1-1. (Contd.)

	Starting cyclic monomer	Polyester structure
	3,9-bis-methylene-2,4,8,10-tetraoxa-spiro[5,5]undecane (16)	cross-linked structure
	9,9-disubstituted-4-methylene-3,5,8,10-tetraoxabicyclo[5.3.0]decane (17)	
	2-methylene-1,3,6-trioxocane (18)	
	2,5-methylene-1,3-dioxane (19)	
	2-ethylidene-4-methyl/ethyl-1,3-dioxalane (20)	
	perfluoro-2-methylene-1,3-dioxane (21)	
	2-difluoromethylene-1,3-dioxane (22)	
	perfluoro-2-methylene-4-methyl-1,3-dioxolane (23)	
	2-difluoromethylene-4-methyl-1,3-dioxolane (24)	
	2-difluoromethylene-1,3-dioxolane (25)	
	$\beta$ -propiolactone (26)	
	cyclic allylic sulphide (27)	

### 1.1.2 Mechanism of Radical Ring-Opening Polymerization

Cyclic ketene acetals (CKAs) hold an exo-methylene double bond on the acetal ring and are widely used as starting monomers for radical ring-opening polymerization. Under radical ring-opening polymerization conditions, it can undergo two possible polymerization routes, ring-opening or ring-retaining polymerization. The combination of the two routes is also possible (Scheme 1-2). In general, the disengagement of ring-strain and/or the stability of the formation of ester bond are the driving force for the radical ring-opening reaction, and based on the report of J. Bailey *et al.*<sup>31</sup>, the bonding energy of a carbon oxygen bond is about 40 Kcal/mol, which is more stable than the carbon-carbon double bond. However, the competitive reaction between the ring-opening (path 1 in Scheme 1-3) and ring-retaining polymerization (path 2 in Scheme 1-2) is depending on the monomer concentration, reactions temperature, ring-size and substituents on the ring of CKAs.<sup>21</sup>

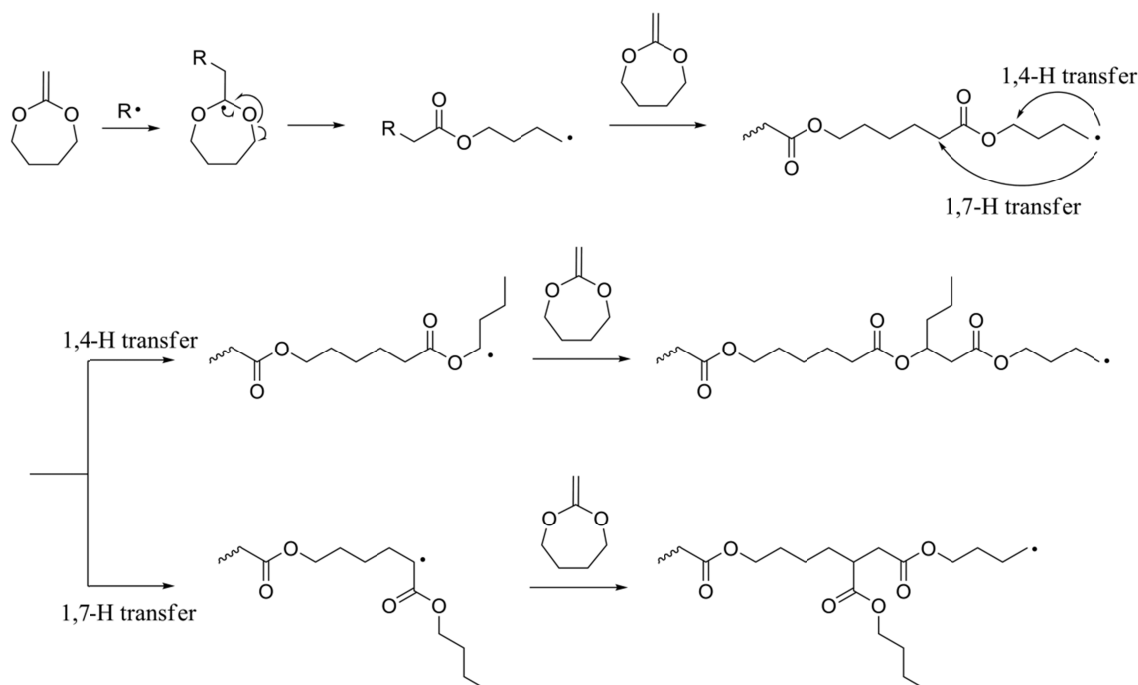


**Scheme 1-3.** Different possibilities during radical ring-opening polymerization of cyclic ketene acetals: path 1: radical ring-opening polymerization leading to polyesters; path 2: radical ring-retaining polymerization leading to polyacetals; path 3: combination of path 1 and path 2.

The ring-size of the CKAs plays a very important role in the competition between the ring-retaining and ring-opening polymerization during the reaction. For instance, 2-methylene-1,3-dioxepane (MDO, Structure **3** in Table 1-1), a CKA with seven members ring, leads to the aliphatic biodegradable polyester with polycaprolactone (PCL) like structure under the radical polymerization conditions at all reaction temperatures between 50 °C and 120 °C.<sup>22, 32</sup> For other examples, 4,7-dimethyl-2-methylene-1,3-dioxepane (Structure **4** in Table 1-1)<sup>27</sup> and 5,6-benzo-2-methylene-1,3-dioxepane (BMDO, Structure **2** in Table 1-1)<sup>33</sup> are another seven-membered CKAs and undergo quantitative ring-opening radical reaction and formed corresponding polyesters at 120 °C. In contrast, due to the stable five-membered ring and the unstable primary radical formed after ring-opening reaction, the CKA 2-methylene-1,3-dioxolane (Structure **15** in Table 1-1) is polymerized with the mixture of ring-opened and ring-retained structures at all temperatures under radical reaction condition.<sup>34</sup> The content of ring-opened structure in the resulting polymer after radical polymerization is increased with the increasing reaction temperature (50 % ring-opening polymerized at 60 °C using AIBN as initiator and 85 % ring-opening polymerized at 130 °C using di-*tert*-butylperoxide as initiator).<sup>34</sup>

In addition, the substituents on the ring of CKAs play another important role during the radical ring-opening polymerization. For instance, both 2-methylene-4-phenyl-1,3-dioxalane (Structure **1** in Table 1-1) and 2-methylene-4-hexyl/decyl-1,3-dioxalane (Structure **5** in Table 1-1) are stable five-membered CKA and they showed different polymerization behaviors during the radical polymerization. Due to the stable benzyl radical formed during the polymerization, 2-methylene-4-phenyl-1,3-dioxalane gives quantitative and regio-selective ring-opened polyester structure at all reaction temperatures from 60 to 150 °C.<sup>23</sup> On the other side, 2-methylene-4-hexyl-1,3-dioxalane gives 50 % ring-opened structure at 60 °C and 73 % ring-opened structure at 110 °C, and 2-methylene-4-decyl-1,3-dioxalane gives 55 % ring-opened structure at 60 °C and 88 % ring-opened structure at 110 °C.<sup>35</sup>

The final topology of the resulting polyesters by radical ring-opening polymerization is also dependent on the growing radical stability on the polymer chain end. The primary radicals formed during RROP process are very reactive and could lead to a backbiting reaction. As a result, branched polyesters could be formed during radical ring-opening polymerization of CKAs.<sup>26, 32, 33, 36</sup> The radical reaction process of 2-methylene-1,3-dioxepane (MDO, Structure **3** in Table 1-1) is used as an example to explain the backbiting occurrence. Similar to the intramolecular hydrogen transfers observed in the radical polymerization of ethylene, the hydrogen transfers are obtained during MDO polymerization (Scheme 1-4). Due to the high reactivity of the primary radicals, 1,4- and/or 1,7-H transfers occurred to form radicals with higher stability. The polyester with branch density of 20 % was produced after radical polymerization of MDO at reaction temperature of 50 °C.<sup>36</sup> Based on the high branch density, poly(MDO) have a different crystallinity and thermal properties in comparison with commercial PCL prepared by ROP of  $\epsilon$ -caprolactone.<sup>37</sup>



**Scheme 1-4.** Occurrence of back-biting in the radical polymerization of 2-methylene-1,3-dioxepane (MDO).

## 1.2 Controlled Radical Ring-Opening Polymerization

Controlled radical polymerization gives the opportunity to produce polymers with low polydispersity, tunable polymer chain length and functional-end groups and also provides the possibility of producing polymers with complex architectures like block, graft and star polymers under radical polymerization condition.<sup>38</sup> Atom-transfer radical polymerization (ATRP),<sup>39, 40</sup> nitroxide mediated polymerization (NMP)<sup>41</sup> and reversible addition fragmentation chain transfer (RAFT) polymerization<sup>42</sup> are the most popular controlled radical polymerization techniques. In recent years, the controlled radical polymerization techniques have been used in the radical ring-opening polymerization of CKAs with the purpose of producing well-defined polyesters.

### 1.2.1 Radical Ring-Opening Polymerization under ATRP Condition

The radical ring-opening polymerization of cyclic ketene acetals under ATRP condition to prepare degradable polyesters mostly use the substituted CKAs, 2-methylene-4-phenyl-1,3-dioxalane (MPDO, Structure 1 in Table 1-1)<sup>43</sup> or 5,6-benzo-2-methylene-1,3-dioxepane (BMDO, structure 2 in Table 1-1)<sup>26, 33, 44-48</sup> as starting monomers. Both BMDO and MPDO are polymerized with controlled polymer chain length and low polydispersities. The resulting polymer structures are dependent on the CKA structures. Similar to the conventional free radical polymerization, 5,6-benzo-2-methylene-1,3-dioxepane (BMDO) gave quantitative formation of complete ring-opened structure under ATRP condition. However, the five membered CKA, 2-methylene-4-phenyl-1,3-dioxalane (MPDO) provided mixed structure: ring-opened and ring-retained polymerized by ATRP.<sup>43</sup> This is in contrast to with the quantitative ring-opened structure obtained under free radical polymerization condition.<sup>23</sup>

Controlled radical ring-opening polymerization using ATRP method were also applied for block copolymers preparation.<sup>46</sup> ATRP was also used for the surface modification with degradable polymer brushes (Figure 1-1).<sup>45</sup> The surface initiated ATRP copolymerization

of 5,6-benzo-2-methylene-1,3-dioxepane (BMDO) and poly(ethylene glycol) methacrylate was used for hydrolytically degradable polymer brushes preparation. The polymer brushes' chain length, i.e. the film thickness, could be controlled by polymerization time.

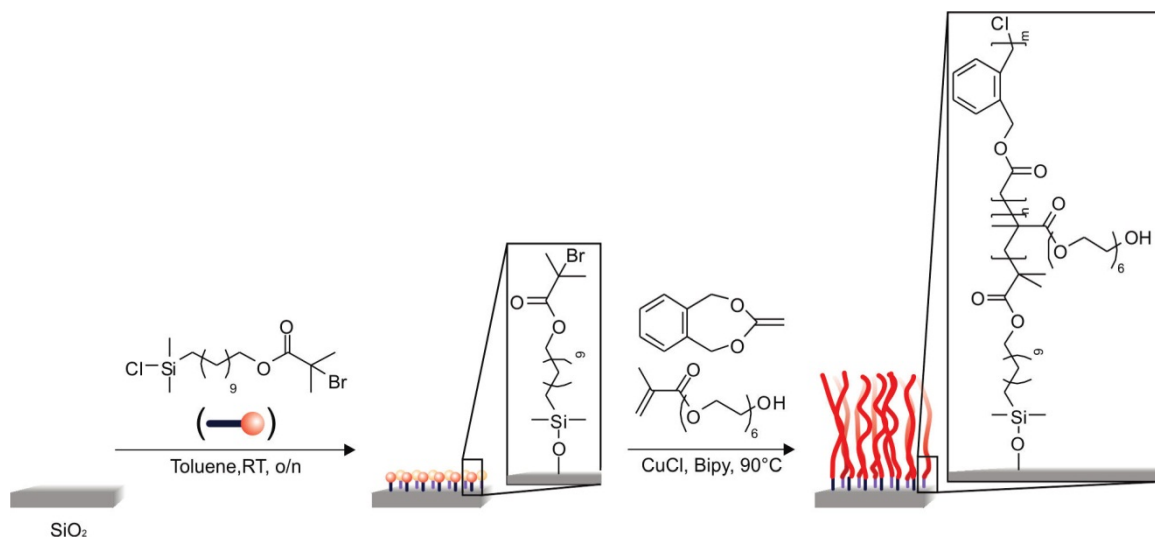


**Figure 1-1.** Surface initiated ATRP copolymerization of 5,6-benzo-2-methylene-1,3-dioxepane and poly(ethylene glycol) methacrylate for degradable polymer brushes preparation.<sup>45</sup> Reprinted with permission from C. Riachi, N. Schüwer and H.-A. Klok, *Macromolecules*, 2009, **42**, 8076-8081. Copyright (2009) American Chemical Society.

## 1.2.2 Radical Ring-Opening Polymerization under RAFT Condition

Reversible addition-fragmentation chain-transfer (RAFT) polymerization is another useful tool for the production of well-defined polymers and also various polymeric architectures.<sup>49</sup> The radical ring-opening polymerization under RAFT condition<sup>49</sup> was first reported by C.-Y. Pan's group in 2002.<sup>50</sup> The acryl-substituted CKA, 5,6-benzo-2-methylene-1,3-dioxepane (BMDO), was used as starting monomer and 1-(ethoxycarbonyl)prop-1-yl-dithiobenzoate was used as chain transfer agent. BMDO was completely ring-opened polymerized and the resulting polymer showed a controllable chain length and low polydispersity.

After that, efforts based on copolymerization of BMDO and vinyl monomers under RAFT condition was carried out.<sup>51-53</sup> For instance, T. Junkers *et al.*<sup>53</sup> reported a degradable star polymers by RAFT copolymerization of BMDO and methyl methacrylate (MMA) using functional RAFT agent with four arms (Figure 1-2). Recently, A. P. Dove and his coworkers<sup>54</sup> reported another CKA for RAFT polymerization. They gave the first example of RAFT copolymerization of 2-methylene-1,3-dioxepane (MDO) and vinyl acetate to produce well-defined and biodegradable polymers.

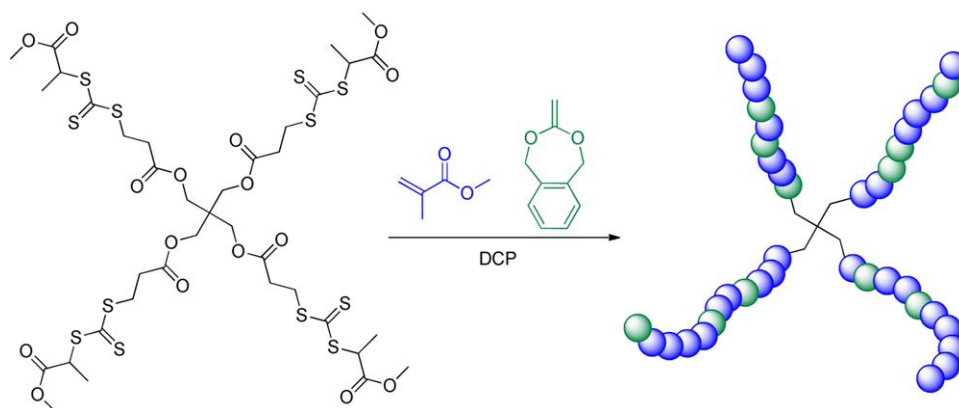


**Figure 1-2.** Schematic illustration of degradable star polymers via RAFT copolymerization of BMDO and MMA.<sup>53</sup> Reprinted with permission from S. Kobben, A. Ethirajan and T. Junkers, *J. Polym. Sci., Part A: Polym. Chem.*, 2014, **52**, 1633-1641. Copyright (2014) Wiley Periodicals, Inc.

### 1.2.3 Radical Ring-Opening Polymerization under NPM Condition

In comparison with RAFT and ATRP, nitroxide mediated (NMP) radical ring-opening polymerizations are rare.<sup>55-58</sup> However, due to the non-requirement of metal catalyst (ATRP) or sulfur-based chain transfer agents (RAFT), it has its own advantages in the preparation of environmental friendly and low cytotoxic materials.<sup>59</sup> The nitroxide mediated radical ring-opening polymerization of CKAs was first reported by Wei *et al.*<sup>57</sup> in presence of 2,2,6,6-tetramethyl-1-piperidinyloxy (TEMPO) and using 2-methylene-1,3-dioxepane (MDO) as starting monomer. MDO was quantitative ring-opened polymerized providing PCL-structure with a low polydispersity (<1.5).

Because of the well-controlled polymerization and low cytotoxicity, this method was employed for the design of biodegradable polymers in the field of biomedical applications.<sup>60</sup> Three different CKAs, 2-methylene-1,3-dioxepane (MDO), 5,6-benzo-2-methylene-1,3-dioxepane (BMDO) and 2-methylene-4-phenyl-1,3-dioxolane (MPDL), were copolymerized with oligo(ethylene glycol) methacrylate (OEGMA) and acrylonitrile (AN) by nitroxide-mediated radical ring-opening polymerization (Figure 1-3). The resulting copolymers showed a well-defined structure, good hydrolytic degradability and low cytotoxicity.

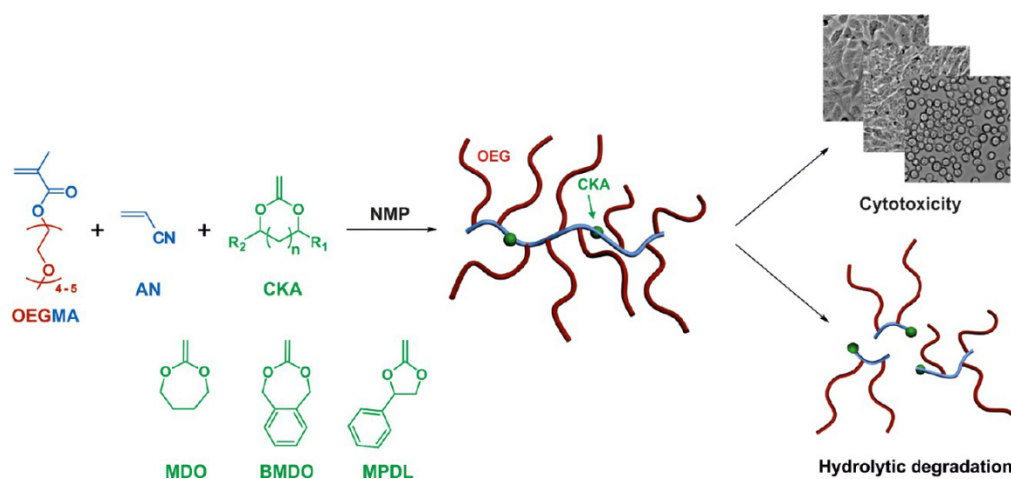


**Figure 1-3.** Schematic illustration of poly(OEGMA-*co*-AN-*co*-CKA) synthesis, cytotoxicity and hydrolytic degradability.<sup>60</sup> Reprinted with permission from V. Delplace, A. Tardy, S. Harrison, S. Mura, D. Gigmes, Y. Guillaneuf and J. Nicolas, *Biomacromolecules*, 2013, **14**, 3769-3779. Copyright (2013) American Chemical Society.

### **1.3 Application of radical ring-opening polymerization for producing functional polyesters**

Radical ring-opening polymerization (RROP) opened a new door for producing functional polyesters. RROP provides a novel synthetic route for the formation of many (bio)degradable materials. This section explores functional polyesters generated by RROP.

#### **1.3.1 Functional polyesters generated by radical ring-opening homopolymerization**

Various substituted cyclic ketene acetals (CKAs) and cyclic allylic sulphide (structure 27 in Table 1-1) were designed and used for radical ring-opening polymerization to generate polyesters with different polyesters with specific properties and functionalities.

Based on the possibility to form polyesters under radical polymerization conditions, CKAs are used for making functional polyesters for biomedical applications. For instance, M. R. Buchmeiser *et al.*<sup>61</sup> reported a porous monolithic supports by electron-beam (EB) initiated free radical polymerization. 2-methylene-4-phenyl- 1,3-dioxolane was used as monomer and trimethylolpropane triacrylate (CL) was used as cross-linker (Figure 1-4). This porous polymeric scaffold could be used in cell cultivation and tissue engineering.

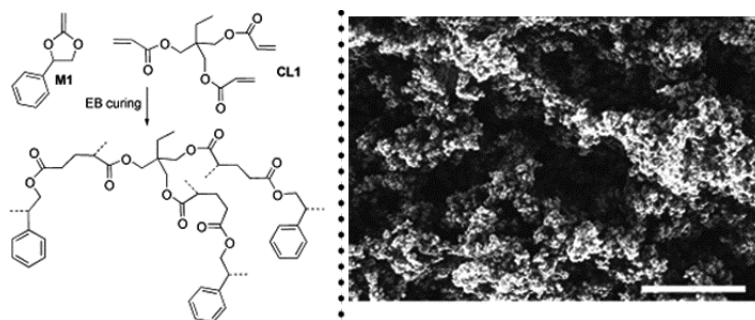
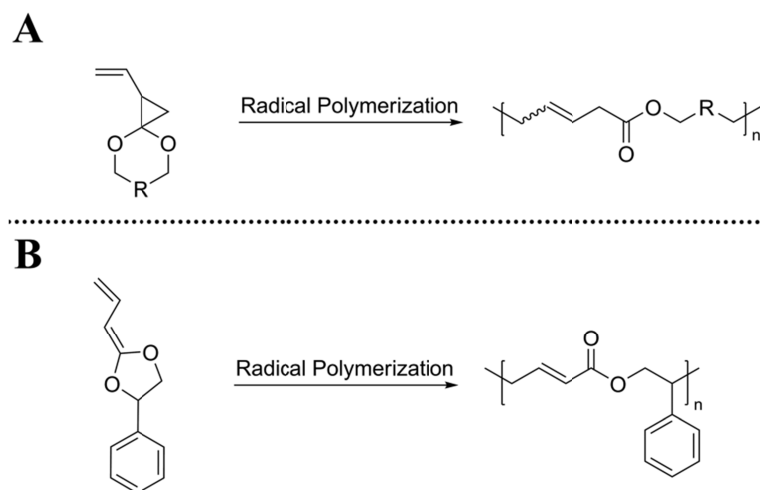


**Figure 1-4.** Monolithic polymers for biomedical applications. Left: synthesis of monolithic polyester using 2-methylene-4-phenyl-1,3-dioxolane as starting monomer for radical ring-opening polymerization; right: porous monolithic scaffolds derived from electron-beam (EB) initiated RROP. Scale bar: 100  $\mu\text{m}$ .<sup>61</sup> Reprinted with permission from A. Löber, A. Verch, B. Schlemmer, S. Höfer, B. Frerich and M. R. Buchmeiser, *Angew. Chem. Int. Ed.*, 2008, **47**, 9138-9141. Copyright (2008) WILEY-VCH Verlag GmbH & Co. KGaA, Weinheim.

Another well-known application of RROP is in producing unsaturated polyesters (UPs) with specially designed CKAs (Scheme 1-5).<sup>62-64</sup> Very interesting monomers, vinylcyclopropanone cyclic acetals (structure details please refer to structure **10-13** in Table 1-1), were reported by T. Endo *et al.*<sup>62</sup> to be used for unsaturated polyesters preparation. These specially designed monomers combine vinylcyclopropane and cyclic ketene acetal structure and were expected to be polymerized as unsaturated polyesters through a double ring-opening process during the radical polymerization (Scheme 1-5A). However, the resulting polymers contain ring-opened unsaturated polyester structure and also ring-retained structures. The resulting polymer has the highest content of unsaturated polyester units with 59 mol-%. Another example for synthesis of UPs by RROP is using 2-methylene-1,3-dioxo-5-pene (structure **8** in Table 1-1), a cyclic ketene acetal with double bond on monomer ring, as the starting monomer.<sup>63</sup> This attempt was not very successful. At higher reaction temperatures, the main product was 5-membered stable cyclic ester, and at lower reaction temperatures, the resulting product was oligomer with ring-opened and also ring-retained structures. 4-phenyl-2-propenylene-1,3-dioxalane (structure **14** in Table 1-1) was reported by S.-K. Kim and his coworker<sup>64</sup> and underwent

quantitative 1,7-type ring-opening polymerization to form unsaturated polyester (Scheme 1-5B).



**Scheme 1-5.** Radical ring-opening polymerization of various CKAs for unsaturated polyester preparation. Starting monomers: A: vinylcyclopropanone cyclic acetal (structure details please cite to structure **10-13** in Table 1-1);<sup>62</sup> B: 4-phenyl-2-propenylene-1,3-dioxalane (structure **14** in Table 1-1)<sup>64</sup>.

Other attempts to synthesis polyesters with *exo*-methylene groups in the main chain were reported using RROP.<sup>28, 30</sup> The preparation and polymerization of *exo*-methylene group substituted CKAs (structure **6** and **7** in Table 1-1) was reported by T. Endo et al.<sup>28</sup>. The ring-opened and ring-retained structures were coexisted in the resulting polymer. In addition, the resulting polymers had a very low molar mass (about 1000 g/mol) and cross-linking behavior appeared during the polymerization process. After that, C. J. Hawker's group reported a new monomer cyclic allylic sulphide (structure **27** in Table 1-1) to prepare polyesters with *exo*-methylene groups using radical ring-opening polymerization (Figure 1-5 A).<sup>30</sup> The monomer was synthesized *via* a two-step reaction and it could undergo polyester with 100 % ring-opened structure under RAFT-mediated radical ring-opening polymerization condition. In addition, these monomers could be copolymerized with commercial vinyl monomers like methyl methacrylate (MMA), *N,N*-dimethylaminoethyl methacrylate (DMAEMA) and hydroxyethylmethacrylate (HEMA).

The copolymers showed a selective bio- and chemical degradability (Figure 1-5 B and C).

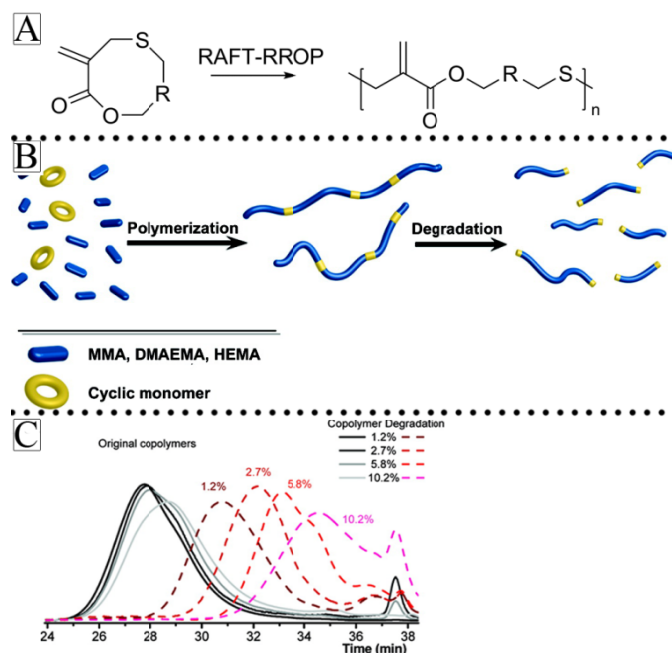
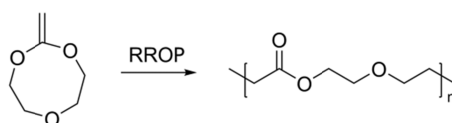


**Figure 1-5.** Radical ring-opening polymerization of cyclic allylic sulphide.<sup>30</sup> A: schematic representation of cyclic allylic sulphide polymerization under RAFT polymerization condition; B: schematic illustration of cyclic allylic sulphide copolymerization with vinyl comonomer and the degradation behavior of resulting copolymer; C: GPC traces of copolymer after degradation (copolymer of cyclic allylic sulphide and MMA as example). Reprinted with permission from J. M. J. Paulusse, R. J. Amir, R. A. Evans and C. J. Hawker, *J. Am. Chem. Soc.*, 2009, **131**, 9805-9812. Copyright (2009) American Chemical Society.

Poly(ester ether) with amorphous and hydrophilic properties is an interesting soft material for tissue engineering. It could be produced *via* RROP of 2-methylene-1,3,6-trioxocane (MTC, structure **18** in Table 1-1).<sup>65</sup> MTC could be polymerized as poly(ester ether) with 100 % ring-opened structure (Scheme 1-6). To optimize the poly(ester ether) property, the copolymerization of MTC and MDO was also reported.



**Scheme 1-6.** Radical ring-opening polymerization of 2-methylene-1,3,6-trioxocane.<sup>65</sup>

### 1.3.2 Functional polyesters generated by copolymerization of CKAs and various vinyl monomers

Radical ring-opening polymerization (RROP) provides a unique chance of bringing ester linkages onto the vinyl polymer backbone providing novel hydrolysable functional materials based on vinyl monomers simply by copolymerization of the cyclic ketene acetals (CKAs) with the corresponding vinyl monomers.<sup>66</sup> This chemistry gives an interesting addition to the conventional functional polyesters producing methods with great advantages.<sup>21</sup> This section explores various biodegradable functional materials prepared using RROP chemistry in the following.

The first example of copolymerization of CKAs with vinyl monomers was reported by W. J. Bailey *et al.*<sup>35</sup>. After that, many other reports about the copolymerization behavior of CKAs with various vinyl monomers like styrene (St),<sup>24</sup> methyl methacrylate (MMA),<sup>67</sup> ethylene,<sup>68</sup> vinyl acetate (VAc)<sup>69</sup> *etc.* were followed. These copolymers can be described as poly(vinyl-*co*-ester), a new class of (bio)degradable vinyl polymer. Due to the differences of monomer reactivity ratios between CKAs and vinyl monomers, copolymers with different microstructures can be prepared. For instance, in the copolymerization system of 5,6-benzo-2-methylene-1,3-dioxepane (BMDO, structure **2** in Table 1-1) and styrene (St), the monomer reactivity ratio was reported as  $r_{\text{BMDO}} = 1.08$  and  $r_{\text{St}} = 8.53$ .<sup>26</sup> Based on the large differences between the reactivity ratios of the comonomers, the resulting St-BMDO copolymer structure was confirmed as random with St-block on the copolymer main chain. Similar results were reported in the copolymerization of BMDO with *n*-butyl acrylate (BA,  $r_{\text{BMDO}} = 0.08$  and  $r_{\text{BA}} = 3.7$ )<sup>47</sup> and the copolymerization of MDO with St ( $r_{\text{MDO}} = 0.021$ ,  $r_{\text{St}} = 22.6$ )<sup>70</sup> and MMA ( $r_{\text{MDO}} = 0.057$ ,  $r_{\text{MMA}} = 34.12$ )<sup>71</sup>. Only a few vinyl monomers can be polymerized with CKAs to form statistical copolymers. For example, the reactivity ratios of BMDO and MMA was reported as  $r_{\text{BMDO}} = 0.53$  and  $r_{\text{MMA}} = 1.96$ ,<sup>33</sup> and reactivity ratios of MDO and vinyl acetate (VAc) was reported as  $r_{\text{MDO}} = 0.93$  and  $r_{\text{VAc}} = 1.71$ .<sup>22</sup> The copolymerization

behavior of MDO with  $\beta$ -methyl-  $\alpha$ -methylene- $\gamma$ -butyrolactone (Tulipalin-A), a bio-based electron-deficient vinyl monomer, was reported by S. Agarwal *et al.* (Figure 1-6).<sup>72</sup> Based on the electron-donor (MDO) and electron-acceptor (Tulipalin-A) comonomers, a charge transfer complex exists during the copolymerization. These two comonomers could lead to an alternating copolymerization and the spontaneous copolymerization could be processed by simple mixing and heating.

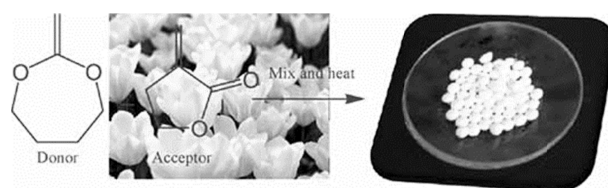


**Figure 1-6.** Copolymerization of MDO and Tulipalin-A.<sup>72</sup> Reprinted with permission from S. Agarwal and R. Kumar, *Macromol. Chem. Phys.*, 2011, **212**, 603-612. Copyright (2011) WILEY-VCH Verlag GmbH & Co. KGaA, Weinheim.

The application of copolymerization of CKAs with functional vinyl monomers to overcome the limitation of polymer materials in non-degradability attracts more and more research interests. For instance, poly(*N,N'*-isopropylacrylamide) (PNIPAAm) is an important thermo-responsive polymer and widely used in bio-medical field.<sup>73-75</sup> The copolymerization of CKAs and NIPAAm provides an opportunity to create a new polymeric material combining lower critical solution temperature (LCST) and biodegradability (Figure 1-7). The copolymerization behavior of BMDO and NIPAAm was reported by our group.<sup>76</sup> BMDO shows quantitative ring-opened structure during the copolymerization and ester-groups are randomly distributed on the polymer main chain. The lower critical solution temperature can be controlled through changing the BMDO and NIPAAm feed ratio.

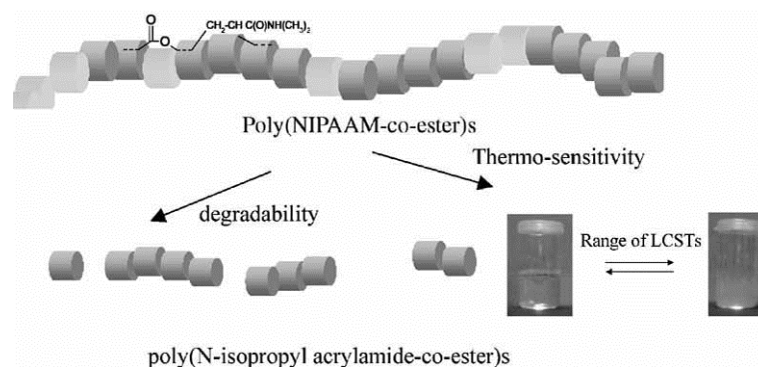


**Figure 1-7.** Schematic illustration of degradable poly(NIPAAAM-*co-ester*) with LCST property.<sup>76</sup> Reprinted with permission from L. Ren and S. Agarwal, *Macromol. Chem. Phys.*, 2007, **208**, 245-253. Copyright (2007) WILEY-VCH Verlag GmbH & Co. KGaA, Weinheim.

Based on the biodegradable thermo-responsive poly(BMDO-*co*-NIPAAAM), K. Matyjaszewski *et al.*<sup>48</sup> developed a cross-linked gel with good biodegradability and biocompatibility. In this report, the well-defined poly(BMDO-*co*-NIPAAAM) was prepared using ATRP or RAFT technology and poly(ethylene glycol-*co*-glycolic acid) diacrylate was used as cross-linker. The resulting hydrogel and its products after degradation showed a low cytotoxicity by *in vitro* cell analysis.

Furthermore, J.-F. Lutz *et al.* reported another biocompatible, thermoresponsive, and biodegradable material (“All-in-One” biorelevant polymer) by simple copolymerization of oligo(ethylene glycol) methacrylate (OEGMA), 2-(2-methoxyethoxy)ethyl methacrylate (MEO<sub>2</sub>MA) and BMDO under ATRP condition.<sup>77</sup> The structure of resulting copolymer was characterized by <sup>1</sup>H-NMR spectroscopy (Figure 1-8 A). The novel “All-in-One” polymer showed a good biodegradability (Figure 1-8 B) and compared with the previously reported poly(BMDO-*co*-NIPAAAM),<sup>76</sup> LCST of this poly(OEGMA-*co*-MEO<sub>2</sub>MA-*co*-BMDO) system could be controlled in a broad range (31 - 67°C) with a sharp phase transition (Figure 1-8 C).

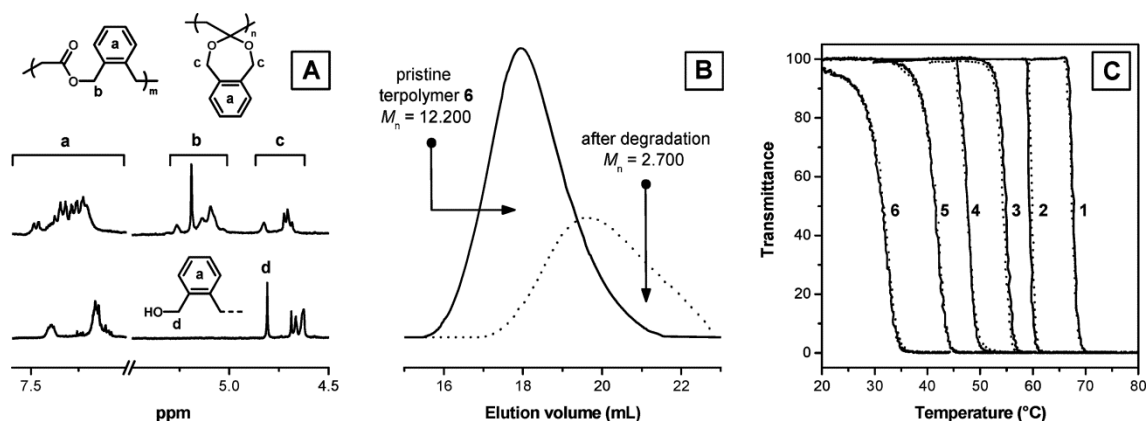


**Figure 1-8.** A: <sup>1</sup>H-NMR spectrum of poly(OEGMA-*co*-MEO<sub>2</sub>MA-*co*-BMDO) before (top) and after (bottom) degradation. B: Comparison of GPC curves of poly(OEGMA-*co*-MEO<sub>2</sub>MA-*co*-BMDO) before and after degradation. C: Measurement of LCST values for poly(OEGMA-*co*-MEO<sub>2</sub>MA-*co*-BMDO) with different composition.<sup>77</sup> Reprinted with permission from J.-F. Lutz, J. Andrieu, S. Üzgün, C. Rudolph and S. Agarwal, *Macromolecules*, 2007, **40**, 8540-8543. Copyright (2007) American Chemical Society.

Due to the good biocompatibility and biodegradability of poly(vinyl-*co*-ester), more and more reports were given using copolymerization of CKAs and vinyl monomers in the biomedical application field like drug and gene delivery. An amphiphilic copolymer was formed by copolymerization of poly(ethylene glycol) methacrylate (PEGMA), MDO and 7-(2-methacryloyloxyethoxy)-4-methylcoumarin methacrylate (CMA).<sup>78</sup> The resulting copolymer was photo cross-linkable and showed biodegradability, biocompatibility. This amphiphilic copolymer has the capability to self-assemble into micelle in aqueous solution (Figure 1-9 A). The polymeric micelle showed degradability in the presence of enzymes (Figure 1-9 B) and was used for anticancer drug doxorubicin (DOX) delivery (Figure 1-9 C).

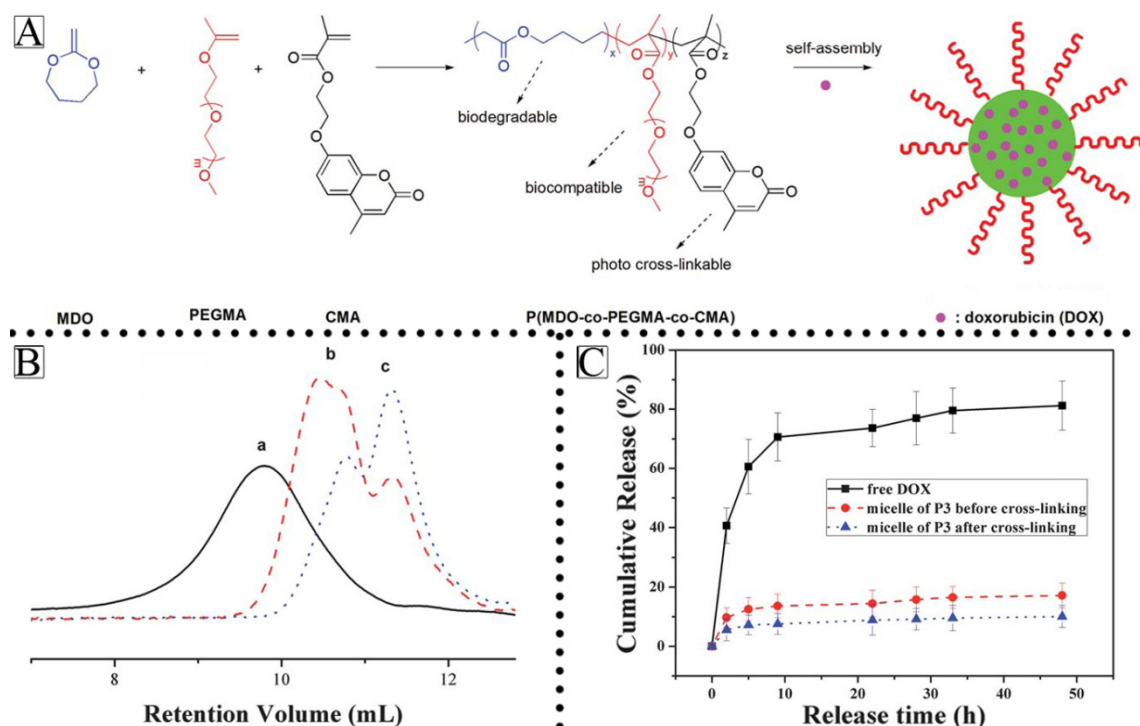
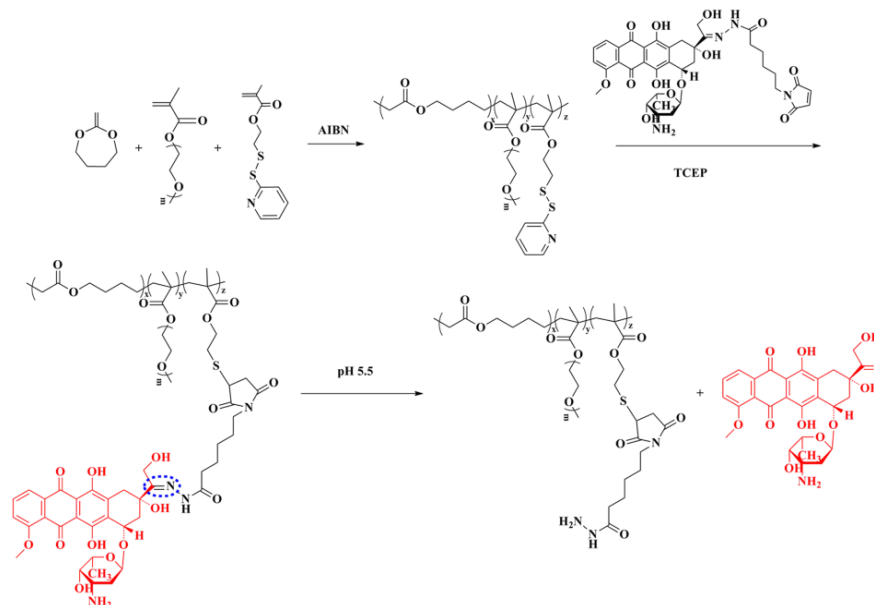


**Figure 1-9.** A: Schematic illustration of P(MDO-*co*-PEGMA-*co*-CMA) preparation and drug loading on the self-assembled micelle. B: GPC traces of P(MDO-*co*-PEGMA-*co*-CMA): (a) before degradation, (b) after 2 days degradation in 10 mg/mL Lipase (from *Pseudomonas cepacia*) solution and (c) after 5 days degradation in 10 mg/mL Lipase (from *Pseudomonas cepacia*) solution. C: cumulative release of DOX from P(MDO-*co*-PEGMA-*co*-CMA) micelles, (free DOX•HCl was used as control).<sup>78</sup> Reprinted with permission from Q. Jin, S. Maji and S. Agarwal, *Polym. Chem.*, 2012, **3**, 2785-2793. Copyright (2012) Royal Society of Chemistry.

After this report, similar biodegradable amphiphilic copolymers were used as a template for micelle formation and drug delivery.<sup>79-81</sup> For instance, J. Ji's group recently reported a MDO-based biodegradable polyester for prodrug construction (Scheme 1-7).<sup>80</sup> The functional terpolymer was simply synthesized through a one-pot radical polymerization of MDO, PEGMA and pyridyldisulfide ethylmethacrylate (PDSMA). Doxorubicin (DOX) was immobilized on the polymer mainchain via thiol-ene click reaction. The resulting copolymer was self-assembled into prodrug micelle and showed pH-sensitivity and good biodegradability.



**Scheme 1-7.** Schematic illustration of biodegradable polymeric prodrug preparation.<sup>80</sup> Taken from T. Cai, Y. Chen, Y. Wang, H. Wang, X. Liu, Q. Jin, S. Agarwal and J. Ji, *Polym. Chem.*, 2014, **5**, 4061-4068 by author open access.

The application of this chemistry in the field of gene delivery was also reported in the last few years.<sup>82-84</sup> The RROP chemistry gives a novel method to reduce toxicity of materials for gene delivery and provides (bio)degradability to the resulting polymer. Poly(*N,N*-dimethylaminoethyl methacrylate) is a well-known cationic polyelectrolyte for gene delivery.<sup>85, 86</sup> A new designed copolymer based on DMAEMA and BMDO was reported for gene delivery (Figure 1-10).<sup>83</sup> To improve water solubility and reduce the toxicity, poly(ethylene oxide) (PEO) azo-initiator was used as radical initiator. The resulting poly(PEG-*b*-(BMDO-*co*-DMAEMA)) showed a good biocompatibility, biodegradability and good results in *p*-DNA transfection.

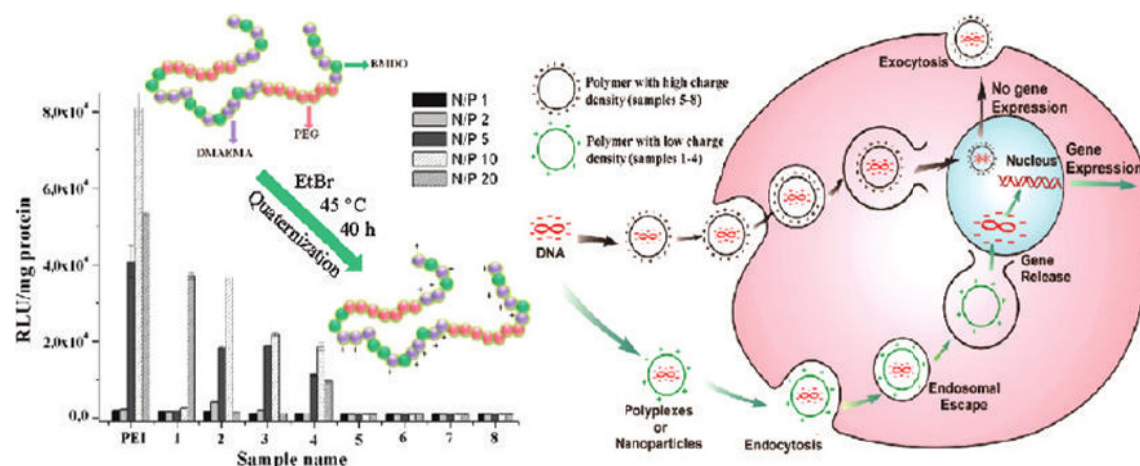


**Figure 1-10.** Schematic illustration of poly(PEG-*b*-(BMDO-*co*-DMAEMA)) for gene delivery.<sup>83</sup> Reprinted with permission from Y. Zhang, M. Zheng, T. Kissel and S. Agarwal, *Biomacromolecules*, 2012, **13**, 313-322. Copyright (2012) American Chemical Society.

Another interesting attempt for application of RROP in the gene delivery field was reported using polymer analogous reaction of poly(viny-*co*-ester).<sup>84</sup> A terpolymer was synthesized *via* radical copolymerization of propargyl acrylate (PA), MDO and DMAEMA. Through an alkyne-azide click reaction, PEG side chains was grafted onto the poly(PA-*co*-MDO-*co*-DMAEMA) main chain to improve water solubility (Figure 1-11 left). The resulting copolymer showed a lower cytotoxic than PEI and has the potential to be used as gene delivery carrier (Figure 1-11 right).

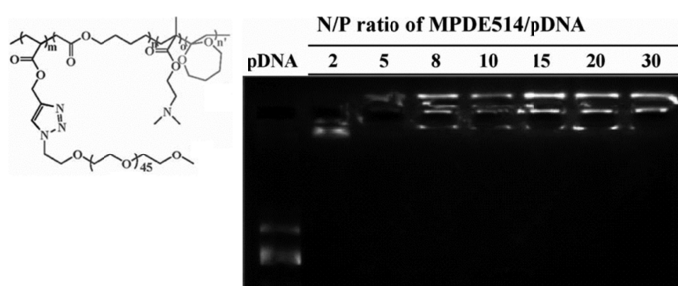


**Figure 1-11.** Left: polymer structure of PEG grafted poly(PA-*co*-MDO-*co*-DMAEMA). Right: Agarose gel electrophoresis of polymer/DNA complexes with different N/P ratios.<sup>84</sup> Reprinted with permission from S. Maji, F. Mitschang, L. Chen, Q. Jin, Y. Wang and S. Agarwal, *Macromol. Chem. Phys.*, 2012, **213**, 1643-1654. Copyright (2012) WILEY-VCH Verlag GmbH & Co. KGaA, Weinheim.

In addition, copolymerization of CKAs and vinyl monomers was also applied for the formation of biodegradable materials like ionomers,<sup>87</sup> thermoplastic elastomers<sup>88</sup> and packaging films<sup>89</sup> *etc.*

## **1.4 Aim of the Thesis**

Radical ring-opening copolymerization of cyclic monomers with vinyl monomers provides a novel and simple synthetic method for producing biodegradable materials. Therefore, the motivation of this thesis was to explore the formation of various polymeric architectures and degradable polymers with novel properties, such as amphiphilic conetworks (APCNs), biomimetic DOPA-containing adhesives and polymeric material with high thermal stability, glass transition temperature and optical transparency. Further aim was to understand the reaction mechanism of radical ring-opening polymerization of special cyclic starting monomers.

## 1.5 References

1. H. Tian, Z. Tang, X. Zhuang, X. Chen and X. Jing, *Prog. Polym. Sci.*, 2012, **37**, 237-280.
2. M. Okada, *Prog. Polym. Sci.*, 2002, **27**, 87-133.
3. L. S. Nair and C. T. Laurencin, *Prog. Polym. Sci.*, 2007, **32**, 762-798.
4. D. Goldberg, *J. Environ. Polym. Degrad.*, 1995, **3**, 61-67.
5. G. Z. Papageorgiou, D. S. Achilias and D. N. Bikiaris, *Macromol. Chem. Phys.*, 2009, **210**, 90-107.
6. S. Målberg, P. Plikk, A. Finne-Wistrand and A.-C. Albertsson, *Chem. Mater.*, 2010, **22**, 3009-3014.
7. A. Mahapatro, A. Kumar, B. Kalra and R. A. Gross, *Macromolecules*, 2004, **37**, 35-40.
8. A. Mahapatro, B. Kalra, A. Kumar and R. A. Gross, *Biomacromolecules*, 2003, **4**, 544-551.
9. A. Mahapatro, A. Kumar and R. A. Gross, *Biomacromolecules*, 2004, **5**, 62-68.
10. D. O'Hagan and N. A. Zaidi, *Polymer*, 1994, **35**, 3576-3578.
11. Y.-b. Lim, Y. H. Choi and J.-s. Park, *J. Am. Chem. Soc.*, 1999, **121**, 5633-5639.
12. M. Labet and W. Thielemans, *Chem. Soc. Rev.*, 2009, **38**, 3484-3504.
13. C. K. Williams, *Chem. Soc. Rev.*, 2007, **36**, 1573-1580.
14. S. Inkinen, M. Hakkarainen, A.-C. Albertsson and A. Södergård, *Biomacromolecules*, 2011, **12**, 523-532.

15. I. K. Varma, A.-C. Albertsson, R. Rajkhowa and R. K. Srivastava, *Prog. Polym. Sci.*, 2005, **30**, 949-981.
16. S. Cajot, P. Lecomte, C. Jerome and R. Riva, *Polym. Chem.*, 2013, **4**, 1025-1037.
17. R. Riva, S. Schmeits, F. Stoffelbach, C. Jerome, R. Jerome and P. Lecomte, *Chem. Commun.*, 2005, 5334-5336.
18. M. Liu, N. Vladimirov and J. M. J. Fréchet, *Macromolecules*, 1999, **32**, 6881-6884.
19. G. Carrot, J. G. Hilborn, M. Trollsås and J. L. Hedrick, *Macromolecules*, 1999, **32**, 5264-5269.
20. A. L. Korich, A. R. Walker, C. Hincke, C. Stevens and P. M. Iovine, *J. Polym. Sci., Part A: Polym. Chem.*, 2010, **48**, 5767-5774.
21. S. Agarwal, *Polym. Chem.*, 2010, **1**, 953-964.
22. J. Undin, T. Illanes, A. Finne-Wistrand and A.-C. Albertsson, *Polym. Chem.*, 2012, **3**, 1260-1266.
23. W. J. Bailey, S.-R. Wu and Z. Ni, *Die Makromolekulare Chemie*, 1982, **183**, 1913-1920.
24. W. J. Bailey, Z. Ni and S.-R. Wu, *J. Polym. Sci., Polym. Chem. Ed.*, 1982, **20**, 3021-3030.
25. S. M. McElvain and M. J. Curry, *J. Am. Chem. Soc.*, 1948, **70**, 3781-3786.
26. H. Wickel and S. Agarwal, *Macromolecules*, 2003, **36**, 6152-6159.
27. W. J. Bailey, Z. Ni and S. R. Wu, *Macromolecules*, 1982, **15**, 711-714.
28. T. Yokozawa, R. Hayashi and T. Endo, *J. Polym. Sci., Part A: Polym. Chem.*, 1990, **28**, 3739-3746.

29. S. Katayama, H. Horikawa and O. Toshima, *J. Polym. Sci., Part A-1: Polym. Chem.*, 1971, **9**, 2915-2932.
30. J. M. J. Paulusse, R. J. Amir, R. A. Evans and C. J. Hawker, *J. Am. Chem. Soc.*, 2009, **131**, 9805-9812.
31. J. Bailey, J. L. Chou, P. Z. Feng, V. Kuruganti and L. L. Zhou, *Acta Polym.*, 1988, **39**, 335-341.
32. S. Jin and K. E. Gonsalves, *Macromolecules*, 1998, **31**, 1010-1015.
33. H. Wickel, S. Agarwal and A. Greiner, *Macromolecules*, 2003, **36**, 2397-2403.
34. W. Liu, F. Mikeš, Y. Guo, Y. Koike and Y. Okamoto, *J. Polym. Sci., Part A: Polym. Chem.*, 2004, **42**, 5180-5188.
35. W. J. Bailey, S.-R. Wu and Z. Ni, *J. Macromol. Sci., Part A: Chem.*, 1982, **18**, 973-986.
36. S. Jin and K. E. Gonsalves, *Macromolecules*, 1997, **30**, 3104-3106.
37. S. Agarwal and C. Speyerer, *Polymer*, 2010, **51**, 1024-1032.
38. W. A. Braunecker and K. Matyjaszewski, *Prog. Polym. Sci.*, 2007, **32**, 93-146.
39. J.-S. Wang and K. Matyjaszewski, *Macromolecules*, 1995, **28**, 7901-7910.
40. J.-S. Wang and K. Matyjaszewski, *J. Am. Chem. Soc.*, 1995, **117**, 5614-5615.
41. C. J. Hawker, A. W. Bosman and E. Harth, *Chem. Rev.*, 2001, **101**, 3661-3688.
42. J. Chiefari, Y. K. Chong, F. Ercole, J. Krstina, J. Jeffery, T. P. T. Le, R. T. A. Mayadunne, G. F. Meijs, C. L. Moad, G. Moad, E. Rizzardo and S. H. Thang, *Macromolecules*, 1998, **31**, 5559-5562.
43. C.-Y. Pan and X.-D. Lou, *Macromol. Chem. Phys.*, 2000, **201**, 1115-1120.
44. J.-Y. Yuan, C.-Y. Pan and B. Z. Tang, *Macromolecules*, 2001, **34**, 211-214.

45. C. Riachi, N. Schüwer and H.-A. Klok, *Macromolecules*, 2009, **42**, 8076-8081.
46. J.-Y. Yuan and C.-Y. Pan, *Eur. Polym. J.*, 2002, **38**, 1565-1571.
47. J. Huang, R. Gil and K. Matyjaszewski, *Polymer*, 2005, **46**, 11698-11706.
48. D. J. Siegwart, S. A. Bencherif, A. Srinivasan, J. O. Hollinger and K. Matyjaszewski, *J. Biomed. Mater. Res., Part A*, 2008, **87A**, 345-358.
49. M. Semsarilar and S. Perrier, *Nat. Chem.*, 2010, **2**, 811-820.
50. T. He, Y.-F. Zou and C.-Y. Pan, *Polym. J.*, 2002, **34**, 138-143.
51. N. Xiao, H. Liang and J. Lu, *Soft Matter*, 2011, **7**, 10834-10840.
52. G. G. d'Ayala, M. Malinconico, P. Laurienzo, A. Tardy, Y. Guillaneuf, M. Lansalot, F. D'Agosto and B. Charleux, *J. Polym. Sci., Part A: Polym. Chem.*, 2014, **52**, 104-111.
53. S. Kobben, A. Ethirajan and T. Junkers, *J. Polym. Sci., Part A: Polym. Chem.*, 2014, **52**, 1633-1641.
54. G. G. Hedir, C. A. Bell, N. S. Jeong, E. Chapman, I. R. Collins, R. K. O'Reilly and A. P. Dove, *Macromolecules*, 2014, **47**, 2847-2852.
55. Y. Wei, E. J. Connors, X. Jia and C. Wang, *J. Polym. Sci., Part A: Polym. Chem.*, 1998, **36**, 761-771.
56. V. Delplace, S. Harrisson, A. Tardy, D. Gigmes, Y. Guillaneuf and J. Nicolas, *Macromol. Rapid Commun.*, 2014, **35**, 484-491.
57. Y. Wei, E. J. Connors, X. Jia and B. Wang, *Chem. Mater.*, 1996, **8**, 604-606.
58. A. Tardy, V. Delplace, D. Siri, C. Lefay, S. Harrisson, B. de Fatima Albergaria Pereira, L. Charles, D. Gigmes, J. Nicolas and Y. Guillaneuf, *Polym. Chem.*, 2013, **4**, 4776-4787.

59. M. Chenal, S. Mura, C. Marchal, D. Gigmes, B. Charleux, E. Fattal, P. Couvreur and J. Nicolas, *Macromolecules*, 2010, **43**, 9291-9303.
60. V. Delplace, A. Tardy, S. Harrisson, S. Mura, D. Gigmes, Y. Guillaneuf and J. Nicolas, *Biomacromolecules*, 2013, **14**, 3769-3779.
61. A. Löber, A. Verch, B. Schlemmer, S. Höfer, B. Frerich and M. R. Buchmeiser, *Angew. Chem. Int. Ed.*, 2008, **47**, 9138-9141.
62. F. Sanda, T. Takata and T. Endo, *Macromolecules*, 1994, **27**, 1099-1111.
63. P. Plikk, T. Tyson, A. Finne-Wistrand and A.-C. Albertsson, *J. Polym. Sci., Part A: Polym. Chem.*, 2009, **47**, 4587-4601.
64. I. Cho and S.-K. Kim, *J. Polym. Sci., Part C: Polym. Lett.*, 1990, **28**, 417-421.
65. J. Undin, P. Plikk, A. Finne-Wistrand and A.-C. Albertsson, *J. Polym. Sci., Part A: Polym. Chem.*, 2010, **48**, 4965-4973.
66. Y. Shi, Z. Zheng and S. Agarwal, *Chem. - Eur. J.*, 2014, **20**, 7419-7428.
67. T. Endo, N. Yako, K. Azuma and K. Nate, *Die Makromolekulare Chemie*, 1985, **186**, 1543-1548.
68. B. Wu and R. Lenz, *J. Environ. Polym. Degrad.*, 1998, **6**, 23-29.
69. S. Agarwal, R. Kumar, T. Kissel and R. Reul, *Polym. J*, 2009, **41**, 650-660.
70. W. J. Bailey, T. Endo, B. Gapud, Y.-N. Lin, Z. Ni, C.-Y. Pan, S. E. Shaffer, S.-R. Wu, N. Yamazaki and K. Yonezawa, *J. Macromol. Sci., Part A: Chem.*, 1984, **21**, 979-995.
71. G. E. Roberts, M. L. Coote, J. P. A. Heuts, L. M. Morris and T. P. Davis, *Macromolecules*, 1999, **32**, 1332-1340.
72. S. Agarwal and R. Kumar, *Macromol. Chem. Phys.*, 2011, **212**, 603-612.
73. N. Rapoport, *Prog. Polym. Sci.*, 2007, **32**, 962-990.

74. A. Kumar, A. Srivastava, I. Y. Galaev and B. Mattiasson, *Prog. Polym. Sci.*, 2007, **32**, 1205-1237.
75. E. S. Gil and S. M. Hudson, *Prog. Polym. Sci.*, 2004, **29**, 1173-1222.
76. L. Ren and S. Agarwal, *Macromol. Chem. Phys.*, 2007, **208**, 245-253.
77. J.-F. Lutz, J. Andrieu, S. Üzgün, C. Rudolph and S. Agarwal, *Macromolecules*, 2007, **40**, 8540-8543.
78. Q. Jin, S. Maji and S. Agarwal, *Polym. Chem.*, 2012, **3**, 2785-2793.
79. T. Cai, Y. Chen, Y. Wang, H. Wang, X. Liu, Q. Jin, S. Agarwal and J. Ji, *Macromol. Chem. Phys.*, 2014, **215**, 1848-1854.
80. T. Cai, Y. Chen, Y. Wang, H. Wang, X. Liu, Q. Jin, S. Agarwal and J. Ji, *Polym. Chem.*, 2014, **5**, 4061-4068.
81. Y. Zhang, D. Chu, M. Zheng, T. Kissel and S. Agarwal, *Polym. Chem.*, 2012, **3**, 2752-2759.
82. S. Agarwal, L. Ren, T. Kissel and N. Bege, *Macromol. Chem. Phys.*, 2010, **211**, 905-915.
83. Y. Zhang, M. Zheng, T. Kissel and S. Agarwal, *Biomacromolecules*, 2012, **13**, 313-322.
84. S. Maji, F. Mitschang, L. Chen, Q. Jin, Y. Wang and S. Agarwal, *Macromol. Chem. Phys.*, 2012, **213**, 1643-1654.
85. S. De Smedt, J. Demeester and W. Hennink, *Pharm. Res.*, 2000, **17**, 113-126.
86. D. N. Nguyen, J. J. Green, J. M. Chan, R. Langer and D. G. Anderson, *Adv. Mater.*, 2009, **21**, 847-867.
87. S. Agarwal and L. Ren, *Macromolecules*, 2009, **42**, 1574-1579.

88. N. Grabe, Y. Zhang and S. Agarwal, *Macromol. Chem. Phys.*, 2011, **212**, 1327-1334.
89. P. K. Roy, M. Hakkarainen, I. K. Varma and A.-C. Albertsson, *Environ. Sci. Technol.*, 2011, **45**, 4217-4227.



## Chapter 2

### Overview of Thesis

This thesis is made up of six chapters. Four publications are included in this thesis and presented in Chapters 3 to 6.

All the chapters in this thesis are presented under the general theme polyester preparation by radical ring-opening polymerization (RROP). My research work is focused on (i) a rare example of the formation of polystyrene-grafted aliphatic polyester in one-pot by radical polymerization (**Chapter 3**), (ii) designed enzymatically degradable amphiphilic conetworks (APCNs) by radical ring-opening polymerization (**Chapter 4**), (iii) developing enzymatically degradable DOPA-containing polyester based adhesives by radical polymerization (**Chapter 5**), and (iv) preparation and characterization of novel thermally stable optically transparent copolymers with degradable ester linkages (**Chapter 6**).

This chapter presents an overview of the main results obtained during the work.

## 2.1 Formation of Polystyrene Grafted Aliphatic Polyester in One-Pot by Radical Polymerization

It is evident from the literature that the grafting of polyesters onto vinyl polymers, such as polystyrene (PSt), requires multistep procedures. Hence, the formation of graft copolymers of polyesters, by radical polymerization in one pot, avoiding cross-linking and thermal degradation could be highly advantageous. In this chapter we highlight a rare example of the formation of PSt-g-aliphatic polyester in one pot by radical polymerization.

Various copolymers of  $\beta$ -propiolactone ( $\beta$ -PL) with St were produced by changing the molar ratio of the two monomers in the initial feed. Polymer blends were formed in reactions with an increased amount of  $\beta$ -PL in the feed. The two fractions of all the resulting polymer blends could be separated by using preparative GPC or Soxhlet extraction. A blend with  $\beta$ -PL–St copolymer (Fraction 1) and homopoly( $\beta$ -PL) (Fraction 2) was synthesized (Figure 2-1).

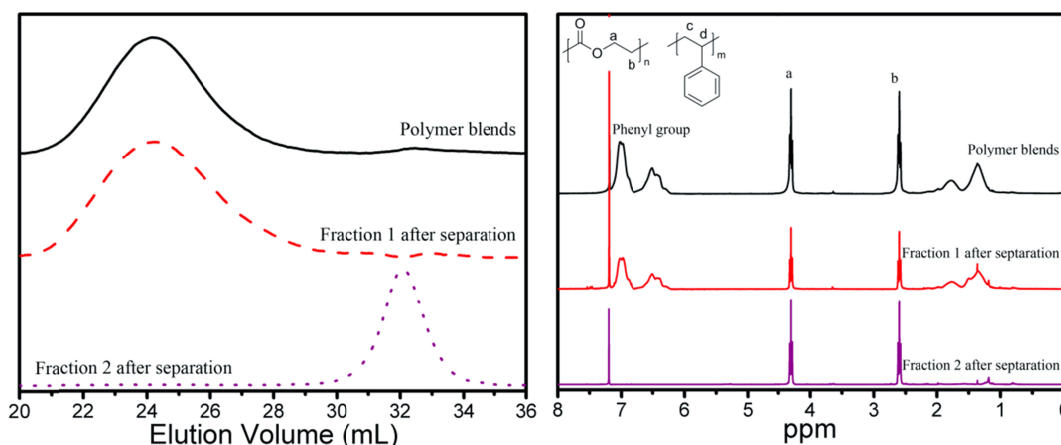


**Figure 2-1.** Separation of polymer blend prepared by radical copolymerization of styrene and  $\beta$ -PL at 120°C (monomer ratio of  $\beta$ -PL:St=1:1 in feed). Comparison of GPC traces before and after separation (left) and <sup>1</sup>H NMR spectra of each fraction (right, original polymer (black); first fraction after separation (red); second fraction after separation (purple)).

To gain insight into the microstructure of the copolymers, alkaline hydrolysis was carried out. Surprisingly, there was no significant difference between the elution volumes and the relative molar mass of the remaining polymers after degradation and the original  $\beta$ -PL–St copolymers as determined against polystyrene standards by using an RI detector (Figure 2-2). The absolute molar mass of the polymers could be interesting and was determined by gel permeation chromatography with multi-angle laser light scattering (GPC-MALLS). The copolymers showed a higher absolute molar mass than the relative molar mass determined by using an RI detector against polystyrene standards. Whereas the degraded polymers had similar absolute and relative molar mass, showing the presence of branched structures from  $\beta$ -PL. These results confirmed that the copolymers were graft copolymers, in which  $\beta$ -PL chains were grafted onto the PSt backbone.

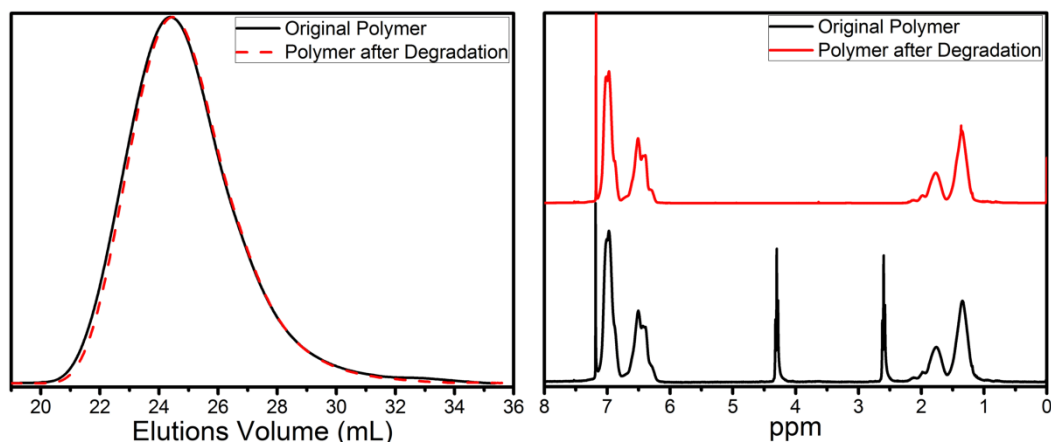


**Figure 2-3.** Degradation behavior of  $\beta$ -PL–St copolymers. Comparison of the relative GPC traces (left) and comparison of the  $^1\text{H}$  NMR spectra (right). Black: original polymer, red: polymer after degradation. Monomer ratio in the feed:  $\beta$ -PL:St = 1:2 as example.

We designed a reaction to define the polymer structure at the grafting point. The degraded polymer was esterified with trifluoroacetic anhydride. The remaining group at the grafting point after degradation was confirmed as  $-\text{CH}_2\text{OH}$  (Figure 2-3). Hence the polymer structure of  $\beta$ -PL–St copolymer at grafting point was confirmed. The mechanism of the copolymerization is summarized in Scheme 2-1. Through radical recombination between the transferred benzyl radical and the active end radical of poly( $\beta$ -PL), the

poly( $\beta$ -PL) side chains were grafted onto the polystyrene main chain.

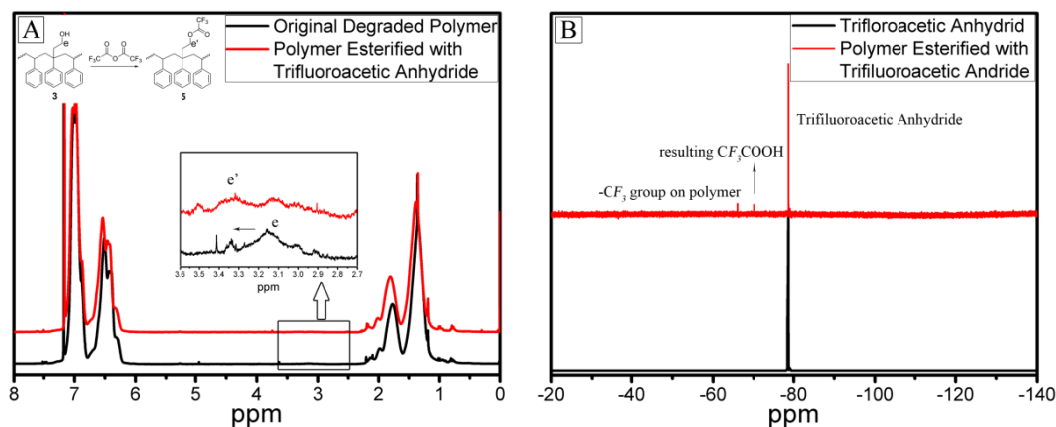
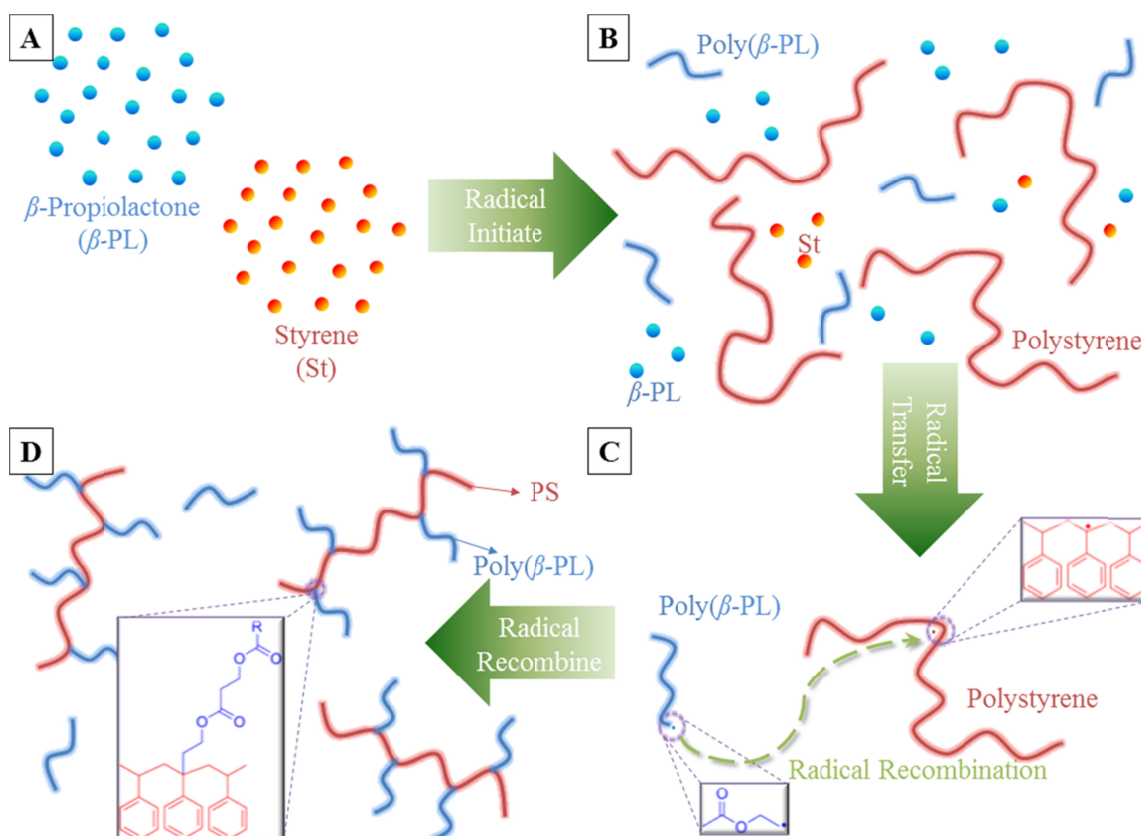


**Figure 2-3.** A) Comparison of  $^1\text{H}$  NMR spectra. Resulting  $\beta$ -PL-g-St copolymer after degradation and polymer after esterification with trifluoroacetic anhydride. B) Comparison of  $^{19}\text{F}$  NMR spectra: trifluoroacetic anhydride and polymer after esterification with trifluoroacetic anhydride.

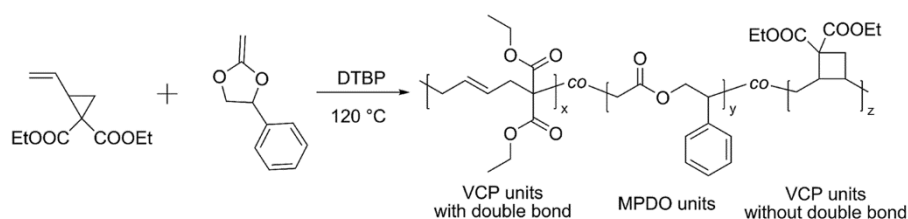


**Scheme 2-1.** Schematic process of  $\beta$ -PL–St copolymerization.

## 2.2 Designed Enzymatically Degradable APCNs by RROP

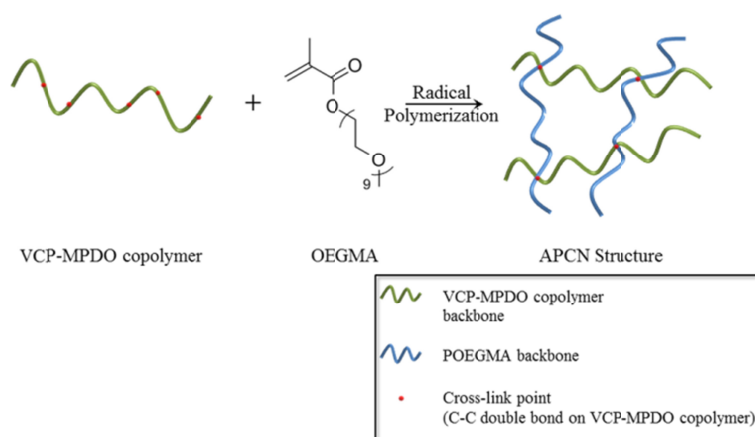
A different route to the preparation of enzymatically degradable amphiphilic conetworks (APCNs) based on unsaturated polyesters by RROP is presented in this chapter. In the first step, the unsaturated biodegradable polyesters were prepared by radical ring-opening copolymerization of vinylcyclopropane (VCP) and 2-methylene-4-phenyl-1,3-dioxolane (MPDO). The unsaturated units were used for cross-linking hydrophilic macromonomer (oligo(ethylene glycol) methacrylate, OEGMA) by radical polymerization in a second step for the formation of enzymatically degradable amphiphilic conetworks (APCNs). This method provides an interesting route for making functional biodegradable APCNs using radical chemistry in the future.

The unsaturated biodegradable polyesters with random distribution of cross-linkable double bonds and degradable ester units were prepared by radical ring-opening copolymerization of VCP and MPDO (Scheme 2-2). Very similar reactivity ratios ( $r_{VCP} = 0.23 \pm 0.08$  and  $r_{MPDO} = 0.18 \pm 0.02$ ), unimodal gel permeation chromatography (GPC) curves and 2D NMR technique showed the formation of random copolymers with unsaturation and ester units.



**Scheme 2-2.** Schematic process of radical ring-opening polymerization (RROP) of VCP and MPDO.

Based on the cross-linkable carbon-carbon double bonds and the almost random VCP-MPDO combination on the copolymer backbone (random distribution of ester units), the VCP-MPDO copolymers were copolymerized with OEGMA for the preparation of biodegradable amphiphilic conetworks (Scheme 2-3).



**Scheme 2-3.** Preparation of biodegradable amphiphilic conetworks. OEGMA = oligo(ethylene glycol) methacrylate,  $M_n \sim 500$  g/mol. Di-*tert*-butyl peroxide was used as initiator and reaction temperature was at 140 °C.

Due to the hydrophilic (HI) and hydrophobic (HO) microphase separation, the APCNs showed swelling in both water and organic solvents with different optical properties. The swelling ratios of all APCNs in water were smaller than in DMF. All APCNs showed a high transparency in DMF (Figure 2-4 top) due to the extension of both hydrophobic and hydrophilic parts. Because of the phase separation between the hydrophilic (POEGMA chains) and hydrophobic (VCP-MPDO copolymer) segments, the APCNs appeared opaque in water (Figure 2-4 below).

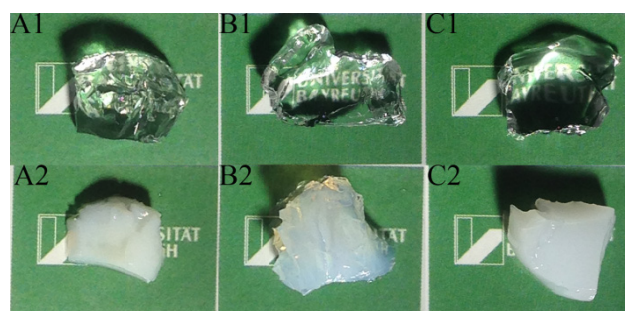


**Figure 2-4.** Photographs of APCNs swollen in different solvent. Top: Gels in DMF; below: Gels in H<sub>2</sub>O.

The degradability of APCNs was realized through cleavage of VCP-MPDO copolymer segments, which act as cross-linking chains in the APCNs. Because of their

amorphous nature, the VCP-MPDO copolymer chains of APCNs have a good degradability. The degradation of VCP-MPDO chain segments causes the release of soluble hydrophilic POEGMA segments, leading to a reduction in gel content (Figure 2-5).

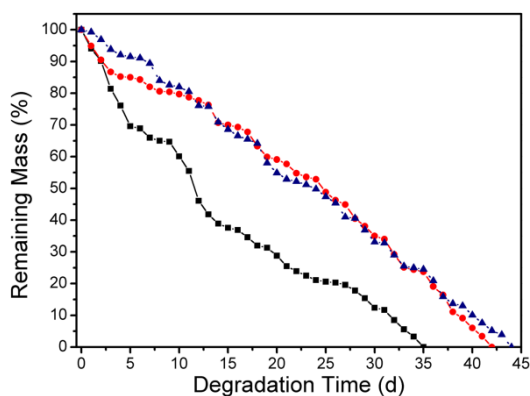
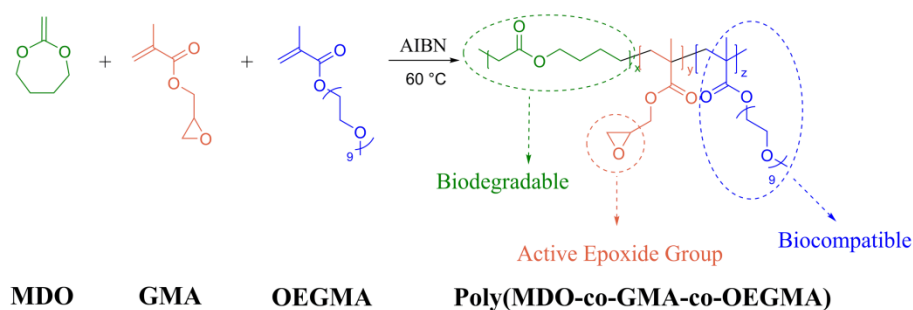


**Figure 2-5.** Mass loss of APCNs against enzyme (Lipase from *Pseudomonas cepacia*) in pH = 7 PBS buffer solution in dependence of degradation time.

## 2.3 Enzymatically Degradable DOPA-containing Polyester Based Adhesives by Radical Polymerization

A designed 3,4-dihydroxyphenylalanine (DOPA) containing enzymatic degradable non-toxic synthetic adhesive with good adhesion to soft tissue and metals made by a simple two-step reaction is presented in this chapter. Due to the high adhesive strength, enzymatic degradability and low toxicity, the material is a promising candidate for future studies as medical glue.

In the first step for DOPA containing polyester based adhesive preparation, a terpolymer of oligo(ethylene glycol) methacrylate (OEGMA), glycidyl methacrylate (GMA) and 2-methylene-1,3-dioxepane (MDO) was produced using radical polymerization (Scheme 2-4). The copolymers showed very high molar mass ( $> 1.0 \times 10^5$  g/mol). Yet, they were transparent viscous liquids.



**Scheme 2-4.** Schematic illustration of the synthesis of poly(OEGMA-co-GMA-co-MDO).

The epoxide ring of GMA in terpolymer was used for immobilisation of 3-(3,4-dihydroxyphenyl)propionic acid, DOPA-mimetic catechol group in the second step (Figure 2-6A). By comparing the UV/Vis spectra of resulting polymer and 3-(3,4-dihydroxyphenyl)propionic acid, it was obvious that the catechol group was immobilized on polymer as its characteristic peak was not changed (Figure 2-6B).

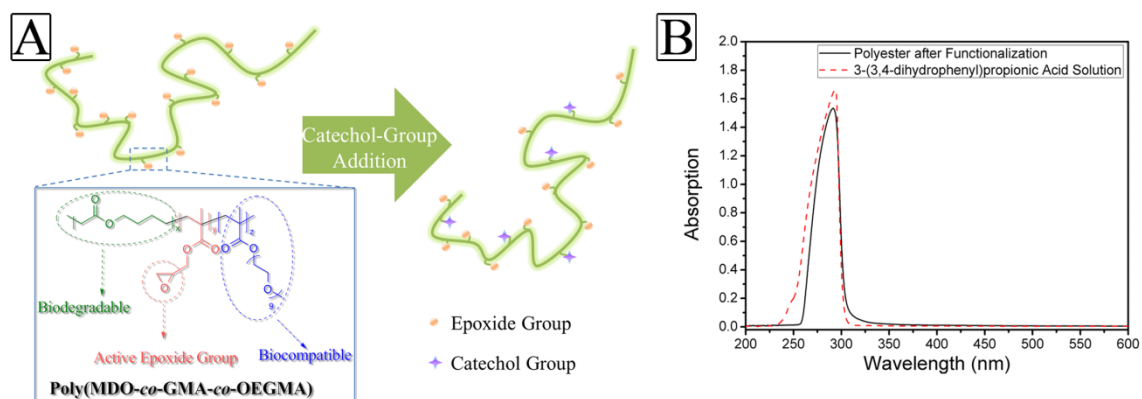


**Figure 2-6.** A: Schematic illustration of immobilization of catechol group onto poly(OEGMA-co-GMA-co-MDO) backbone. B: Comparison of UV/Vis spectra of catechol functionalized poly(OEGMA-co-GMA-co-MDO) (black) and 3-(3,4-dihydroxyphenyl)propionic acid (red) in THF.

For adhesive application, medical grade hydrogen peroxide (30% in water) or  $\text{Fe}(\text{acac})_3$  (10 wt% in water) were used as cross-linking agents. Fresh porcine skin was used as representative soft tissue for studying the adhesion property as determined by lap shear strength test measurement (Figure 2-7A). The adhesion properties with/without cross-linkers were shown in Figure 2-7B. The adhesive, which contained 15 mol% catechol group on backbone and cross-linked by  $\text{Fe}(\text{acac})_3$ , exhibited the best adhesive property. The lap adhesion strength value of our system was much greater than the existing medical adhesive CoSeal and fibrin glue obtained in the previous studies.

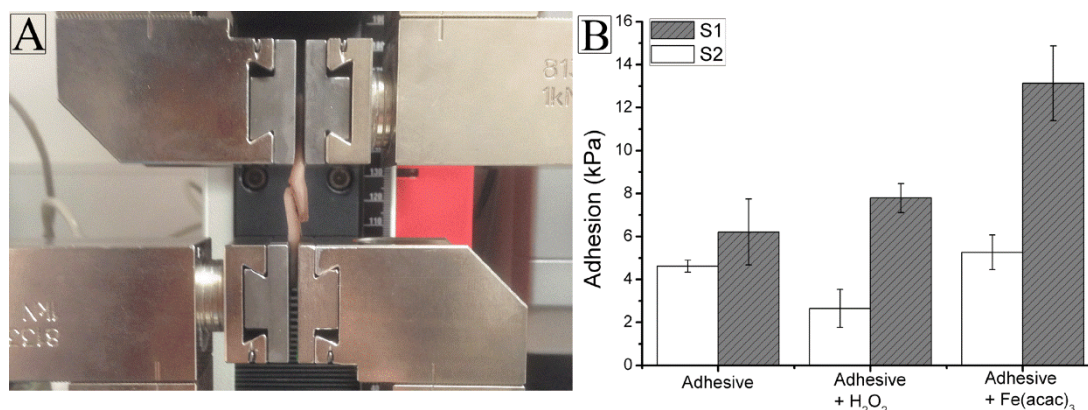


**Figure 2-7.** Adhesion test on porcine skin. A: photograph of lap shear strength test on fresh porcine skin. B: Adhesion properties of prepared adhesives with different cross-linking agents.

It was interesting to check the effect of PBS buffer on adhesion strength as these materials could be interesting as medical glue, and aluminium sheets were used for this test. The cross-linked adhesive showed good adhesion stability in pH 7 PBS buffer at 37 °C for at least one week (Figure 2-8).

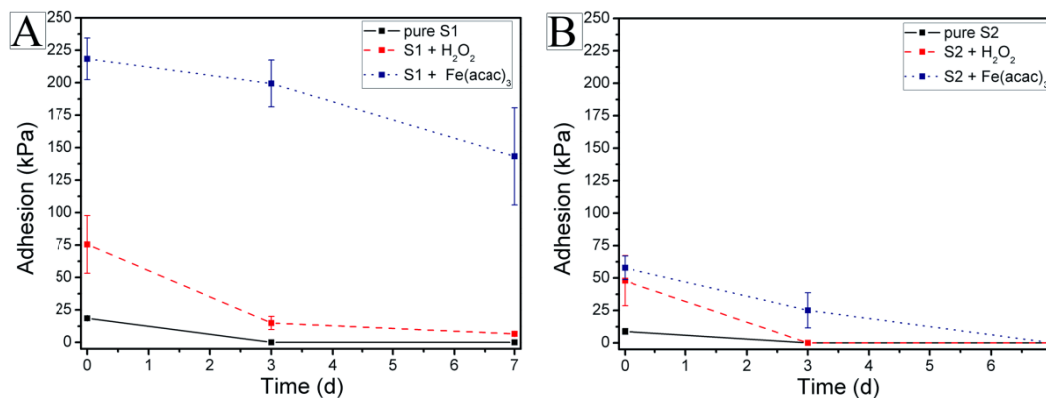


**Figure 2-8.** Lap shear strength of adhesives after placing in pH = 7 PBS buffer solution for different time.

The intended use of MDO in terpolymers was to provide enzymatically degradable ester linkages in the polymer backbone. Therefore, further enzymatic degradation studies were carried out using Fe(acac)<sub>3</sub> cross-linked sample in PBS buffer (pH = 7) in presence of lipase from *Pseudomonas cepacia*. It's obvious that the prepared adhesive could be degraded in the presence of lipase from *Pseudomonas cepacia* (Figure 2-9).

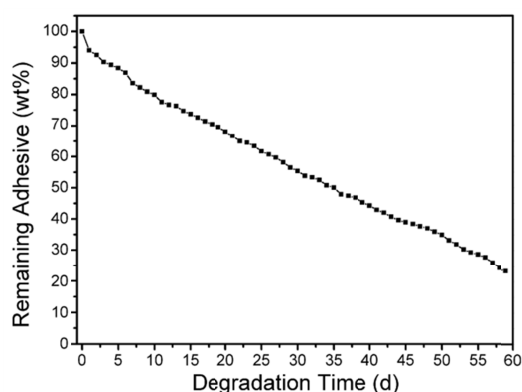
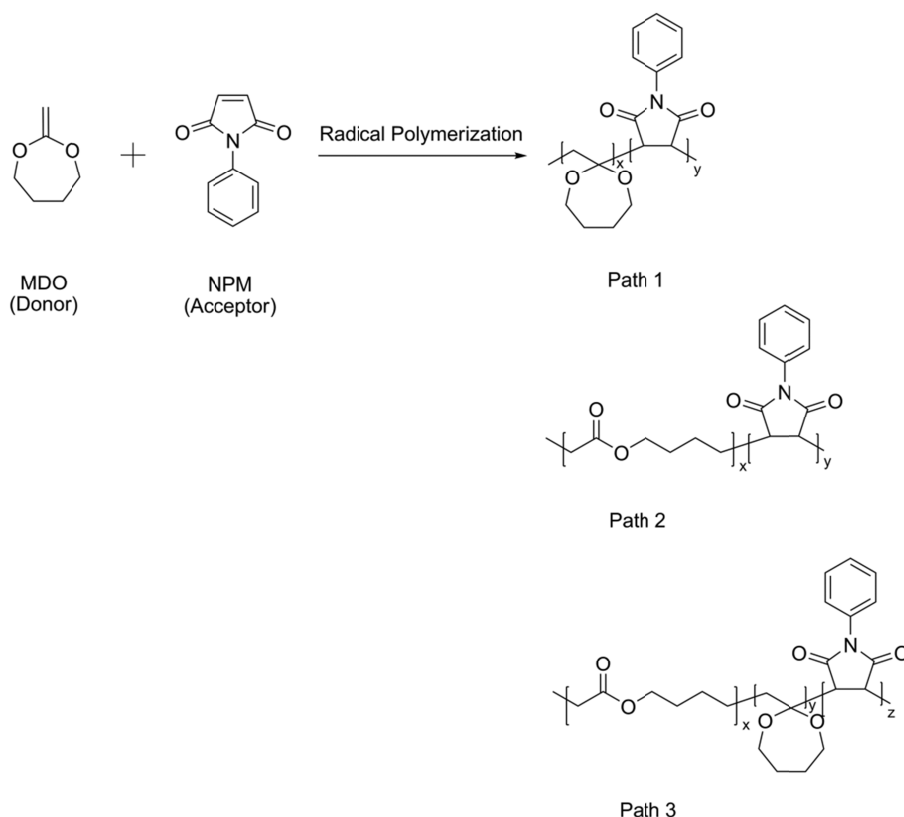


**Figure 2-9.** Mass loss profiles of adhesive S1 cross-linked by Fe(acac)<sub>3</sub>.

## 2.4 Thermally stable optically transparent copolymers with degradable ester linkages

The copolymers of 2-methylene-1,3-dioxepane (MDO) and *N*-phenyl maleimide (NPM) prepared by radical polymerization with high thermal stability, glass transition temperature and optical transparency are presented in this chapter. Formation of charge-transfer complex between MDO and NPM also led to the formation of high molar mass copolymers by simple mixing and heating of monomers without use of any initiator.

Various reactions for the copolymerization of MDO with NPM were carried out by changing the molar ratio of two monomers in feed at 60 °C and 120 °C. During copolymerization, MDO could undergo either ring-opening polymerization giving ester units, vinyl polymerization producing acetal rings or a combination of two (Scheme 2-5).



**Scheme 2-5.** Different possibilities during MDO-NPM copolymerization. Path 1: MDO copolymerized with ring-retained structure; Path 2: MDO copolymerized with ring-opened structure; Path 3: MDO copolymerized with ring-opened and ring-retained structure.

The microscopic structure of MDO-NPM copolymers was characterized by  $^1\text{H-NMR}$  (Figure 2-10A) and  $^{13}\text{C-NMR}$  (Figure 2-10B) with full assignments. All copolymers in  $^{13}\text{C-NMR}$  spectra showed the presence of ketal carbon at  $\delta = 100$  ppm due to ring-retained acetal units from MDO. Compared with the  $^1\text{H-NMR}$  spectrum of resulting copolymers prepared at  $60\text{ }^\circ\text{C}$  (Figure 2-10A, black curve), the peak at  $\delta = 4.0$  ppm in  $^1\text{H-NMR}$  spectrum due to the  $-\text{OCH}_2-$  protons of ester units formed by ring-opening of MDO during copolymerization at  $120\text{ }^\circ\text{C}$  was obvious (Figure 2-10A, red curve). For the copolymerization at  $120\text{ }^\circ\text{C}$ , on reducing the amount of MDO below 50 mol% in the initial feed, the amount of ring-opened MDO was strongly decreased and could not be determined with accuracy.

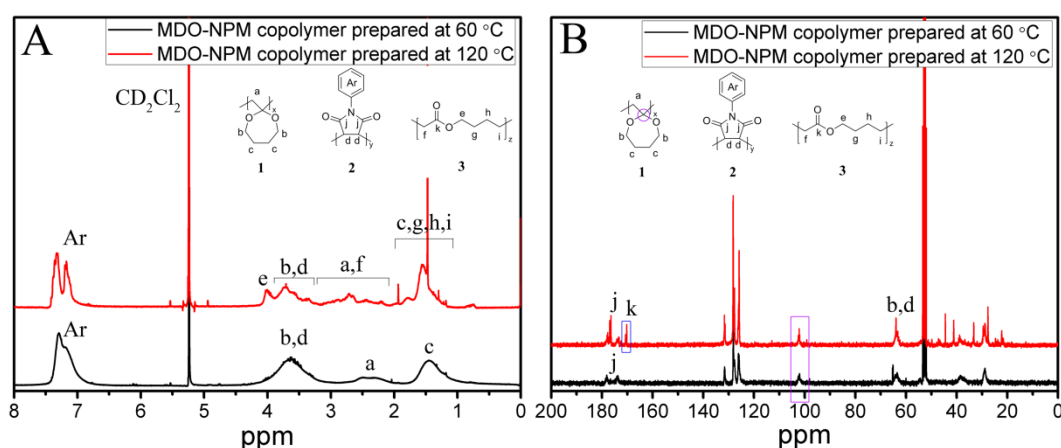


**Figure 2-10.**  $^1\text{H-NMR}$  and  $^{13}\text{C-NMR}$  spectra of MDO-NPM copolymer, monomer ratio of MDO:NPM = 7:3 in feed as an example. A:  $^1\text{H-NMR}$  and B:  $^{13}\text{C-NMR}$ , black curve: copolymerization at  $60\text{ }^\circ\text{C}$ , red curve: copolymerization at  $120\text{ }^\circ\text{C}$ .

The comonomer-copolymer composition curves for copolymerization at  $60$  and  $120\text{ }^\circ\text{C}$  were shown in Figure 2-11. The monomer reactivity ratios at different temperatures could be determined on the basis of comonomer-copolymer composition curves for the MDO and NPM copolymerization at  $60\text{ }^\circ\text{C}$  and  $120\text{ }^\circ\text{C}$ . These results also suggested the alternating copolymerization tendency of MDO and NPM at  $60\text{ }^\circ\text{C}$ .

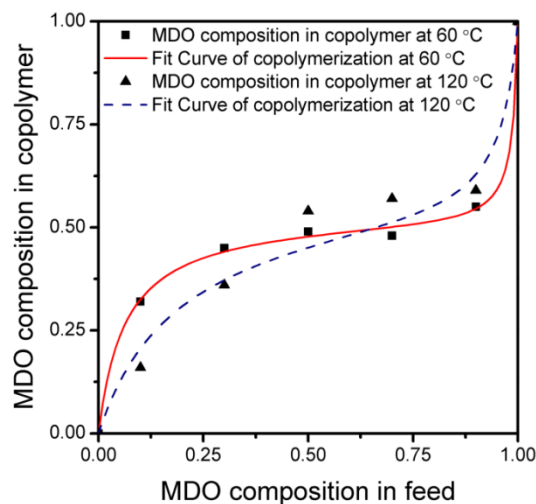


**Figure 2-11.** Comonomer-copolymer composition curves for the MDO and NPM copolymerization at different temperatures. Using nonlinear least-squares curve fitting method, the curve was drawn. Red curve: Fit curve of copolymerization at 60 °C; Navy curve: Fit curve of copolymerization at 120 °C. Copolymerization at 60 °C:  $r_{MDO} = 0.0241$ ,  $r_{NPM} = 0.1202$ ,  $R^2 = 0.998$ ; Copolymerization at 120 °C:  $r_{MDO} = 0.0839$ ,  $r_{NPM} = 0.3208$ ,  $R^2 = 0.972$ .

To get insight into the mechanism of polymerization, equimolar amounts of MDO and NPM were dissolved in  $CDCl_3$  and stirred under argon for 1 h. Due to formation of the MDO-NPM complex, the other proton signals of the MDO and NPM monomer also showed a small shift in the peaks in  $^1H$ -NMR spectrum (Figure 2-12). This result strongly suggested the interaction between the double bonds of MDO and NPM.

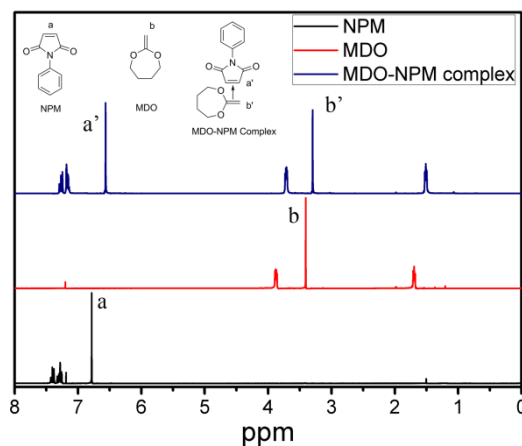


**Figure 2-12.** Comparison of  $^1H$ -NMR spectra of MDO-NPM complex with the monomer MDO and NPM.

The thermal stability of the MDO-NPM copolymers made by radical polymerization was performed by TGA analysis. All polymers were highly thermally stable (decomposition temperature was higher than 300°C). The glass transition temperatures for the copolymers prepared at 120°C were determined using DSC-technique. Due to this immiscible random structure of the resulting copolymer (*i.e.* block of ring-remained MDO-*co*-NPM and block of ring-opened MDO-*co*-NPM), two glass transition temperatures between the  $T_g$  of homopoly(NPM) and poly(MDO) with fully ring-opened structure were observed in the DSC curves (Figure 2-13A). The films of MDO-NPM copolymers with higher ester content were prepared using spin coating and showed a high transparency (Figure 2-13B).

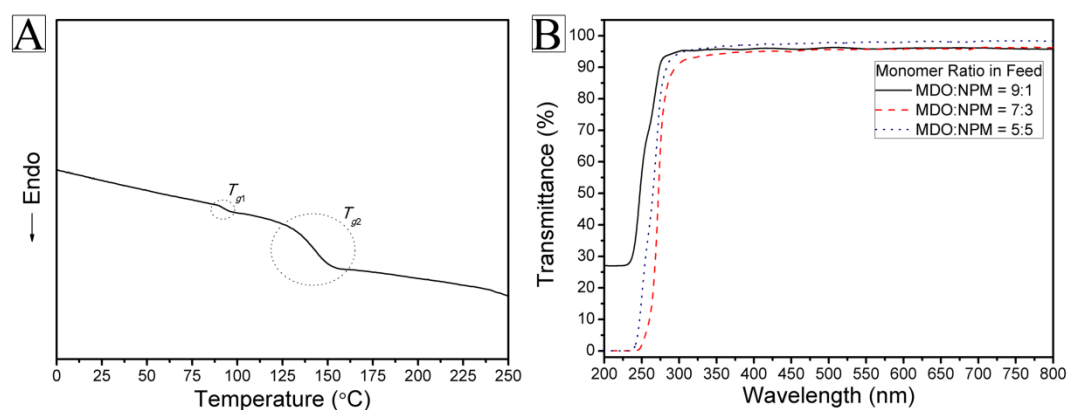


**Figure 2-13.** A: DSC trace of MDO-NPM copolymer (monomer ratio in feed: MDO:NPM = 5:5, reaction temperature: 120°C). B: UV-Vis transmittance spectra of MDO-NPM copolymer films prepared using spin coating, copolymerization temperature: 120°C.

## 2.5 Individual Contributions to Joint Publications

The results presented in his thesis were obtained in collaboration with others, and have been published or are submitted for publication as indicated below. In the following, the contributions of all the coauthors to the different publications are specified. The asterisk denotes the corresponding author.

### Chapter 3

This work is published in the journal *Chem. Eur. J.*, **2014**, *20*, 7419-7428, under the title:

**“A Rare Example of the Formation of Polystyrene-Grafted Aliphatic Polyester in One-Pot by Radical Polymerization”**

by Yinfeng Shi, Zhicheng Zheng, and Seema Agarwal\*

I designed concept, conducted all the experiments and wrote the publication, except that:

- Zhicheng Zheng was involved in scientific discussions and correcting the publication;
- Seema Agarwal was involved in designing concept, overall supervision, scientific discussions and correcting the publication.

### Chapter 4

This work is submitted to *Macromolecules* under the title:

**“Designed Enzymatically Degradable Amphiphilic Conetworks by Radical Ring-Opening Polymerization”**

by Yinfeng Shi, Holger Schmalz, and Seema Agarwal\*

I designed concept, conducted all the experiments and wrote the publication, except that:

- Holger Schmalz was involved in scientific discussions and correcting the publication;

- Seema Agarwal was involved in designing concept, overall supervision, scientific discussions and correcting the publication.

## Chapter 5

This work is submitted to *Macromolecules* under the title:

### **“Enzymatically Degradable DOPA-containing Polyester Based Adhesives by Radical Polymerization”**

by Yinfeng Shi, Peiran Zhou, Valérie Jérôme, Ruth Freitag, and Seema Agarwal\*

I designed concept, conducted all the experiments and wrote the publication, except that:

- Peiran Zhou assisted the synthesis of polyester based adhesives as a practical trainee in lab course.
- Valérie Jérôme and Ruth Freitag conducted the cytotoxicity measurements;
- Seema Agarwal was involved in designing concept, overall supervision, scientific discussions and correcting the publication.

## Chapter 6

This work is submitted to *e-polymers* under the title:

### **“Thermally stable optically transparent copolymers of 2-methylene-1,3-dioxepane and *N*-phenyl maleimide with degradable ester linkages”**

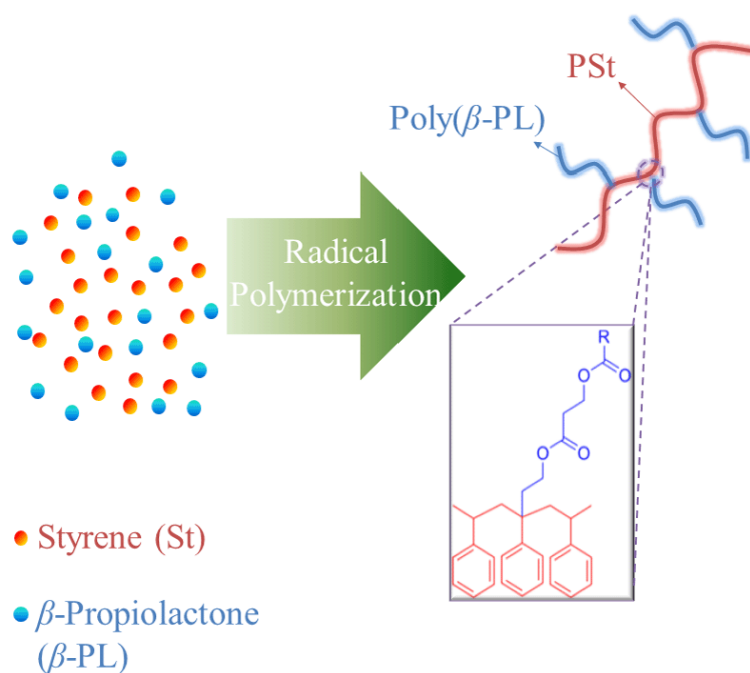
by Yinfeng Shi and Seema Agarwal\*

I designed concept, conducted all the experiments and wrote the publication, except that:

- Seema Agarwal was involved in designing concept, overall supervision, scientific discussions and correcting the publication.

## Chapter 3

### Formation of Polystyrene Grafted Aliphatic Polyester in One-Pot by Radical Polymerization



The results of this chapter have been published as:

“A Rare Example of the Formation of Polystyrene-Grafted Aliphatic Polyester in One-Pot  
by Radical Polymerization”

by Yinfeng Shi, Zhicheng Zheng, and Seema Agarwal\*

in *Chem. Eur. J.*, **2014**, *20*, 7419-7428.



### 3.1 Abstract

The radical copolymerization of cyclic ester  $\beta$ -propiolactone ( $\beta$ -PL) with styrene (St) at 120 °C, with a complete range of monomer ratios, is a rare example of a system providing graft copolymers (PSt-*g*- $\beta$ -PL) in one pot. The structure of the resulting  $\beta$ -PL-St copolymers was proven by using a combination of different characterization techniques, such as 1D and 2D NMR spectroscopy and gel permeation chromatography (GPC), before and after alkaline hydrolysis of the polymers. The number of grafting points increased with an increasing amount of  $\beta$ -PL in the feed. A significant difference in the reactivity of St and  $\beta$ -PL and radical chaintransfer reactions at the polystyrene (PSt) backbone, followed by combination with the active growing poly( $\beta$ -PL) chains, led to the formation of graft copolymers by a grafting-onto mechanism.



## 3.2 Introduction

Aliphatic polyesters are widely used as biomaterials for various biorelevant applications.<sup>1-5</sup> The synthesis of polyesters by conventional cationic, anionic, metal-catalyzed ring-opening polymerization of cyclic esters, and condensation polymerization of diols and diacids has already been studied in detail.<sup>2,4-7</sup> Recently, the number of reports regarding the synthesis of polyesters by radical ring-opening polymerization (RROP) has increased.<sup>8-17</sup> RROP provides an opportunity to introduce ester linkages onto a vinyl polymer backbone, providing novel hydrolysable functional materials based on vinyl monomers, simply by the copolymerization of cyclic ketene acetals (CKAs) with the corresponding vinyl monomers.<sup>11</sup> By using this method we have shown the formation of various degradable functional polymers, such as ionomers,<sup>15</sup> thermoplastic elastomers,<sup>18</sup> and polymers for gene transfection.<sup>19</sup>

$\beta$ -propiolactone ( $\beta$ -PL) is an interesting four-membered cyclic ester capable of undergoing not only cationic, anionic, and metal-catalyzed ring-opening polymerization, but also radical polymerization. The resulting polymer, poly( $\beta$ -propiolactone), is a biodegradable aliphatic polyester with good mechanical properties and biocompatibility.<sup>20</sup> The first radical polymerization of  $\beta$ -PL was reported by Ohse *et al.*<sup>21</sup>, without structural and mechanistic clarifications. Katayama *et al.*<sup>22</sup> provided the mechanism for RROP of  $\beta$ -PL, showing the formation of ester (-C(O)OCH<sub>2</sub>CH<sub>2</sub>-) repeat units. During copolymerization with vinyl monomers, such as acrylonitrile and styrene (St),  $\beta$ -PL showed a large difference in reactivity, with the formation of blocky statistical copolymers, possessing long blocks of the vinyl polymer separated by one ester unit from  $\beta$ -PL.<sup>22</sup> In an attempt to utilize free-radical copolymerization reactions of  $\beta$ -PL with vinyl monomers (e.g. styrene) for the formation of degradable functional polymers, we observed the formation of an unusual polymer architecture (graft copolymers (PSt-*g*- $\beta$ -PL)) in one step, depending upon the feed composition. Heating St and  $\beta$ -PL in the presence of a radical initiator at 120 °C provided graft copolymers for complete range

of monomer ratios. Herein, we report the detailed studies that were carried out to provide evidence of the polymer structure and the mechanism of polymerization.

It is well known that graft copolymers, including polymer brushes, are an important type of polymer architecture.<sup>23,24</sup> Normally, the main and side chains of graft copolymers have different chemical natures and compositions, resulting in special properties. Therefore, graft copolymers are used in a variety of applications in the fields of biomaterials, interfacial materials, thermoplastic elastomers, and medical applications, amongst others.<sup>25-33</sup> In general, three synthetic methods were developed to prepare graft copolymers: a) the “grafting-onto” approach, which is a coupling reaction of end-functional polymer side chains onto a random functional backbone; b) the “grafting-from” approach, in which a monomer is polymerized as side chains from multiple functional groups of main chain; and c) the “grafting-through” approach, in which the main chain is polymerized by macromonomers that are presynthesized as side chains.<sup>23,24,30,34-36</sup> Owing to the low cost and simplicity, graft copolymerization based on free-radical polymerization is particularly attractive.<sup>37-41</sup> The melt extrusion process was used to realize the grafting process for free-radical polymerization with vinyl monomers. However, this melt free-radical process requires a high processing temperature (usually higher than 180 °C), which could result in a low grafting degree of the monomer, severe cross-linking, or even thermal degradation of the polymer.<sup>37,38</sup> Besides these factors, the presynthesized main chain of the resulting graft copolymer is also required, making this method a multistep process.

Wilhelm *et al.*<sup>42</sup> have already reported the formation of polyesters grafted by polystyrene (PSt) by random copolymerization of styrene and the double bonds in the polyester chains by a grafting-through radical mechanism. The double bonds of unsaturated polyesters were copolymerized with styrene. The problems encountered during this synthesis were achieving high molecular weights, in particular high molecular weights of the PSt chains, and the occurrence of multigrafting reactions at the double bonds, leading to cross-linked products. In another approach, polyester-g-PSt was

made by host-guest chemistry based on the bis(m-phenylene)-32-crown-10/paraquat recognition motif by Gibson *et al.* A polyester host containing crown ether units in its main chain and a paraquat-terminated polystyrene guest were used to produce supramolecular graft copolymers.<sup>43</sup> PSt macromonomers with carboxyl groups were also used as comonomers in condensation with diols for the formation of polyester-g-PSt.<sup>44</sup> Recently, click chemistry has been used to synthesize aliphatic polyesters, such as poly(lactic acid-co-glycolic acid), grafted onto polystyrene in a multistep process. The azido-functionalized PSt main chain (PSt-N<sub>3</sub>) was produced by copolymerization of styrene and chlorostyrene by nitroxide-mediated radical polymerization, followed by the conversion of chlorine groups to azido groups. Propargyl-functionalized polyesters were produced by metal-catalyzed ring-opening polymerization, at 130 °C, in the presence of propargyl alcohol. Graft copolymers were then produced by an azide-alkyne click reaction and were used for making biocompatible microspheres for drug-release applications.<sup>45, 46</sup>

It is evident from the literature that the grafting of polyesters onto vinyl polymers, such as PSt, requires multistep procedures. Hence, the formation of graft copolymers of polyesters, by radical polymerization in one pot, avoiding cross-linking and thermal degradation could be highly advantageous. The present work highlights a rare example of the formation of PSt-g-aliphatic polyester in one pot by radical polymerization.

### 3.3 Results and Discussion

#### 3.3.1 Homopolymerization of $\beta$ -propiolactone

Initially, the behavior of the homopolymerization of  $\beta$ -PL under radical polymerization conditions at 120 °C was studied. Representative  $^1\text{H}$ -NMR and  $^{13}\text{C}$ -NMR spectra of poly( $\beta$ -PL) are shown in Figure 3-1. The characteristic proton signals of  $\beta$ -PL were observed and marked. In the  $^1\text{H}$  NMR spectrum, the triplet at  $\delta = 2.6$  ppm corresponds to the  $-\text{OCH}_2-$  group, and the triplet at  $\delta = 4.3$  ppm corresponds to the  $-\text{CH}_2\text{CH}_2\text{C}(\text{O})\text{O}-$  group (Figure 3-1A). The integral ratio of these two groups is exactly 1:1. In the  $^{13}\text{C}$  NMR spectrum, characteristic signals were found at  $\delta = 170$  ppm ( $-\text{C}=\text{O}$ ),  $\delta = 59$  ppm ( $-\text{OCH}_2-$ ), and  $\delta = 32$  ppm ( $-\text{CH}_2\text{CH}_2\text{C}(\text{O})\text{O}-$ ). During the radical polymerization at 120 °C, all reacted  $\beta$ -PL underwent ring-opening polymerization (Figure 3-1B) with low molar mass ( $M_w \approx 8200$ , characterized by GPC with refractive index (RI) detector, calibration with polylactide standard). The corresponding aliphatic polyester was semicrystalline with a glass transition temperature ( $T_g$ ) of -20 °C and a melting point of 67 °C (Figure 3-S1 in the Supporting Information). The radical ring-opening reaction of  $\beta$ -PL at 50 and 80 °C, using azobisisobutyronitrile (AIBN) and benzoylperoxide (BPO) initiators, was previously shown by Katayama *et al.*<sup>22</sup> and is described in Scheme 3-1.

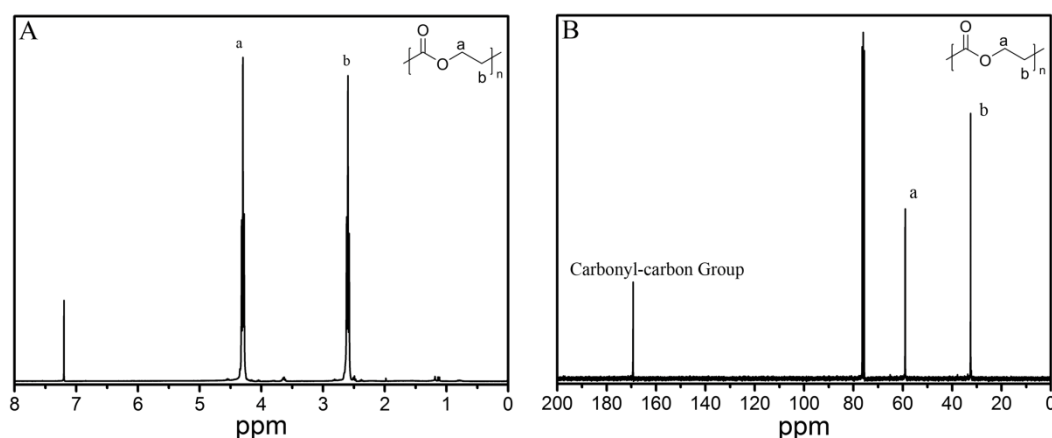
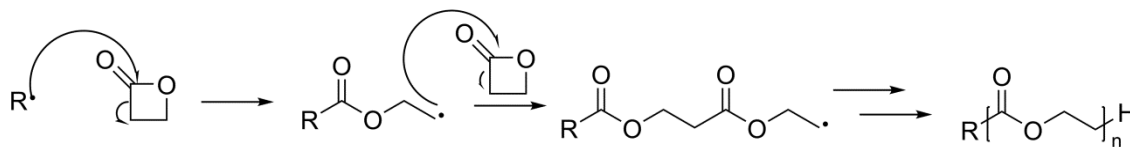


**Figure 3-1.** NMR spectra of  $\beta$ -PL homopolymer. A)  $^1\text{H}$  NMR spectrum; B)  $^{13}\text{C}$  NMR spectrum.



**Scheme 3-1.** Radical ring-opening mechanism of  $\beta$ -PL.<sup>22</sup>

### 3.3.2 Copolymerization of $\beta$ -propiolactone with styrene

Various copolymers of  $\beta$ -PL with St were produced by changing the molar ratio of the two monomers in the initial feed. The GPC trace for the reaction product of  $\beta$ -PL:St=1:2 was unimodal (solid curve in Figure 3-2) in comparison with other feed ratios of  $\beta$ -PL:St (1:1, 2:1, and 5:1). This result suggested the formation of polymer blends in reactions with an increased amount of  $\beta$ -PL in the feed.

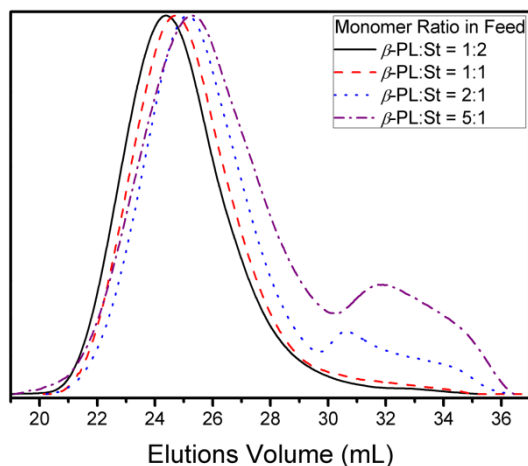


**Figure 3-2.** GPC traces of polymers prepared by radical polymerization at 120°C with different monomer ratios of  $\beta$ -PL and styrene in feed.

The two fractions of all the resulting polymer blends ( $\beta$ -PL:St=1:1, 2:1, and 5:1 in the feed composition) could be separated by using preparative GPC or Soxhlet extraction with methanol/ethyl acetate (50:1) as solvent. Through NMR analysis, the composition of the fractions could be studied. In the first fraction (the elution volume from 20 mL to 29 mL), the characteristic proton signals of both  $\beta$ -PL and St units were present in the  $^1\text{H}$ -NMR spectra, whereas in the second fraction (the elution volume from 30 mL to

34 mL), only the characteristic proton signals of homopoly( $\beta$ -propiolactone) existed (Figure 3-3). In conclusion, a blend with  $\beta$ -PL–St copolymer and homopoly( $\beta$ -propiolactone) was synthesized. The fractionated copolymers were used for further analysis.

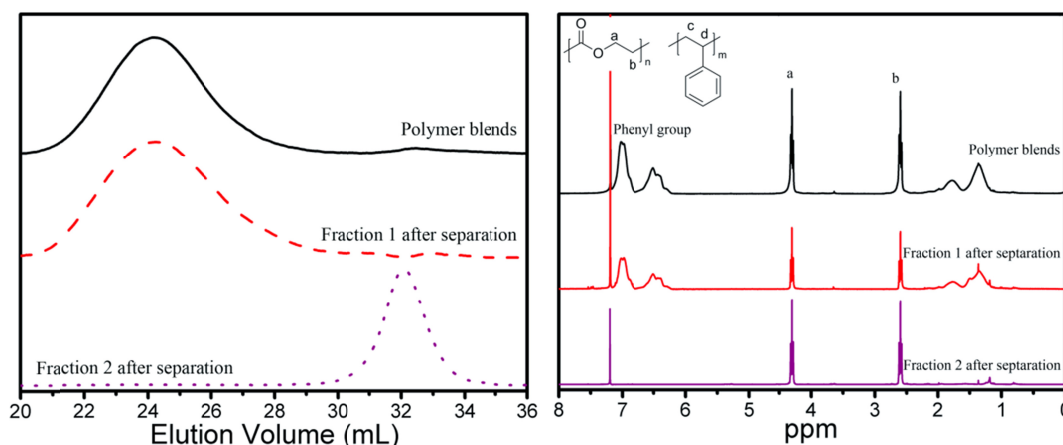


**Figure 3-3.** Separation of polymer blend prepared by radical copolymerization of styrene and  $\beta$ -PL at 120°C (monomer ratio of  $\beta$ -PL:St=1:1 in feed). Comparison of GPC traces before and after separation (left) and  $^1\text{H}$  NMR spectra of each fraction (right, original polymer (black); first fraction after separation (red); second fraction after separation (purple)).

The fractionated copolymers were analyzed by  $^1\text{H}$  NMR spectroscopy to investigate the copolymer composition. In the  $^1\text{H}$  NMR spectrum, the triplet peak at  $\delta = 2.6$  ppm corresponding to the  $-\text{OCH}_2-$  group from  $\beta$ -PL and the broad peaks from  $\delta = 6.2$  to 7.2 ppm corresponding to the phenyl group from St were observed. The peak integration of these signals was used for the determination of the copolymer composition. Although increasing the amount of  $\beta$ -PL incorporated into the copolymers was possible by increasing its amount in the initial feed, this increase also led to the formation of more homopoly( $\beta$ -PL) (Table 3-1); 0, 39, 48, and 73 mol% of reacted  $\beta$ -PL was converted to the homopolymer on changing the  $\beta$ -PL/St ratio in the feed to 1:2, 1:1, 2:1, and 5:1, respectively. The 1:2 ( $\beta$ -PL:St) feed composition provided 100% graft copolymers without impurities from homopoly( $\beta$ -PL), compared with 89, 82, and 51 wt% graft copolymers formed on changing the feed ratio to 1:1, 2:1, and 5:1, respectively. The

molar mass of the resulting copolymers after fractionation was analyzed by THF-GPC analysis with an RI detector and ranged from  $9.42 \times 10^4$  to  $1.65 \times 10^5$ . The polydispersity index (PDI) ranged from 1.6 to 1.9 (Table 3-1).

**Table 3-1.** Copolymerization data and reaction conditions for  $\beta$ -PL–St copolymers.<sup>a</sup>

Entry	Feed ratio [molar ratio]		Copolymer in blend <sup>b</sup> [wt%]	$M_w^c$	PDI	Polymer composition [molar ratio] <sup>d</sup>	
	$\beta$ -PL	St				$\beta$ -PL	St
1	1.0	2.0	100	$1.65 \times 10^5$	1.9	1.0	5.2
2	1.0	1.0	89	$1.40 \times 10^5$	1.6	1.0	2.8
3	2.0	1.0	82	$1.17 \times 10^5$	1.8	1.0	2.3
4	5.0	1.0	51	$9.42 \times 10^4$	1.7	1.0	1.1

<sup>a</sup> Initiator: Di-*tert*-butyl peroxide; 1 wt% of monomer; reaction temperature: 120 °C; reaction time: 20 h.

<sup>b</sup> Comparison of the copolymer composition of the blend (before fractionation) and the purified polymer (after fractionation) was used for this calculation. Characterized by <sup>1</sup>H NMR spectroscopy of the polymer blend and  $\beta$ -PL–St copolymers after separation.

<sup>c</sup> Characterized by GPC analysis with RI detector, calibration with PS standard.

<sup>d</sup> Characterized by <sup>1</sup>H NMR spectroscopy of  $\beta$ -PL–St copolymers after separation of homopoly( $\beta$ -PL).

More information about the polymer structure was gained by using 2D NMR spectroscopy techniques. Cross-peaks from HMBC correlation of the proton signal at 1.5 ppm with carbonyl-carbon group signal at 170 ppm were most informative (Figure 3-4, F). These peaks correspond to the coupling of the carbonylcarbon atoms of monomer  $\beta$ -PL with the backbone methylene groups of St. This finding confirmed the covalent linkage between  $\beta$ -PL and St units in the fractionated copolymer.

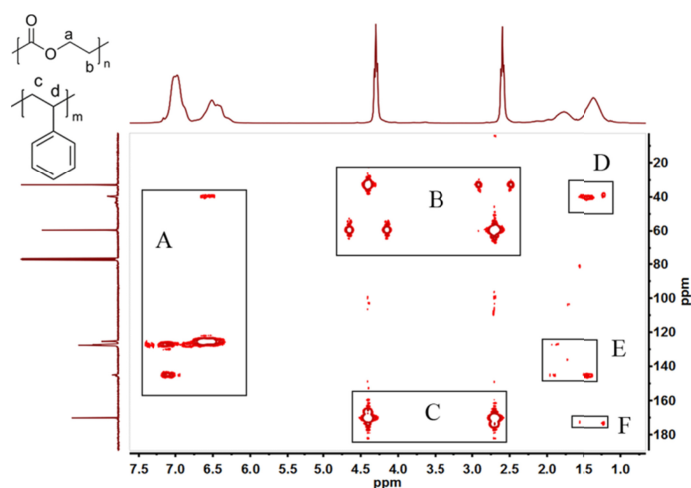


**Figure 3-4.** HMBC spectrum of  $\beta$ -PL–St copolymer (Table 1, entry 2): crosspeaks A) coupling between phenyl groups; B, C) coupling between groups a and b; D) coupling between groups c and d; E) coupling between phenyl groups and groups c, d; F) coupling between groups c and d from the styrene monomer and the carbonyl-carbon atom of monomer  $\beta$ -PL.

To gain insight into the microstructure of the copolymers, alkaline hydrolysis was carried out. Ester bonds resulting from ring opening of  $\beta$ -PL in the  $\beta$ -PL–St copolymers are hydrolytically unstable, causing a decrease in molar mass. NMR characterization of the copolymers could give an indication of the microstructure. For the  $\beta$ -PL–St copolymers with a copolymer composition of 1:2.3, 1:2.8 and 1:5.2 ( $\beta$ -PL/St; Table 1, entries 1–3), the  $^1\text{H}$  NMR spectra of the remaining polymer after degradation showed the presence of only styrene signals (Figure 3-5). This suggested the degradation of all the ester groups on the  $\beta$ -PL–St copolymer chains. Surprisingly, there was no significant difference between the elution volumes and the relative molar mass of the remaining polymers after degradation and the original  $\beta$ -PL–St copolymers as determined against polystyrene standards by using an RI detector (Table 3-2). Katayama *et al.*<sup>22</sup> reported a huge reactivity difference and temperature-dependent reactivity between  $\beta$ -PL and styrene (reactivity ratios ( $r$ ) were:  $r_{\text{st}} = 32$ ;  $r_{\beta\text{-PL}} = 0$  at  $80^\circ\text{C}$  using BPO as the initiator, and  $r_{\text{st}} = 6.2$ ;  $r_{\beta\text{-PL}} = 0$  at  $50^\circ\text{C}$  using AIBN as the initiator), with the formation of long blocks of styrene separated by single ester units (from RROP of  $\beta$ -PL during copolymerization) without clear evidence of copolymerization. The degradation results carried out in our work ruled out the formation of statistical block-type copolymers from  $\beta$ -PL and St at

120°C.  $\beta$ -PL and St seemed to be an interesting system that could provide different macromolecular architectures owing to the huge change in the reactivity of the two co-monomers with temperature. In this situation, the absolute molar mass of the polymers could be interesting and was determined by gel permeation chromatography with multi-angle laser light scattering (GPC-MALLS).

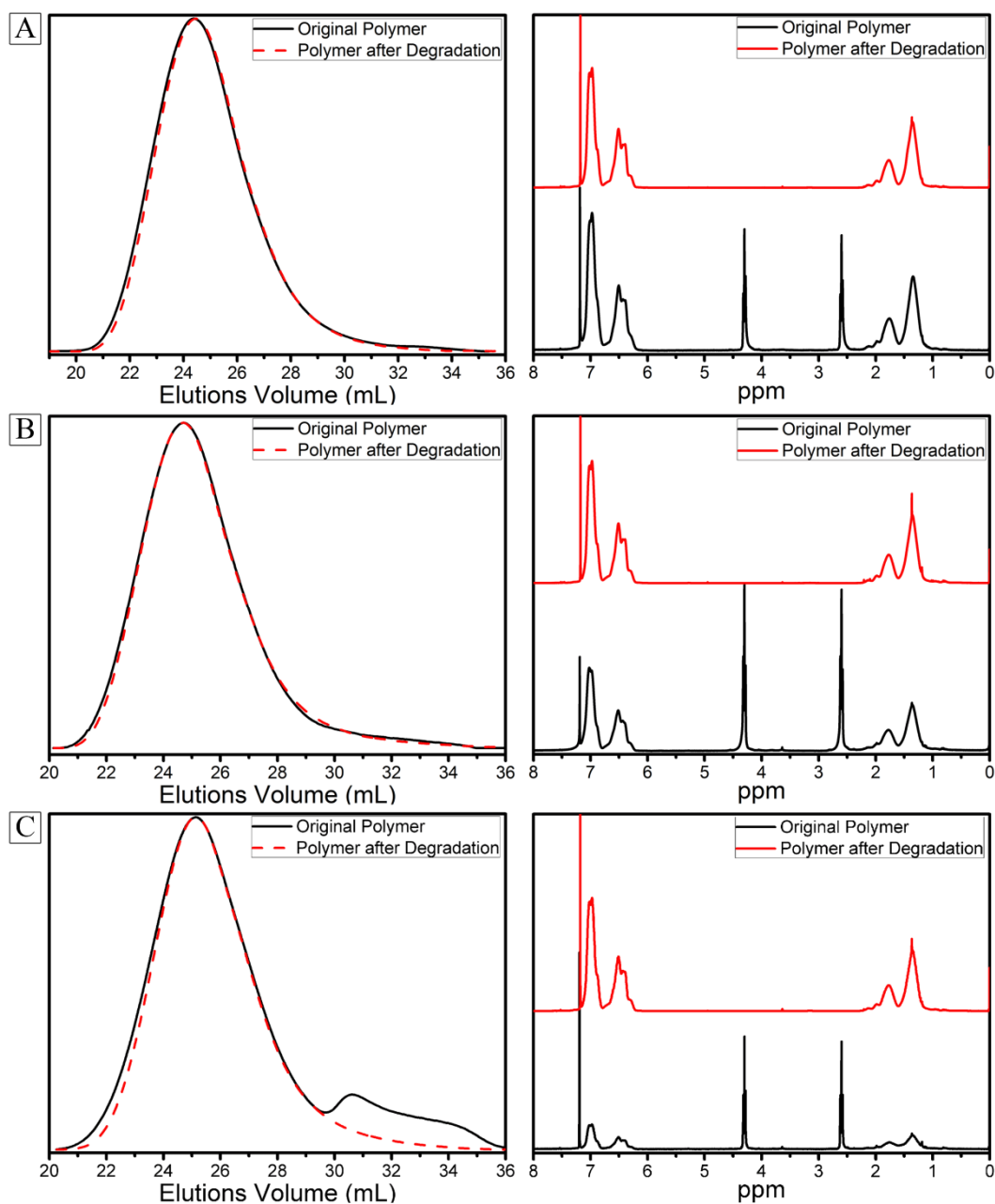


**Figure 3-5.** Degradation behavior of  $\beta$ -PL–St copolymers. Comparison of the relative GPC traces (left) and comparison of the  $^1\text{H}$  NMR spectra (right; bottom spectrum shows original polymer, top spectrum shows polymer after degradation); Monomer ratio in the feed: A)  $\beta$ -PL:St=1:2 (Table 3-1, entry 1); B)  $\beta$ -PL:St=1:1 (Table 3-1, entry 2) ; C)  $\beta$ -PL:St=2:1 (Table 3-1, entry 3).

The copolymers showed a higher absolute molar mass ( $M_{w,MALLS}$ ) than the relative molar mass ( $M_{w,GPC}$ ) determined by using an RI detector against polystyrene standards (Table 3-2) Whereas the degraded polymers had similar absolute  $M_{w,MALLS}$  and relative  $M_{w,GPC}$ , showing the presence of branched structures from  $\beta$ -PL. After 24h hydrolysis, the ester side chains were degraded. From the results of GPC-MALLS, the absolute molar mass was indeed decrease after degradation (Table 3-2). After degradation, the remaining polymers were linear (polystyrene), which had an absolute molar mass  $M_{w,MALLS}$  similar to the relative molar mass  $M_{w,GPC}$  (against PS standards). These results confirmed that the copolymers were graft copolymers, in which  $\beta$ -PL chains were grafted onto the PS backbone.

**Table 3-2.** Molar mass of  $\beta$ -PL–St copolymers and remaining polymers after degradation.<sup>a</sup>

Entry	Polymer composition		Molar mass of $\beta$ -PL–St copolymers		Molar mass of remaining polymers after degradation	
	[molar ratio] <sup>b</sup>		$M_{w,GPC}$ <sup>c</sup>	$M_{w,MALLS}$ <sup>d</sup>	$M_{w,GPC}$ <sup>c</sup>	$M_{w,MALLS}$ <sup>d</sup>
	$\beta$ -PL	St				
1	1.0	5.2	$1.65 \times 10^5$	$1.88 \times 10^5$	$1.58 \times 10^5$	$1.68 \times 10^5$
2	1.0	2.8	$1.40 \times 10^5$	$1.72 \times 10^5$	$1.36 \times 10^5$	$1.32 \times 10^5$
3	1.0	2.3	$1.17 \times 10^5$	$1.50 \times 10^5$	$1.11 \times 10^5$	$1.08 \times 10^5$

<sup>a</sup> Same as entry 1–3 in Table 1.

<sup>b</sup> Characterized by <sup>1</sup>H NMR spectroscopy of  $\beta$ -PL–St copolymers after separation.

<sup>c</sup> Characterized by relative THF-GPC analysis with RI detector, calibration with PS standard.

<sup>d</sup> Characterized by GPC analysis with multi-angle light scattering (GPC-MALLS).

The copolymer synthesized by using a higher amount of  $\beta$ -PL monomer in the feed composition ( $\beta$ -PL:St=5:1; Table 3-1, entry 4) showed a slight decrease in relative molar mass  $M_{w,GPC}$  (against PS standards) after alkaline hydrolysis (Figure 3-6). This result raised a question regarding the microstructure of the copolymer changing to that of a statistical copolymer, with or without  $\beta$ -PL graft, on increasing the amount of  $\beta$ -PL in the feed. The microstructure of the resulting  $\beta$ -PL–St copolymer with the monomer ratio of  $\beta$ -PL:St=5:1 in feed was confirmed by comparing the degradation behavior of the copolymers made at different time intervals.  $\beta$ -PL and St were copolymerized with the

monomer ratio of  $\beta$ -PL:St=5:1 in feed at 120°C with a reaction time of 12 min. The resulting polymer was analyzed by THF-GPC analysis and  $^1\text{H}$  NMR spectroscopy and then degraded by cleaving the ester bond in the polymer chains. The  $^1\text{H}$  NMR spectrum of the remaining polymer showed that only St-units existed, whereas there was no shift in the GPC peak on comparison of the original  $\beta$ -PL–St copolymer (elution volume from 22–32 mL) and the remaining polymer (Figure 3-7). This result confirmed that  $\beta$ -PL and St were also copolymerized as a graft copolymer with the monomer ratio of  $\beta$ -PL:St = 5:1 in feed. With the increase in the amount of  $\beta$ -PL in feed, its amount in the copolymer grafts also increased (copolymer composition  $\beta$ -PL:St = 1:1.1) and led to the change in the hydrodynamic volume compared with the polystyrene backbone, thereby showing a slight decrease in molar mass after degradation. In conclusion, the monomer  $\beta$ -PL could be graft copolymerized as the side chain on the polystyrene main chain. The resulting  $\beta$ -PL–St graft copolymer had a similar elution volume as the original linear polystyrene.

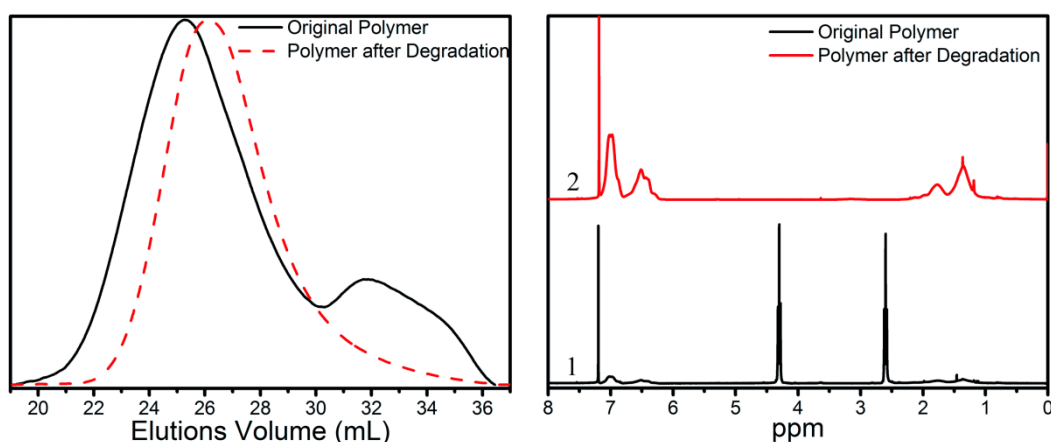


**Figure 3-6.** Degradation behavior of  $\beta$ -PL–St copolymer (Table 3-1, entry 4). Comparison of the GPC traces (right) and comparison of the  $^1\text{H}$  NMR spectra (left; bottom spectrum (1) shows original polymer, top spectrum (2) shows polymer after degradation).

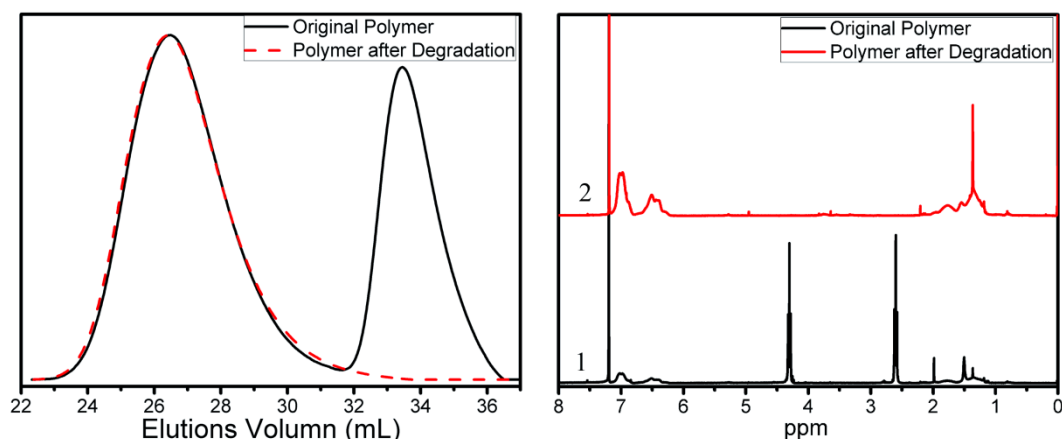


**Figure 3-7.** Degradation behavior of  $\beta$ -PL–St copolymer ( $\beta$ -PL:St = 5:1 in feed, reaction temperature: 120°C, reaction time: 12 min). Comparison of the GPC traces (right) and comparison of the  $^1\text{H}$  NMR spectra (left; bottom spectrum (1) shows original polymer, top spectrum (2) shows polymer after degradation).

The time-dependent consumption of the two co-monomers by  $^1\text{H}$  NMR spectroscopy showed a significant reactivity difference between the St and  $\beta$ -PL monomers for all feed compositions (Figure 3-8). The consumption of styrene monomer was much faster than that of  $\beta$ -PL. For the feed composition with more styrene ( $\beta$ -PL:St=1:2), 50% of the styrene monomer was already consumed before  $\beta$ -PL started to polymerize (Figure 3-8A; left). The GPC curves remained unimodal all throughout the reaction for this particular composition, although  $\beta$ -PL started to be consumed after around 90 min of polymerization (Figure 3-8A; right). On increasing the amount of  $\beta$ -PL in the feed, bimodality with a low molar mass fraction (homopoly( $\beta$ -PL)) appeared at low reaction times in GPC (Figure 3-8B, 3-8C). The fraction of homopoly( $\beta$ -PL) decreased with time, although the consumption of  $\beta$ -PL increased. Time-dependent characterization of the polymers and GPC studies, before and after alkaline degradation, clearly suggested the formation of polystyrene followed by grafting of  $\beta$ -PL.

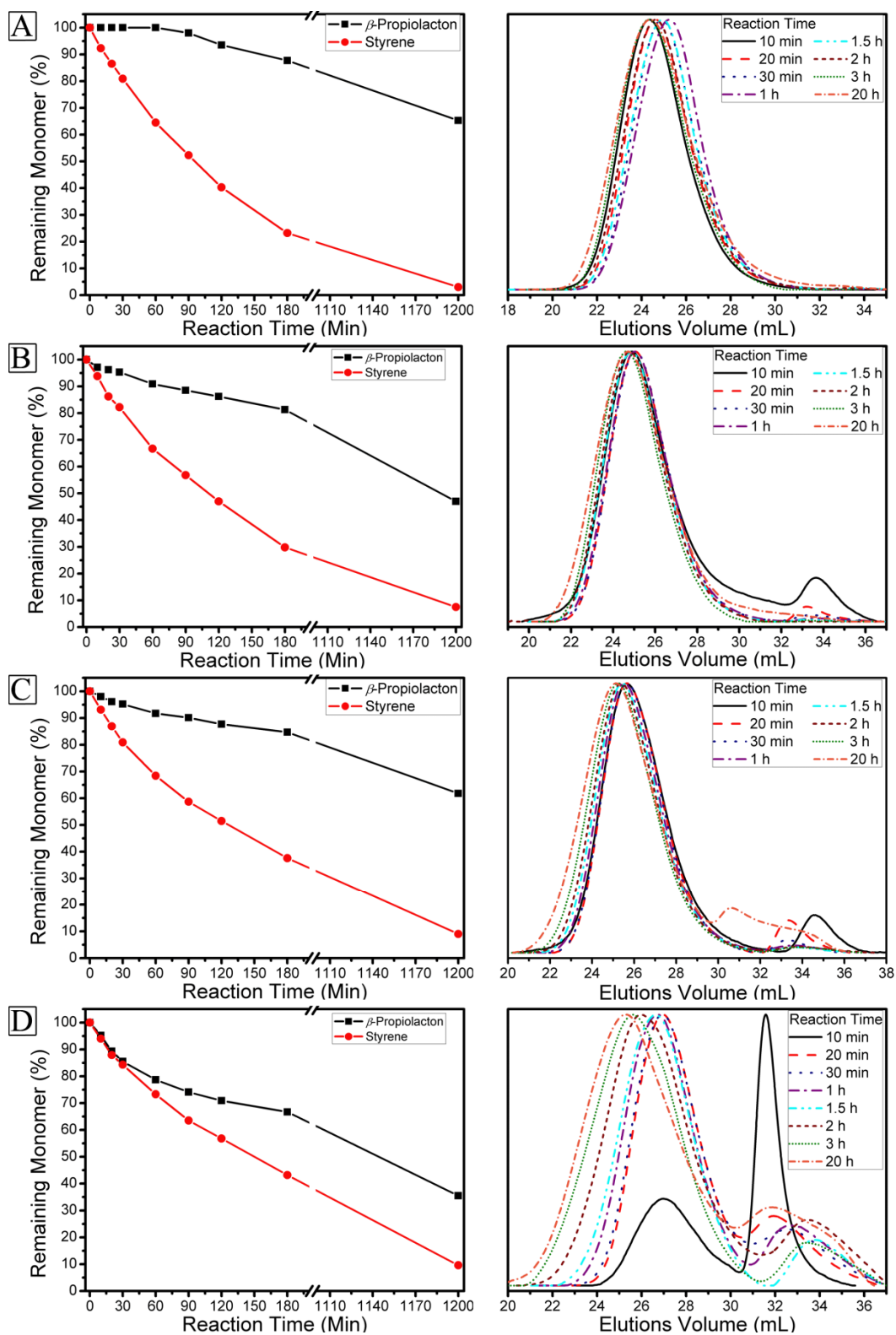


**Figure 3-8.** Kinetic study of  $\beta$ -PL-St copolymerization. Monomer consumption versus time for the copolymerization (left) and GPC traces with different reaction times (right). Monomer ratio in feed: A)  $\beta$ -PL:St=1:2; B)  $\beta$ -PL:St=1:1; C)  $\beta$ -PL:St=2:1; D)  $\beta$ -PL:St=5:1.

In free-radical polymerization, grafting can occur only if chain transfer to the dead polymer chains is possible. Therefore, a blank reaction for the polymerization of  $\beta$ -PL in the presence of a presynthesized polystyrene (by anionic polymerization,  $M_{w, GPC} = 20300$ ) was carried out at 120 °C. The GPC trace of the resulting polymer showed bimodality (Figure 3-9, dashed line). The fraction with lower molecular weight (elution volume from 33 to 36 mL; homopoly( $\beta$ -PL)) was removed through dialysis (Figure 3-9, dotted line). There was no difference between the elution volume of the resulting polymer and the original polystyrene (Figure 3-9), whereas the absolute molar mass, as determined by  $M_{w, MALLS}$ , was increased to 48200 (characterized by GPC-MALLS) on polymerization with  $\beta$ -PL. The characteristic proton signals of both the  $\beta$ -PL and St units were present in the NMR spectrum of the resulting purified copolymer. The purified copolymer was further analyzed by using 2D NMR techniques. Cross-peaks from HMBC correlation of the proton signal at 1.5 ppm with carbonylcarbon signal at 170 ppm existed (Figure 3-10). This correlation could be due to chain-transfer reactions leading to the generation of radicals at the polystyrene backbone, and subsequent grafting of  $\beta$ -PL. Chain-transfer reactions at polystyrene backbones, leading to branched structures with high conversions have been reported previously.<sup>47</sup>

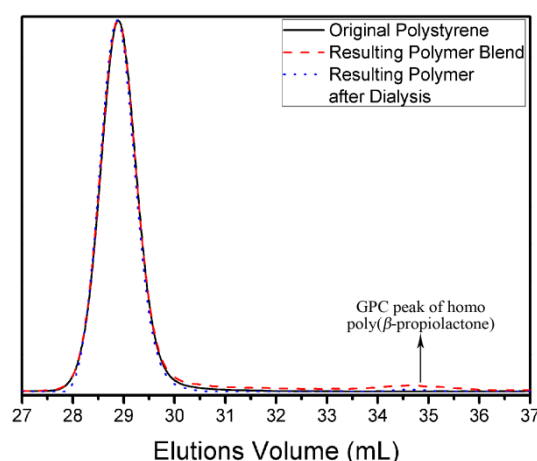


**Figure 3-9.** GPC traces of the resulting polymer from  $\beta$ -PL graft copolymerization with polystyrene, including original polystyrene (solid line), resulting polymer blend (dashed line), and resulting polymer purified by dialysis (dotted line).

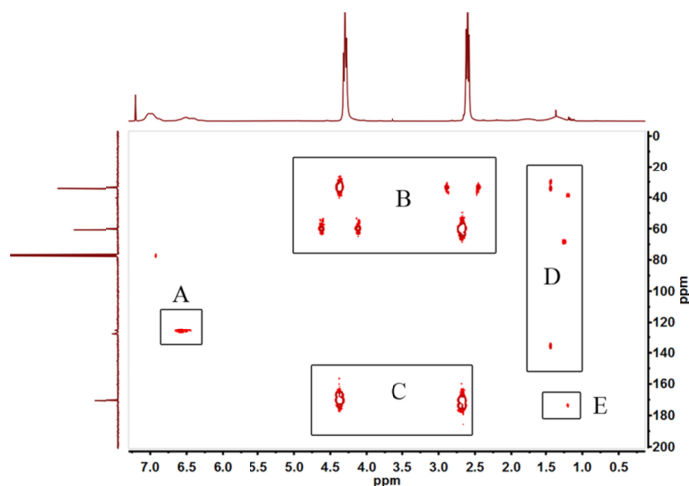
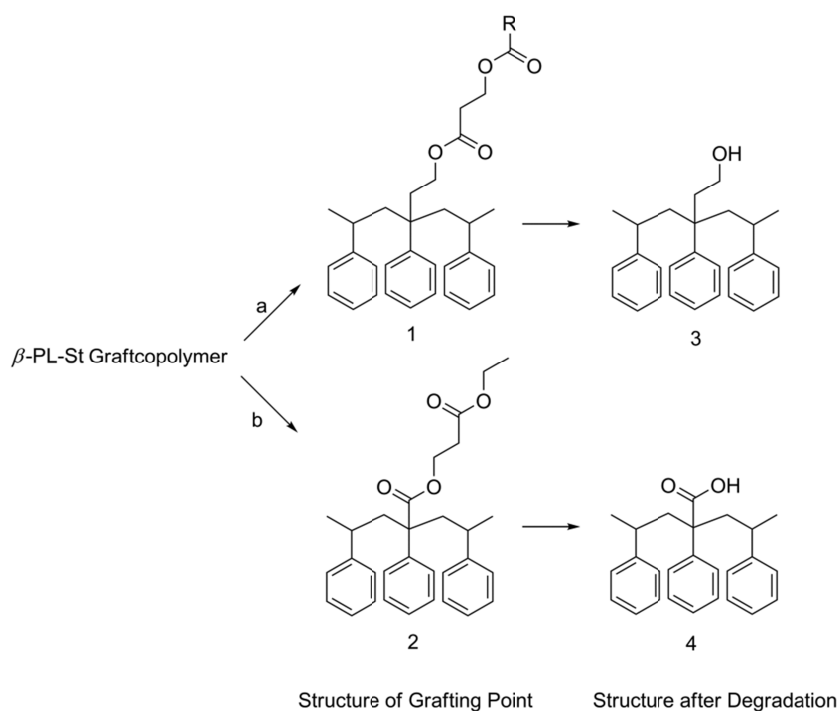


**Figure 3-10.** HMBC spectrum of the resulting polymer from  $\beta$ -PL polymerization with polystyrene. Cross-peaks A) coupling between phenyl groups; B, C) coupling between groups from monomer  $\beta$ -PL; D) coupling between alkyl groups of polystyrene; E) coupling between carbonyl-carbon atom of monomer  $\beta$ -PL and alkyl groups from polystyrene.

### 3.3.3 Mechanism study of $\beta$ -PL–St copolymerization

There could be different possibilities of grafting of  $\beta$ -PL onto PSt chains, as shown in Scheme 3-2. One possibility is coupling of the side chain poly( $\beta$ -PL) onto the polystyrene main chain by a grafting-onto mechanism (Scheme 3-2, route a). During the polymerization process, the chain-transfer reaction could lead to the formation of radicals at the PSt backbone, and by radical combination the growing poly( $\beta$ -PL) could be grafted onto the polystyrene main chain. After degradation of poly( $\beta$ -PL), the remaining end group at the grafting sites would be a hydroxyl group (Scheme 3-2, 3). Another possibility is that the side chain poly( $\beta$ -PL) could be coupled on the polystyrene main chain by a grafting-from mechanism (Scheme 3-2, route b). The radical generated at the PSt backbone due to chain-transfer reactions could start RROP of  $\beta$ -PL. After degradation of poly( $\beta$ -PL), the remaining end group at the grafting sites would be an acid group (Scheme 3-2, 4).



**Scheme 3-2.** Different possibilities for the structure of the  $\beta$ -PL-*g*-St copolymer at the grafting point. a) grafting-onto approach; b) grafting-from approach.

We designed a reaction to define the polymer structure at the grafting point. The degraded polymer was esterified with trifluoroacetic anhydride. The  $^1\text{H}$  NMR spectrum of the polymer after esterification was compared with the spectrum of the originally degraded polymer. The magnified inset in Figure 3-11A shows a characteristic proton signal at  $\delta = 2.90\text{-}3.35$  ppm, which is assigned to the  $-\text{CH}_2\text{OH}$  group (e) from the originally degraded polymer. Furthermore, after trifluoroacetic anhydride esterification, the protons from the  $-\text{CH}_2\text{OOCF}_3$  group shifted to  $\delta = 3.10\text{-}3.55$  ppm (assigned to group e'; see Figure 3-11 A). The  $^{19}\text{F}$  NMR spectrum of the polymer after esterification was compared with the spectrum of trifluoroacetic anhydride (Figure 3-11 B). A characteristic fluorine signal of the  $-\text{CH}_2\text{OOCF}_3$  group from the esterified polymer is present at  $\delta = -66.01$  ppm, and the fluorine signal of resulting  $\text{CF}_3\text{COOH}$  is present at  $\delta = -70.05$  ppm. The polymer structure at the grafting point was confirmed as structure **1** (Scheme 3-2), formed by the coupling of active poly( $\beta$ -PL) chains with radicals generated at the PSt backbone by transfer reactions (Scheme 3-2, route a).

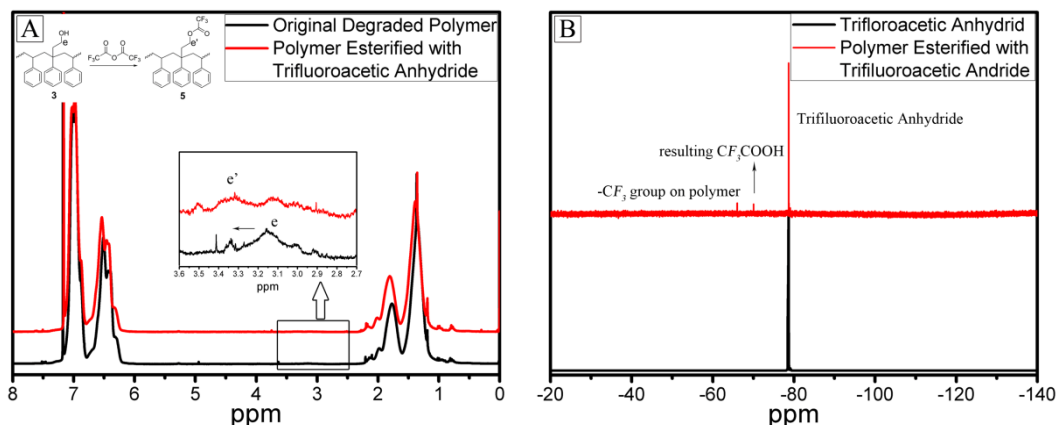


**Figure 3-11.** A) Comparison of  $^1\text{H}$  NMR spectra (300 MHz, 2048 scans). Resulting  $\beta\text{-PL-g-St}$  copolymer after degradation (lower spectrum; see Table 3-1, entry 2) and polymer after esterification with trifluoroacetic anhydride (top). B) Comparison of  $^{19}\text{F}$  NMR spectra: trifluoroacetic anhydride (lower spectrum) and polymer after esterification with trifluoroacetic anhydride (top).

Through comparing the peak integral ratios for  $\delta = 6.0\text{--}7.2$  ppm (corresponding to the phenyl group) and  $\delta = 3.1\text{--}3.6$  ppm (corresponding to the  $-\text{CH}_2\text{OH}$  end group after degradation) in the  $^1\text{H}$  NMR spectra of the  $\beta\text{-PL-St}$  copolymers after degradation, the number of grafting points could be calculated. From the composition of the  $\beta\text{-PL-St}$  copolymer, the molecular weight of the copolymer after degradation and the number of grafting points, the chain length of the polystyrene main chain and poly( $\beta\text{-PL}$ ) side chain could be calculated (Table 3-3). On increasing the amount of  $\beta\text{-PL}$  monomer in feed, the number of grafting points on the graft copolymer main chain also increased. Since the integration area of the peak at  $\delta = 3.1\text{--}3.6$  ppm (corresponding to the  $-\text{CH}_2\text{OH}$  end group after degradation) was very small, an error in this calculation cannot be ruled out. The molecular weight ( $M_n$ ) of the side chains was around 3000, which is similar to the molecular weight of poly( $\beta\text{-PL}$ ) prepared under homo radical-polymerization conditions. The grafted copolymers showed thermal phase transitions of both poly( $\beta\text{-PL}$ ) and polystyrene with two glass transitions at  $-18$  to  $-19$   $^\circ\text{C}$  and  $102$  to  $103$   $^\circ\text{C}$  from poly( $\beta\text{-PL}$ ) and polystyrene respectively and a melting point of  $72\text{--}77$   $^\circ\text{C}$  for poly( $\beta\text{-PL}$ ) (Figure 3-S1 in the Supporting Information).

**Table 3-3.** Data for  $\beta$ -PL-*g*-St Copolymer.<sup>a</sup>

Entry	Composition [molar ratio] <sup>b</sup>		Average number of grafting points <sup>c</sup>	$P_n$	
	$\beta$ -PL	St		PSt main chain <sup>d</sup>	poly( $\beta$ -PL) side chain <sup>e</sup>
1	1.0	5.2	5	1490	57
2	1.0	2.8	8	1308	58
3	1.0	2.3	9	1067	52
4	1.0	1.1	21	684	30

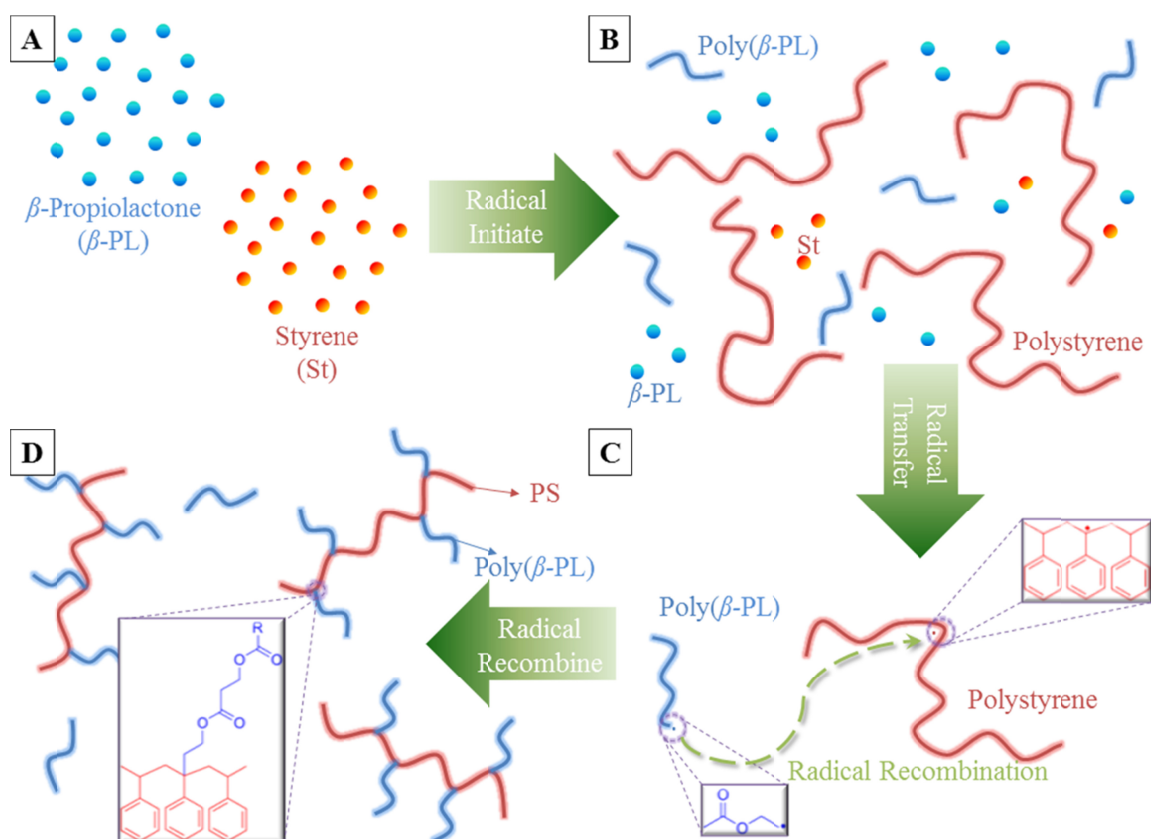
<sup>a</sup> Same as entry 1–4 in Table 1.

<sup>b</sup> Characterized by <sup>1</sup>H NMR spectroscopy of  $\beta$ -PL–St copolymers after separation.

<sup>c</sup> Characterized by <sup>1</sup>H NMR spectroscopy and GPC analysis of  $\beta$ -PL–St copolymers after degradation, calibration with PS standard.

<sup>d,e</sup> Calculated from the composition of the  $\beta$ -PL–St copolymer, the molecular weight of the copolymer after degradation and the number of grafting points.

The mechanism of the copolymerization is summarized in Scheme 3-3. Because of the higher monomer reactivity, styrene was initiated and polymerized first. As the polymerization progressed,  $\beta$ -PL was also initiated (Scheme 3, Step B). The monomer reactivity of styrene is much higher than  $\beta$ -PL, therefore,  $\beta$ -PL and styrene could not be copolymerized as a random copolymer. During the course of the polymerization, the radical was transferred to the benzyl group on the polystyrene chain (Scheme 3, Step C). The resulting benzyl radical was a stable radical and could not initiate  $\beta$ -PL polymerization. The active end radical of poly( $\beta$ -PL) was more reactive than the end phenyl radical of polystyrene and had a higher potential to react with the transferred benzyl radical on the polystyrene chain. Through radical recombination between the transferred benzyl radical and the active end radical of poly( $\beta$ -PL), the poly( $\beta$ -PL) side chains were grafted onto the polystyrene main chain (Scheme 3-3, Step D).



**Scheme 3-3.** Schematic process of  $\beta$ -PL–St copolymerization.

### 3.4 Conclusion

The radical copolymerization of  $\beta$ -PL and styrene at 120 °C for all monomer feed ratios led to the formation of St-*g*- $\beta$ -PL copolymers in one pot. 100% graft copolymers were obtained for 0.5:1 molar ratio of  $\beta$ -PL:St in feed. Increasing the amount of  $\beta$ -PL in feed gave graft copolymers, but also led to the formation of homopoly( $\beta$ -PL). A purification step was required to obtain pure graft copolymers for feed compositions ( $\beta$ -PL:St) 1:1, 2:1, and 5:1. The formation of graft copolymers was proven by a combination of characterization techniques, such as 1D and 2D NMR spectroscopy and GPC analysis before and after alkaline hydrolysis of the polymers. A significant difference in the reactivity of styrene and  $\beta$ -PL and radical chain-transfer reactions at the PSt backbone followed by combination with the active growing poly( $\beta$ -PL) chains led to the formation of graft copolymers by a grafting-onto mechanism.

## 3.5 Experimental Section

### 3.5.1 Materials

Di-*tert*-butyl peroxide (Aldrich), trifluoroacetic anhydride (Aldrich), and potassium hydroxide (Merck) were used as received.  $\beta$ -propiolactone (Acros) was distilled over  $\text{CaH}_2$ . Styrene (Aldrich), THF (Aldrich), ethyl acetate (Aldrich), and methanol (Aldrich) were distilled before use.

### 3.5.2 Instrumentation

$^1\text{H}$  (300 MHz),  $^{13}\text{C}$  (75 MHz) NMR spectra were recorded on a Bruker Ultrashield-300 spectrometer in  $\text{CDCl}_3$ , with tetramethylsilane (TMS) as an internal standard.  $^{19}\text{F}$  (282 MHz) NMR spectra were recorded by using a Bruker Ultrashield-300 spectrometer, with hexafluorobenzene as an external standard. HMBC/HMQC correlation experiments were recorded on a Bruker Ultrashield-300, with a 5 mm multinuclear gradient probe and using *gs*-HMQC and *gs*-HMBC pulse sequences. 2D NMR data were acquired with 2048 points in  $t_2$ , and the number of increments for  $t_1$  was 256. Thirty and sixty scans were used for HMQC and HMBC experiments. A relaxation delay of 1 s was used for all 1D experiments and 2 s for all 2D experiments.

Molecular weights ( $M_{n,\text{GPC}}$  and  $M_{w,\text{GPC}}$ ) and polydispersity indexes (PDI) of the polymers were determined by gel permeation chromatography (GPC) with a Knauer system equipped with 4 PSS-SDV gel columns (particle size = 5 mm), with porosity ranges from  $10^2$  to  $10^5$  Å (PSS, Mainz, Germany), together with a differential refractive index detector (RI-101 from Shodex). THF (HPLC grade) was used as a solvent (for dissolving the polymer and as the eluting solvent) with a flow rate of 1.0 mL/min. A polystyrene calibration was employed as a reference.

Preparative GPC was carried out with a Knauer system equipped with 2×2 PSS gel columns (particle size=10 mm) with a porosity range of  $10^2$  and  $10^4$  Å, together with a

differential refractive index detector and a UV detector. THF (p.a. grade) was used as a solvent (for dissolving the polymer and as the eluting solvent) with flow rate of 10 mL/min.

The absolute weight-average molecular weight ( $M_{w,MALLS}$ ) was evaluated by gel permeation chromatography multi-angle laser light scattering (GPC-MALLS), in THF at room temperature, by using an Agilent system with three 30 cm PSS-SDV columns with porosities of  $10^4$ ,  $10^5$ , and  $10^6$  Å, equipped with a Wyatt DAWN HELEOS laser light scattering detector (50 mW solid state laser;  $\lambda = 658$  nm). The flow rate of THF was 0.8 mL/min. Data evaluation was carried out with Astra Software.  $dn/dc$  was determined by using an interferometer.

Mettler thermal analyzer with 821 DSC module was used for the thermal characterization of the copolymers. DSC scans were recorded in a nitrogen atmosphere at a heating rate of  $10^\circ\text{C}/\text{min}$ . A sample size of  $10 \pm 1$  mg was used in each experiment.

### 3.5.3 General procedure for the homo- and copolymerization of $\beta$ -PL and styrene

For the homopolymerization of  $\beta$ -PL, the mixture of  $\beta$ -PL (0.90 g) and di-*tert*-butyl peroxide (DTBP, 11.3 mL, 1 wt% of monomer) was added into a 10 mL Schlenk tube equipped with a magnetic bar under argon. The liquid was degassed by three freeze-vacuumthaw cycles. The tube was sealed under argon, and then placed in a preheated oil bath at  $120^\circ\text{C}$  for 20h with stirring. After the tube was opened, the reaction mixture was precipitated into methanol. The precipitate was dried at  $40^\circ\text{C}$  under vacuum for 48 h. Yield: 39%.

A similar procedure was used for copolymerization reactions by taking a mixture of  $\beta$ -PL and styrene with different molar ratios ( $\beta$ -PL/St = 1:2, 1:1, 2:1, and 5:1) and DTBP (1 wt% of monomer). Yield: 71% ( $\beta$ -PL/St = 1:2 in feed); 54% ( $\beta$ -PL/St = 1:1 in feed); 42% ( $\beta$ -PL/St = 2:1 in feed); 40% ( $\beta$ -PL/St = 5:1 in feed).

### 3.5.4 Methanolysis of $\beta$ -PL–St copolymer

0.30 g of  $\beta$ -PL–St copolymer was dissolved in a mixture of KOH in methanol (25 mL, 5 wt%) and THF (15 mL) in a round-bottomed flask and was heated at reflux for two days. After 24 h, concentrated hydrochloric acid (3 mL) was added. The mixture was extracted with chloroform and washed with water. The solvent was evaporated under reduced pressure. The remaining solid was dried under vacuum at 40 °C for 48 h. The polymer was obtained as white solid.

### 3.5.5 $\beta$ -PL copolymerized with polystyrene

Polystyrene was presynthesized by anionic polymerization with  $M_n = 20000$  and PDI = 1.02. A mixture of  $\beta$ -PL (0.81 g), polystyrene (0.45 g), and DTBP (10.2 mL) was dissolved in anisole (3 mL) and added to a 10 mL Schlenk tube equipped with a magnetic bar under argon. The liquid was degassed by three freeze-vacuumthaw cycles. The tube was sealed under argon, and then placed in a preheated oil bath at 120°C for 20 h with stirring. After the tube was opened, the reaction mixture was precipitated into methanol. The precipitate was dried at 40°C for 48 h.

*Acknowledgements:* We acknowledge Prof. Dr. Jun Ling from Zhejiang University, and Prof. Andreas Greiner from Bayreuth University for helpful discussions. DFG is kindly acknowledged for financial support.

### 3.6 References

1. A. L. Sisson, M. Schroeter and A. Lendlein, in *Handbook of Biodegradable Polymers*, Wiley-VCH Verlag GmbH & Co. KGaA, 2011, pp. 1-21.
2. H. R. Kricheldorf, T. Mang and J. M. Jonte, *Macromolecules*, 1984, **17**, 2173-2181.
3. J. W. Pack, S. H. Kim, I. W. Cho, S. Y. Park and Y. H. Kim, *J. Polym. Sci., Part A: Polym. Chem.*, 2002, **40**, 544-554.
4. S. Agarwal, M. Karl, K. Dehnicke, G. Seybert, W. Massa and A. Greiner, *J. Appl. Polym. Sci.*, 1999, **73**, 1669-1674.
5. S. Agarwal, N. Naumann and X. Xie, *Macromolecules*, 2002, **35**, 7713-7717.
6. N. E. Kamber, W. Jeong, R. M. Waymouth, R. C. Pratt, B. G. G. Lohmeijer and J. L. Hedrick, *Chem. Rev.*, 2007, **107**, 5813-5840.
7. O. Dechy-Cabaret, B. Martin-Vaca and D. Bourissou, *Chem. Rev.*, 2004, **104**, 6147-6176.
8. S. Agarwal, C. Mast, K. Dehnicke and A. Greiner, *Macromol. Rapid Commun.*, 2000, **21**, 195-212.
9. W. J. Bailey, S.-R. Wu and Z. Ni, *Die Makromolekulare Chemie*, 1982, **183**, 1913-1920.
10. S. Jin and K. E. Gonsalves, *Macromolecules*, 1998, **31**, 1010-1015.
11. S. Agarwal, *Polym. Chem.*, 2010, **1**, 953-964.
12. S. Agarwal and C. Speyerer, *Polymer*, 2010, **51**, 1024-1032.
13. L. Ren, C. Speyerer and S. Agarwal, *Macromolecules*, 2007, **40**, 7834-7841.

14. H. Wickel, S. Agarwal and A. Greiner, *Macromolecules*, 2003, **36**, 2397-2403.
15. S. Agarwal and L. Ren, *Macromolecules*, 2009, **42**, 1574-1579.
16. H. Wickel and S. Agarwal, *Macromolecules*, 2003, **36**, 6152-6159.
17. J.-F. Lutz, J. Andrieu, S. Üzgün, C. Rudolph and S. Agarwal, *Macromolecules*, 2007, **40**, 8540-8543.
18. N. Grabe, Y. Zhang and S. Agarwal, *Macromol. Chem. Phys.*, 2011, **212**, 1327-1334.
19. Y. Zhang, M. Zheng, T. Kissel and S. Agarwal, *Biomacromolecules*, 2012, **13**, 313-322.
20. T. Mathisen, M. Lewis and A.-C. Albertsson, *J. Appl. Polym. Sci.*, 1991, **42**, 2365-2370.
21. V. H. Ohse, H. Cherdron and F. Korte, *Die Makromolekulare Chemie*, 1965, **86**, 312-315.
22. S. Katayama, H. Horikawa and O. Toshima, *J. Polym. Sci., Part A-1: Polym. Chem.*, 1971, **9**, 2915-2932.
23. D. W. Jenkins and S. M. Hudson, *Chem. Rev.*, 2001, **101**, 3245-3274.
24. N. Hadjichristidis, H. Iatrou, M. Pitsikalis and J. Mays, *Prog. Polym. Sci.*, 2006, **31**, 1068-1132.
25. X. Jiang, E. B. Vogel, M. R. Smith and G. L. Baker, *Macromolecules*, 2008, **41**, 1937-1944.
26. Y. Nakagawa, P. J. Miller and K. Matyjaszewski, *Polymer*, 1998, **39**, 5163-5170.
27. B. H. Cao, M. W. Kim and D. G. Peiffer, *Langmuir*, 1995, **11**, 1645-1652.
28. S. Wu, E. T. Kang, K. G. Neoh, H. S. Han and K. L. Tan, *Macromolecules*, 1998, **32**, 186-193.

29. Y. Iwasaki and K. Akiyoshi, *Biomacromolecules*, 2006, **7**, 1433-1438.
30. M. Ouchi, T. Terashima and M. Sawamoto, *Chem. Rev.*, 2009, **109**, 4963-5050.
31. H.-K. Lao, E. Renard, I. Linossier, V. Langlois and K. Vallée-Rehel, *Biomacromolecules*, 2006, **8**, 416-423.
32. Z. Zheng, M. Müllner, J. Ling and A. H. E. Müller, *ACS Nano*, 2013, **7**, 2284-2291.
33. Z. Zheng, A. Daniel, W. Yu, B. Weber, J. Ling and A. H. E. Müller, *Chem. Mater.*, 2013, **25**, 4585-4594.
34. K. Matyjaszewski and J. Xia, *Chem. Rev.*, 2001, **101**, 2921-2990.
35. R. K. Iha, K. L. Wooley, A. M. Nyström, D. J. Burke, M. J. Kade and C. J. Hawker, *Chem. Rev.*, 2009, **109**, 5620-5686.
36. Z. Zheng, J. Ling and A. H. E. Müller, *Macromol. Rapid Commun.*, 2014, **35**, 234-241.
37. E. Passaglia, S. Coiai and S. Augier, *Prog. Polym. Sci.*, 2009, **34**, 911-947.
38. H. Yang, S. Luan, J. Zhao, H. Shi, Q. Shi, J. Yin and P. Stagnaro, *React. Funct. Polym.*, 2010, **70**, 961-966.
39. T. Paunikallio, M. Suvanto and T. T. Pakkanen, *React. Funct. Polym.*, 2008, **68**, 797-808.
40. H. Yang, S. Luan, J. Zhao, H. Shi, X. Li, L. Song, J. Jin, Q. Shi, J. Yin, D. Shi and P. Stagnaro, *Polymer*, 2012, **53**, 1675-1683.
41. H. Huang, C. Y. Zhu, Z. F. Zhou and N. C. Liu, *React. Funct. Polym.*, 2002, **50**, 49-55.
42. V. Wilhelm and G. P. Hellmann, *Polymer*, 2000, **41**, 1905-1915.
43. M. Lee, R. B. Moore and H. W. Gibson, *Macromolecules*, 2011, **44**, 5987-5993.

44. M. Sato, T. Mangyo, K. Nakadera, K.-i. Mukaida, F. Yazaki and Y. Oyanagi, *Macromol. Rapid Commun.*, 1994, **15**, 243-250.
45. M. Kukut, O. Karal-Yilmaz and Y. Yagci, *Des. Monomers Polym.*, 2012, **16**, 233-240.
46. M. Kukut, O. Karal-Yilmaz and Y. Yagci, *J. Microencapsulation*, 2014, **31**, 254-261.
47. G. Henrici-Olivé and S. Olivé, *Journal of Polymer Science*, 1960, **48**, 329-333.

## 3.7 Supporting Information

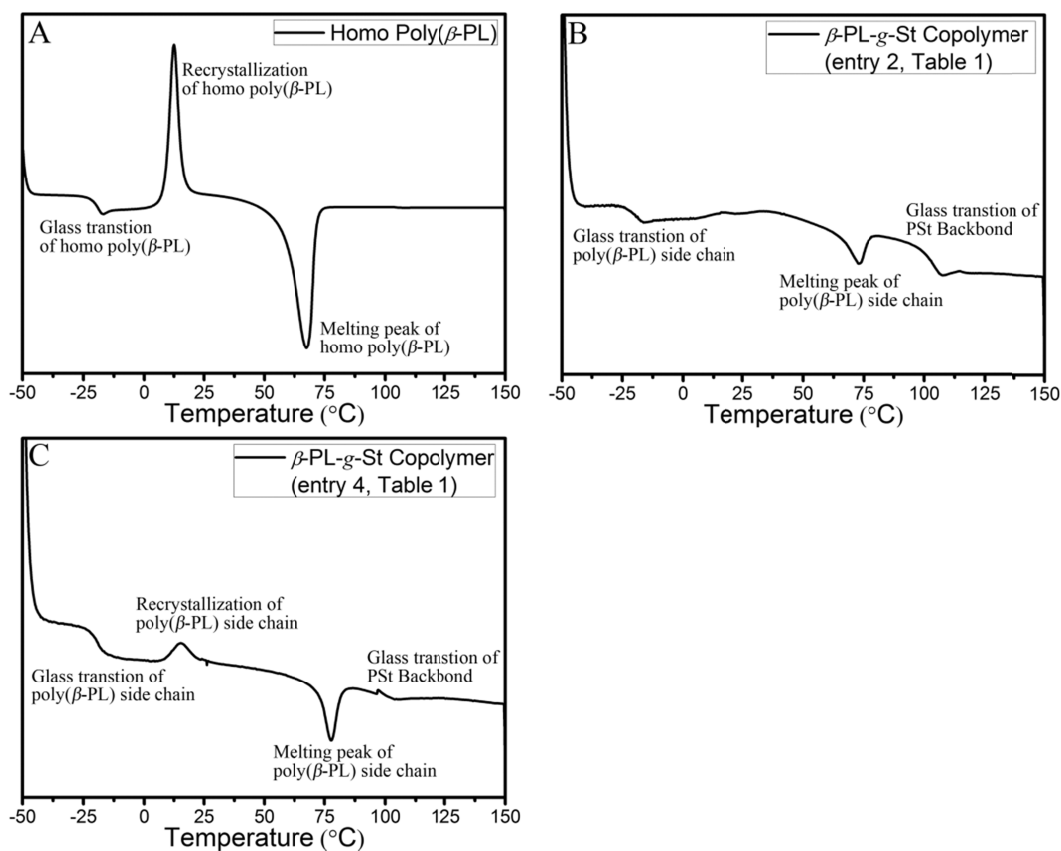
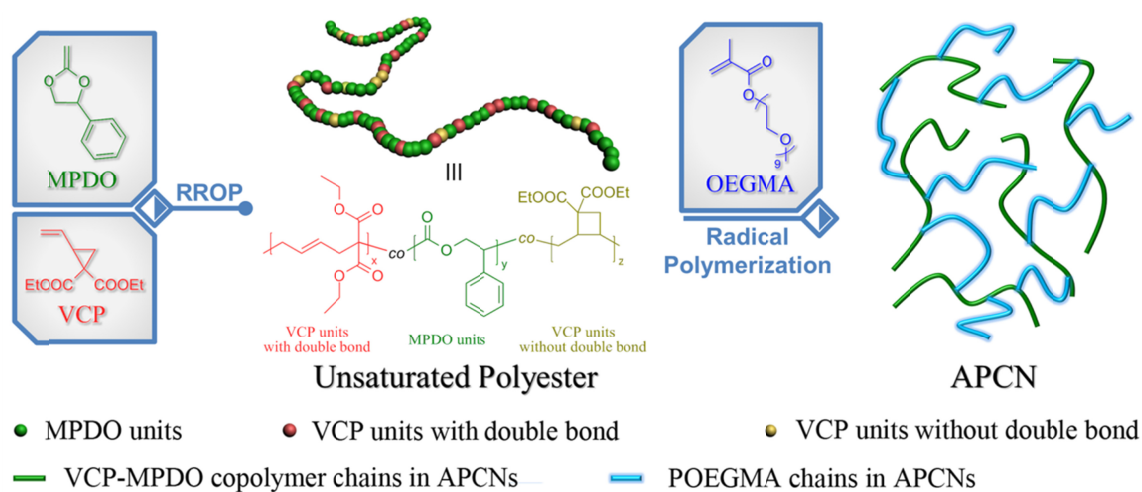


**Figure 3-S1.** DSC Analysis of resulting polymers. A: homo poly( $\beta$ -PL),  $T_g = -20$  °C,  $T_c = 13$  °C,  $T_m = 67$  °C; B: purified  $\beta$ -PL-*g*-St Copolymer (entry 2, Table 1),  $T_{g1} = -18$  °C,  $T_m = 72$  °C,  $T_{g2} = 102$  °C; C: purified  $\beta$ -PL-*g*-St Copolymer (entry 4, Table 1),  $T_{g1} = -19$  °C,  $T_c = 15$  °C,  $T_m = 77$  °C,  $T_{g2} = 103$  °C



## Chapter 4

### Designed Enzymatically Degradable Amphiphilic Conetworks by Radical Ring-Opening Polymerization



The results of this chapter have been submitted to *Macromolecules* as:

“Designed Enzymatically Degradable Amphiphilic Conetworks by Radical Ring-Opening Polymerization”

by Yinfeng Shi, Holger Schmalz, and Seema Agarwal\*



## 4.1 Abstract

A different route to the preparation of enzymatically degradable amphiphilic conetworks (APCNs) based on unsaturated polyesters by radical ring-opening polymerization of vinylcyclopropane (VCP) with cyclic ketene acetal (CKA) is presented in this article. In the first step, the unsaturated biodegradable polyesters with random distribution of cross-linkable double bonds and degradable ester units were prepared by radical ring-opening copolymerization of VCP and CKA such as 2-methylene-4-phenyl-1,3-dioxolane (MPDO). Very similar reactivity ratios ( $r_{VCP} = 0.23 \pm 0.08$  and  $r_{MPDO} = 0.18 \pm 0.02$ ), unimodal gel permeation chromatography (GPC) curves and 2D NMR technique (heteronuclear multiple bond correlation, HMBC) showed the formation of random copolymers with unsaturation and ester units. The unsaturated units were used for cross-linking hydrophilic macromonomer (oligo(ethylene glycol) methacrylate, OEGMA) by radical polymerization in a second step for the formation of enzymatically degradable amphiphilic conetworks (APCNs). Enzymatic degradability was studied using Lipase from *Pseudomonas cepacia*. Due to the hydrophilic (HI) and hydrophobic (HO) microphase separation, the APCNs showed swelling in both water and organic solvents with different optical properties. The method provides an interesting route for making functional biodegradable APCNs using radical chemistry in the future.



## 4.2 Introduction

Amphiphilic conetworks (APCNs), composed of covalently linked hydrophilic and hydrophobic (HI/HO) chain segments, have the capability of swelling in both water and organic solvents.<sup>1-5</sup> Owing to the unique structures and properties, APCNs were developed for various applications.<sup>6-15</sup> The most common method of making APCNs, in fact one of the first examples, was using radical copolymerization of polymerizable telechelics (low molar mass polymers with polymerizable chain-ends) with a suitable comonomer.<sup>16-18</sup> Other methods used for the formation of APCNs were click chemistry,<sup>5</sup> thiol-ene reaction,<sup>19</sup> Diels-Alder reaction<sup>20</sup> *etc.*.

Biodegradable APCNs would be highly interesting for many biomedical applications and have also been made using photo, thermal radical / controlled radical polymerization of  $\alpha,\omega$ -acrylate chain-end functionalized common biodegradable polymers such as poly(*L*-lactide), polyglycolide and poly( $\epsilon$ -caprolactone) (PCL) with comonomers like 2-hydroxyethyl methacrylate and *N,N*-dimethylaminoethyl methacrylate.<sup>21-24</sup> In all these examples aliphatic polyesters made by metal catalyzed ring-opening polymerization (ROP) of corresponding cyclic esters were used as degradable hydrophobic segment. Both chain-ends were modified with polymerizable double bonds, i.e. acrylate units, to make them suitable as cross-linker in radical copolymerization with hydrophilic comonomers in a second step. In addition, azide-alkyne coupling of diazide chain-end functionalised ABA triblock copolymers of PCL and PEO with tetrakis(2-propynyloxymethyl) methane (TMOP) was applied.<sup>5</sup>

Polyesters, in general, can also be made by radical ring-opening polymerization (RROP) of cyclic ketene acetals (CKAs). This method provides opportunities of making functional polyesters in a simple way by simple copolymerization of CKAs with a large variety of vinyl comonomers available.<sup>25-37</sup>

Vinylcyclopropane (VCP) and its derivatives are interesting vinyl monomers

undergoing radical ring-opening polymerization for the formation of polymers with unsaturated units in the backbone<sup>38-46</sup> and have been intensively studied for dental applications as low volume shrinkage monomers (Scheme 1A). The copolymerization of VCP with CKAs could provide new polymers with cross-linkable unsaturated units and biodegradable ester linkages randomly distributed on the polymer backbone (Scheme 1C), which could be useful for making APCNs. Unsaturated biodegradable amphiphilic hydrogels made by condensation polymerization of diol functionalised poly( $\epsilon$ -caprolactone) and poly(ethylene glycol) with diacid functionalised poly(propylene fumarate), followed by cross-linked with poly(acrylamide) are known in the literature with main focus on swellability in water.<sup>47,48</sup> The present method of making APCNs by radical copolymerization would have the advantage of introducing functional groups in a simple way by choosing appropriate vinyl comonomers for copolymerization with VCP and CKAs.

We highlight the formation of APCNs, in which the hydrophobic part is made by radical ring-opening copolymerization of vinylcyclopropane (VCP) and 2-methylene-4-phenyl-1,3-dioxolane (MPDO), followed by cross-linking with a hydrophilic macromonomer oligo(ethylene glycol) methacrylate (OEGMA,  $M_n \sim 500$ ). The copolymerization of VCP and MPDO provides an unsaturated polyester with random distribution of carbon-carbon double bonds and ester units, as characterized by reactivity ratio determination. This is a new method of making unsaturated polyesters (UPs) by radical polymerization with the advantage of easy introduction of additional functional groups simply by choosing appropriate vinyl comonomers. The state-of-the art method of making UPs is by condensation polymerization using high temperatures that restricts the use of many functional monomers. The APCNs were characterized by swelling studies in water and DMF, and the enzymatic degradability of APCNs was studied using Lipase from *Pseudomonas cepacia* in pH= 7 PBS buffer solution. The unique swelling property and biodegradability of the prepared APCNs suggests the potential application in the biomaterial field.

## 4.3 Experimental Section

### 4.3.1 Materials

1-Phenyl-1,2-ethanediol (Aldrich), potassium *tert*-butoxide (Acros), *p*-toluenesulfonic acid (Aldrich), 1,4-dibromo-2-butene (Aldrich), diethyl malonate (Aldrich), sodium (Aldrich), di-*tert*-butyl peroxide (DTBP, Aldrich) and Lipase (from *Pseudomonas cepacia*,  $\geq 30$  U/mg, Aldrich) were used as received. All solvents were distilled before use. Oligo(ethylene glycol) methacrylate (OEGMA,  $M_n \sim 500$ , Aldrich) was passed through a basic alumina column to remove the inhibitor.

2-Methylene-4-phenyl- 1,3-dioxolane (MPDO) was synthesized using the literature method of W. J. Bailey *et al.*<sup>49</sup> with some modifications. 2-vinylcyclopropane-1,1-dicarboxylate (VCP) was synthesized using the literature method of T. Endo *et al.*<sup>38</sup>.

### 4.3.2 Instrumentation

<sup>1</sup>H (300 MHz), <sup>13</sup>C (75 MHz) NMR spectra were recorded on a Bruker Ultrashield-300 spectrometer in CDCl<sub>3</sub>, using tetramethylsilane (TMS) as an internal standard. Molecular weights and polydispersity indexes (PDI) of the polymers were determined by gel permeation chromatography (GPC) with a Knauer system equipped with 4 PSS-SDV gel columns (particle size = 5  $\mu$ m) with pore sizes ranging from 10<sup>2</sup> to 10<sup>5</sup> Å (PSS, Mainz, Germany) together with a differential refractive index detector (RI-101 from Shodex). THF (HPLC grade) was used as solvent at a flow rate of 1.0 mL/min. A Mettler thermal analyzer with 851 TG and 821 DSC modules was used for the thermal characterization of copolymers. Thermal stability was determined by recording TGA traces at a heating rate of 10 K/min in nitrogen atmosphere (flow rate = 50 ml/min). DSC scans were recorded in nitrogen atmosphere (flow rate = 80 ml/min) at a scanning rate of 10 K/min. A sample mass of 10 $\pm$ 1 mg was used in both DSC and TGA analysis.

### 4.3.3 Copolymerization of MPDO and VCP under free radical condition

The mixture of MPDO and VCP with different molar ratios and di-*tert*-butyl peroxide as initiator were added into a 10 mL Schlenk tube equipped with a magnetic stir bar under argon. After degassing by freeze-vacuum-thaw cycles three times, the tubes were sealed under argon, and then placed in a preheated oil bath at 120 °C for 48 h while stirring. Subsequently, the tubes were opened and the reaction mixture was poured into methanol while stirring to cause polymer precipitation. Finally, the purified polymer was dried under vacuum at 60 °C for 48 h. Copolymerization of MPDO and VCP for reactivity ratios calculation was carried out with various feed ratios at 120 °C and stopped at low conversion (reaction time 6h). The reactivity ratios were calculated using Kelen-Tüdös method.<sup>50</sup> Details are given in the Supporting Information.

### 4.3.4 APCN preparation using VCP-MPDO copolymers and OEGMA under free radical condition

VCP-MPDO copolymer, OEGMA and DTBP were dissolved in 0.5 mL dioxane at a molar ratio of carbon-carbon double bonds : OEGMA : DTBP = 1:25:1. After degassing with argon for 1 h, the reaction mixture was placed in a preheated oil bath at 140 °C for 24 h without stirring. After the polymerization, the resulting gel was extracted with chloroform overnight to remove the unreacted VCP-MPDO copolymer. Finally, the purified APCNs were dried in vacuum at 60 °C for 24 h.

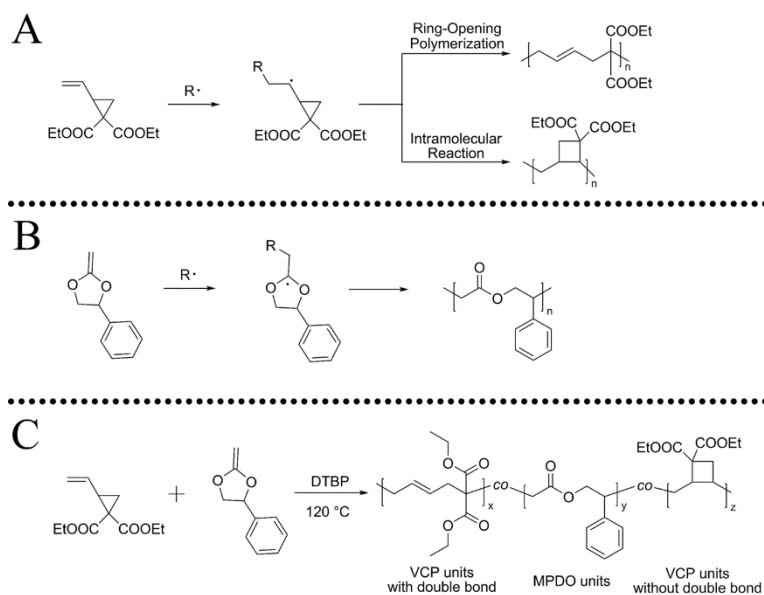
### 4.3.5 *In vitro* degradation study of APCNs

*In vitro* degradation studies of APCNs were carried out by placing APCNs in pH = 7 PBS buffer solution with the enzyme concentration of 15 U/mL (Lipase from *Pseudomonas cepacia*) at 37 °C. The degradation medium was replaced every 24 h. The remaining mass of APCNs was recorded after freeze drying at different degradation time.

## 4.4 Results and Discussion

### 4.4.1 Copolymerization of VCP with MPDO

Various copolymers of VCP with MPDO were prepared by changing the molar ratio of the two monomers in the initial feed (Scheme 4-1, Table 4-1).



**Scheme 4-1.** Schematic process of radical ring-opening polymerization (RROP) of A) vinylcyclopropane (VCP)<sup>38</sup>, B) 2-methylene-4-phenyl-1,3-dioxolane (MPDO)<sup>49</sup>, and C) VCP and MPDO.

**Table 4-1.** Copolymerization data for VCP-MPDO copolymers<sup>a</sup>

Entry	Feed ratio (-mol%)		Yield (%)	$M_n^b$ (g/mol)	PDI <sup>b</sup>	copolymer composition (mol-%) <sup>c</sup>		
	VCP	MPDO				VCP (ring-opened)	VCP (ring-opened)	MPDO
1	30	70	33	$5.4 \times 10^3$	1.4	25	20	55
2	50	50	43	$8.3 \times 10^3$	1.3	31	28	41
3	70	30	46	$1.2 \times 10^4$	1.8	29	35	36

<sup>a</sup> Initiator: DTBP (1 wt% of monomer); reaction temperature: 120 °C; reaction time: 48 h.

<sup>b</sup> Determined by THF-GPC with RI detector; PS-standard used for calibration (Figure 4-3).

<sup>c</sup> Determined by <sup>1</sup>H-NMR spectra of resulting VCP-MPDO copolymers (Figure 4-1A).

After purification, the resulting copolymers were obtained as white solids. The copolymer structure was analyzed by NMR spectroscopy (Figure 4-1). According to the NMR spectra of PVCP (please see Supporting Information, Figure 4-S1) and PMPDO<sup>49</sup> homopolymer, the characteristic peaks of VCP and MPDO units were confirmed and marked in Figure 1. In the <sup>13</sup>C-NMR spectrum (Figure 4-1B), the absence of peaks between  $\delta = 90 - 110$  ppm confirms that all MPDO units were copolymerized as ring-opened structure providing ester units in the polymer backbone (structure **3** in Figure 4-1). In the <sup>1</sup>H-NMR spectrum (Figure 4-1A), the broad peak *c* at  $\delta = 4.7-5.3$  ppm originates from the carbon-carbon double bond  $-CH=CH-$  of VCP units with ring-opened structure (structure **1** in Figure 4-1), the peak *a* at  $\delta = 0.9-1.1$  ppm from the  $CH_3CH_2O-$  group of VCP units with ring-opened and also ring-closed structure (structures **1** and **2** in Figure 4-1) and peak *b,i* between  $\delta = 3.7-4.5$  ppm were assigned to the  $-CH_2-CH(Ph)-$  group of MPDO units and  $CH_3CH_2O-$  group of VCP units in the copolymer. Through comparing the areas of these 3 peaks, the VCP-MPDO copolymer composition was calculated.

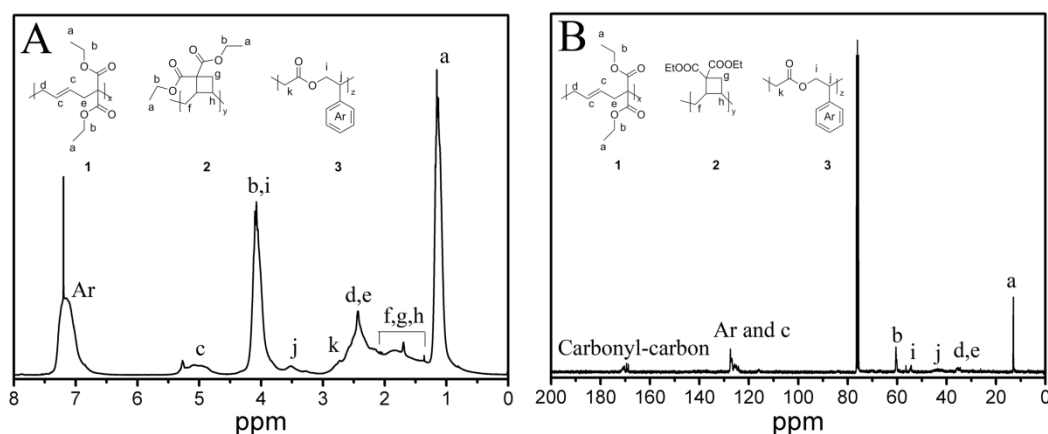


**Figure 4-1.** NMR-spectra of VCP-MPDO copolymer (entry 1 in Table 1). A: <sup>1</sup>H-NMR spectrum; B: <sup>13</sup>C-NMR spectrum. Structure **1**: VCP unit with ring-opened structure in copolymer; structure **2**: VCP unit with ring-closed structure in copolymer; structure **3**: MPDO unit in copolymer.

The 2D HMBC NMR spectrum (Figure 4-2) shows correlation of the proton peaks originating from *d,e* of VCP units (structure **1**) at 2.4 ppm with the aromatic carbon

signals of MPDO units (structure **3**) at 128 ppm, confirming covalent linkage between VCP and MPDO units in the copolymer. The compositions of VCP-MPDO copolymers with different monomer ratio in feed were summarized in Table 1. An increase of VCP in the initial feed led to the higher VCP composition in the VCP-MPDO copolymer.

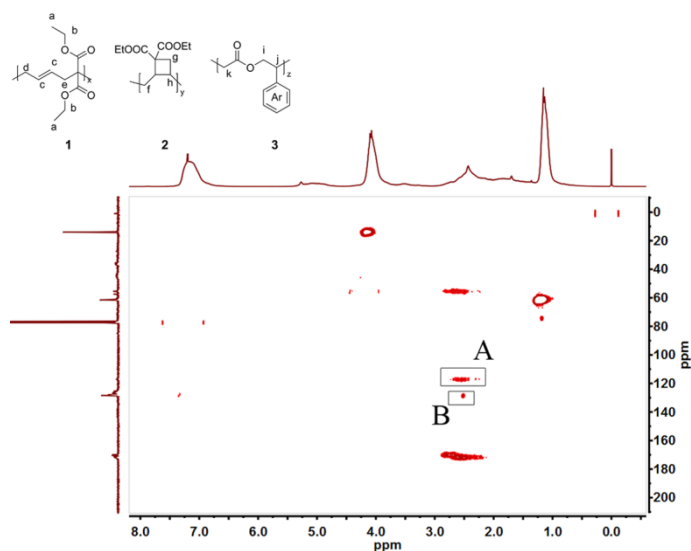


**Figure 4-2.** HMBC spectrum of VCP-MPDO copolymer (entry 1 in Table 1). Cross-peak A: Coupling between group *d,e* of VCP unit with ring-opened structure (structure **1**) and carbon-carbon double bond *c* of VCP unit with ring-opened structure (structure **1**); cross-peak B: Coupling between group *d,e* of VCP unit with ring-opened structure (structure **1**) and phenyl group of MPDO unit (structure **3**).

The number-average molecular weights of the resulting VCP-MPDO copolymers were determined by THF-GPC applying a polystyrene calibration and ranged from  $5.4 \times 10^3$  to  $1.2 \times 10^4$  g/mol (Table 4-1). The corresponding GPC-traces show unimodal molecular weight distributions for all copolymers (Figure 4-3). An increase of VCP in the initial feed led to a higher molar mass of the resulting copolymer.

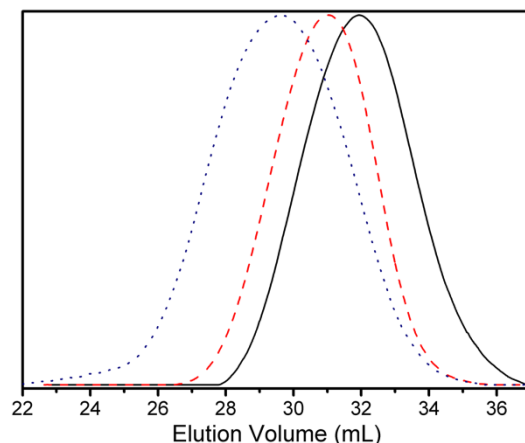


**Figure 4-3.** THF-GPC traces of VCP-MPDO copolymers with different comonomer ratios in feed. Reaction temperature: 120 °C, reaction time: 48 h. Composition in feed: black: VCP:MPDO = 30:70; red: VCP:MPDO = 50:50; navy: VCP:MPDO = 70:30.

The reactivity ratios of the two monomers were calculated using the Kelen-Tüdös method.<sup>50</sup> To that end, a series of VCP-MPDO copolymers with low yields (< 5%) were prepared. The composition of the resulting polymers was determined using <sup>1</sup>H-NMR technique as described above. A detailed discussion on the determination of the reactivity ratios can be found in the Supporting Information (Tables 4-S1, 4-S2 and Figures 4-S3, 4-S4). From the corresponding Kelen-Tüdös plot (Figure 4-S3) the reactivity ratios of VCP and MPDO were determined to  $r_{VCP} = 0.23 \pm 0.08$  and  $r_{MPDO} = 0.18 \pm 0.02$ . There are no big differences between the reactivity ratios of VCP and MPDO and both values are below 1. Consequently, depending on the monomer unit at the active chain end, i.e., VCP or MPDO, the incorporation of the respective other comonomer, i.e., MPDO or VCP, is slightly preferred (copolymerization diagram in Figure 4-S4). This suggests a nearly random distribution of MPDO and VCP units in the copolymer.

Thermal characterization of VCP-MPDO copolymers was carried out using TGA and DSC techniques. The glass transition temperatures and decomposition temperatures of the copolymers are listed in Table 4-2.

**Table 4-2.** Thermal properties of VCP-MPDO copolymers <sup>a</sup>

Entry	copolymer composition (mol-%) <sup>b</sup>			T <sub>g</sub> (°C) <sup>c</sup>	dec. Temp. (°C) <sup>d</sup>
	VCP (ring-opened)	VCP (ring-opened)	MPDO		
1	25	20	55	45	402
2	31	28	41	43	410
3	29	35	36	49	410

<sup>a</sup> Initiator: DTBP (1 wt% of monomer); reaction temperature: 120 °C; reaction time: 48 h; same as entry 1-3 in Table 4-1.

<sup>b</sup> Determined by <sup>1</sup>H-NMR spectra (Figure 4-1A).

<sup>c</sup> Determined by DSC (Figure 4-5).

<sup>d</sup> Determined by TGA (Figure 4-4).

The copolymers show a high thermal stability (T<sub>max</sub>: temperature at which rate of decomposition was maximum = 400-410 °C) with single step decomposition (Figure 4-4). Single glass transition was obtained for copolymers with different comonomer ratios (Figure 4-5), reconfirming the nearly random incorporation of MPDO and VCP in the copolymer chains.

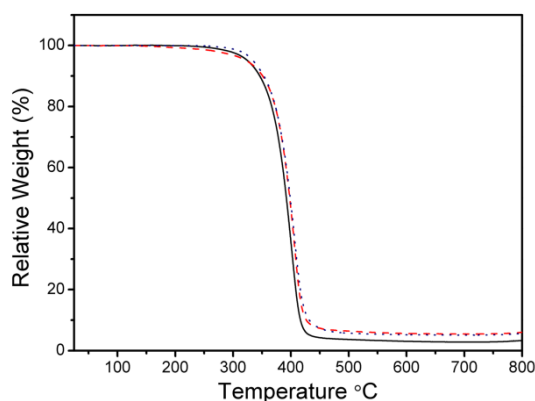


**Figure 4.** TGA profiles of VCP-MPDO copolymers with different comonomer ratios in feed.

Black: VCP:MPDO = 30:70; red: VCP:MPDO = 50:50; navy: VCP:MPDO = 70:30.

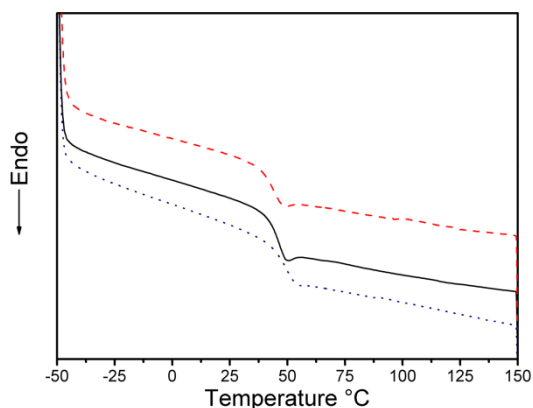
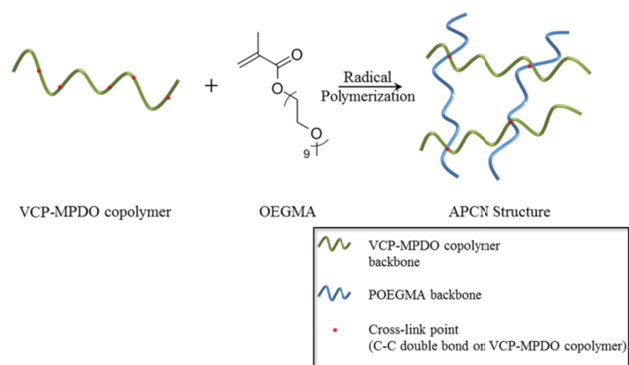


**Figure 4-5.** DSC heating traces of VCP-MPDO copolymers with different comonomer ratios in feed. Black: VCP:MPDO = 30:70; red: VCP:MPDO = 50:50; navy: VCP:MPDO = 70:30.

#### 4.4.2 Synthesis of biodegradable amphiphilic networks using VCP-MPDO copolymers

Based on the cross-linkable carbon-carbon double bonds and the almost random VCP-MPDO combination on the copolymer backbone (random distribution of ester units), the VCP-MPDO copolymers have the potential to be used for the preparation of biodegradable amphiphilic conetworks (APCNs). As shown in Scheme 4-2, APCNs were prepared from a reaction mixture of VCP-MPDO copolymer, OEGMA and DTBP in dioxane with a molar ratio of carbon-carbon double bonds:OEGMA:DTBP = 1:25:1 at 140 °C. After 24 h reaction, colorless cross-linked gels with very high gel fractions were obtained. The gel fraction was determined by calculating the ratio of the gel dry mass to polymer precursor mass (Table 4-3). The FT-IR showed the presence of characteristic peaks for both VPC-MPDO copolymer and POEGMA segments in the APCNs (please see Supporting Information Figure 4-S2).



**Scheme 4-2.** Preparation of biodegradable amphiphilic conetworks. OEGMA = oligo(ethylene glycol) methacrylate,  $M_n \sim 500$  g/mol. Di-*tert*-butyl peroxide was used as initiator and reaction temperature was at 140 °C.

### 4.4.3 Characterization of biodegradable APCNs

The swelling property is one of the most important properties of APCNs and it was studied by immersing dry gels in different solvents. The swelling ratio was calculated using the equation:

$$\text{Weight Swelling Ratio (w/w)} = [(\text{Weight}_{\text{swollen gel}}/\text{Weight}_{\text{dry gel}})-1] \times 100\%$$

Because of the co-existence of hydrophilic (HI) and hydrophobic (HO) structure in the copolymer network, the APCNs show different swelling properties in various solvents. The swelling properties of APCNs in water and DMF are shown in Figure 4-6 and listed in Table 4-3.

**Table 4-3.** Physical properties of APCNs prepared using VCP-MPDO copolymers<sup>a</sup>

Sample	gel fraction (%)	Weight swelling ratio (w/w) after equilibration (%)	
		in water	in DMF
Gel 1 <sup>b</sup>	79	1130	1230
Gel 2 <sup>c</sup>	91	1030	1160
Gel 3 <sup>d</sup>	93	1070	1150

<sup>a</sup> The OEGMA :VCP-MPDO (feed molar ratio) was 6.25:1, 7.75:1 and 7.25:1 for gels 1, 2 and 3, respectively.

<sup>b</sup> APCNs Gel 1: prepared by VCP-MPDO copolymer of entry 1 in Table 4-1.

<sup>c</sup> APCNs Gel 2: prepared by VCP-MPDO copolymer of entry 2 in Table 4-1.

<sup>d</sup> APCNs Gel 3: prepared by VCP-MPDO copolymer of entry 3 in Table 4-1.

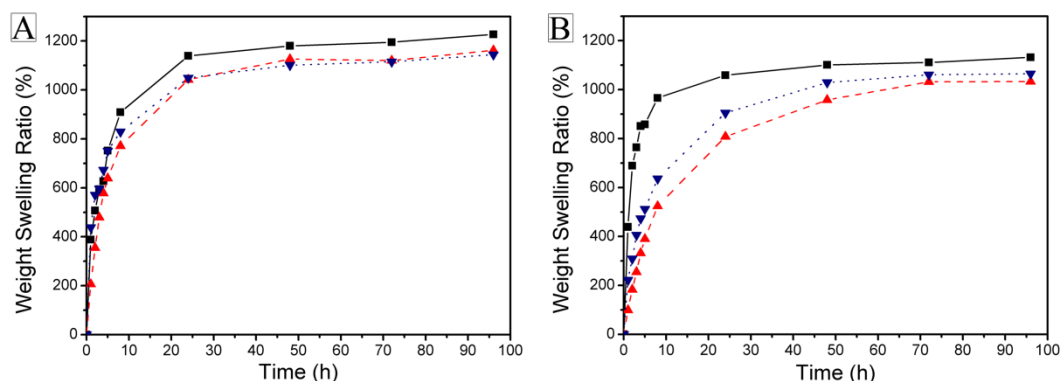


**Figure 4-6.** Weight swelling ratio of APCNs (black: Gel 1, red: Gel 2, navy: Gel 3) in (A) DMF and (B) water.

The gels showed equilibration in water and also DMF in approximately 8 h. DMF is a good solvent for both the hydrophilic and hydrophobic phases in the resulting APCNs and results in an extension of all polymer chains in the networks. However, water is a selective solvent only for the hydrophilic phase and only the poly[oligo(ethylene glycol) methacrylate] (POEGMA) segments extend in water. Due to the lowest content of VCP units with carbon-carbon double bond in the VCP-MPDO copolymer for network preparation, Gel 1 has the lowest concentration of cross-linking points in the network and hence showed the maximum swelling ratio of 1130% in water (Figure 4-6B) and 1230% in DMF (Figure 4-6A). It was larger than Gel 2 (1030% in water and 1160% in DMF) and Gel 3 (1070% in water and 1150% in DMF). The swelling ratios of all APCNs in water were smaller than in DMF. All APCNs showed a high transparency in DMF (Figure 4-7 top) due to the extension of both hydrophobic and hydrophilic parts. Because of the phase separation between the hydrophilic (POEGMA chains) and hydrophobic (VCP-MPDO copolymer) segments, the APCNs appeared opaque in water (Figure 4-7 below).

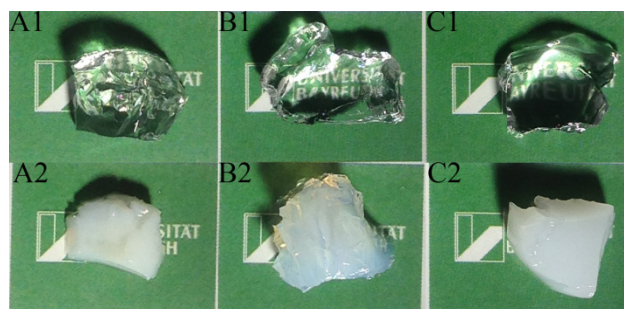


**Figure 4-7.** Photographs of APCNs swollen in different solvent. A1: Gel 1 in DMF; A2: Gel 1 in H<sub>2</sub>O; B1: Gel 2 in DMF; B2: Gel 2 in H<sub>2</sub>O; C1: Gel 3 in DMF; C2: Gel 3 in H<sub>2</sub>O.

Due to the influence of polymer crystallinity to the drug permeation and biodegradability of the whole network in the aim of biomedical application,<sup>51</sup> the thermal properties of APCNs were studied through DSC technique (Figure 4-8). The APCNs showed a low melting temperature around -3 °C due to oligo(ethylene glycol) side-chains. The glass transition temperature of the VCP-MPDO copolymer segments in the conetwork was observed at 45 °C and  $T_g$  of POEGMA backbone at 85 °C, respectively. Due to the higher glass transition temperature of the hydrophobic segments in the conetwork, the APCNs could keep their shape at room temperature.

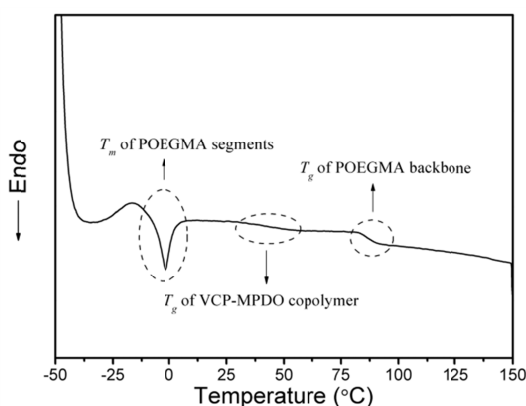


**Figure 4-8.** DSC heating trace of purified APCNs, Gel 3 as an example.

The degradation behavior of APCNs was studied by placing APCNs in pH = 7 PBS buffer solution with the enzyme concentration of 15 U/mL at 37 °C (Lipase from *Pseudomonas cepacia*) (Figure 4-9). The degradability of APCNs was realized through cleavage of VCP-MPDO copolymer segments, which act as cross-linking chains in the

APCNs. Because of their amorphous nature, the VCP-MPDO copolymer chains of APCNs have a good degradability. The degradation of VCP-MPDO chain segments causes the release of soluble hydrophilic POEGMA segments, leading to a reduction in gel content. Due to the highest content of ester bonds from MPDO-units and the lowest content of carbon-carbon double bonds as cross-linking points from ring-opened VCP-units in the conetwork, Gel 1 exhibited the fastest decomposition rate and was decomposed in 35 d in the presence of Lipase from *Pseudomonas cepacia*.

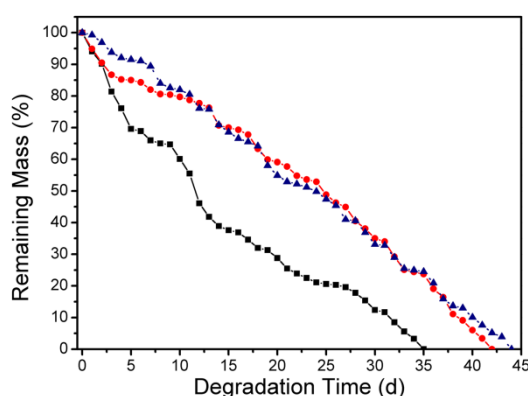


**Figure 4-9.** Mass loss of APCNs against enzyme in pH = 7 PBS buffer solution in dependence of degradation time. Black: Gel 1; red: Gel 2; navy: Gel 3.

## 4.5 Conclusion

Cross-linkable unsaturated polyesters were prepared by radical ring-opening copolymerization of VCP and MPDO. The unsaturated and ester units were provided by ring-opening of VCP and cyclic ketene acetal (MPDO), respectively, and were distributed almost randomly along the copolymer backbone. The VCP-MPDO copolymers were used as hydrophobic (HO) precursors for the formation of amphiphilic conetworks (APCNs) *via* copolymerization with OEGMA, forming the hydrophilic (HI) part. Through the free radical polymerization of OEGMA in the presence of VCP-MPDO copolymer, the APCNs were successfully produced. The concentration of the cross-linking points and hence the swelling property of APCNs in DMF and water depend on the amount of double bonds in the hydrophobic precursor. The APCNs provided unique swelling property with excellent enzymatic degradability. The method provides an interesting route for making functional biodegradable APCNs using radical chemistry in the future.

## 4.6 References

1. C. S. Patrickios and T. K. Georgiou, *Curr. Opin. Colloid Interface Sci.*, 2003, **8**, 76-85.
2. G. Erdodi and J. P. Kennedy, *Prog. Polym. Sci.*, 2006, **31**, 1-18.
3. L. Mespouille, J. L. Hedrick and P. Dubois, *Soft Matter*, 2009, **5**, 4878-4892.
4. M. Rikkou-Kalourkoti, E. Loizou, L. Porcar, K. Matyjaszewski and C. S. Patrickios, *Polym. Chem.*, 2012, **3**, 105-116.
5. Y. Yuan, A.-K. Zhang, J. Ling, L.-H. Yin, Y. Chen and G.-D. Fu, *Soft Matter*, 2013, **9**, 6309-6318.
6. J. Zednik, R. Riva, P. Lussis, C. Jérôme, R. Jérôme and P. Lecomte, *Polymer*, 2008, **49**, 697-702.
7. L. Bromberg, M. Temchenko and T. A. Hatton, *Langmuir*, 2002, **18**, 4944-4952.
8. C. Lin and I. Gitsov, *Macromolecules*, 2010, **43**, 10017-10030.
9. J. P. Kennedy, *Macromol. Symp.*, 2001, **175**, 127-132.
10. I. Gitsov and C. Zhu, *J. Am. Chem. Soc.*, 2003, **125**, 11228-11234.
11. I. Gitsov and C. Zhu, *Macromolecules*, 2002, **35**, 8418-8427.
12. R. Haigh, N. Fullwood and S. Rimmer, *Biomaterials*, 2002, **23**, 3509-3516.
13. S. Rimmer, M. J. German, J. Maughan, Y. Sun, N. Fullwood, J. Ebdon and S. MacNeil, *Biomaterials*, 2005, **26**, 2219-2230.
14. N. Bruns and J. C. Tiller, *Nano Lett.*, 2004, **5**, 45-48.
15. G. Savin, N. Bruns, Y. Thomann and J. C. Tiller, *Macromolecules*, 2005, **38**,

- 7536-7539.
16. D. Chen, J. P. Kennedy and A. J. Allen, *J. Macromol. Sci., Part A: Chem.*, 1988, **25**, 389-401.
  17. E. Themistou and C. S. Patrickios, *Macromolecules*, 2004, **37**, 6734-6743.
  18. E. Loizou, A. I. Triftaridou, T. K. Georgiou, M. Vamvakaki and C. S. Patrickios, *Biomacromolecules*, 2003, **4**, 1150-1160.
  19. C. N. Walker, K. C. Bryson, R. C. Hayward and G. N. Tew, *ACS Nano*, 2014, **8**, 12376-12385.
  20. M. Delerba, J. R. Ebdon and S. Rimmer, *Macromol. Rapid Commun.*, 1997, **18**, 723-728.
  21. A. S. Sawhney, C. P. Pathak and J. A. Hubbell, *Macromolecules*, 1993, **26**, 581-587.
  22. I. Barakat, P. Dubois, R. Jérôme, P. Teyssié and E. Goethals, *J. Polym. Sci., Part A: Polym. Chem.*, 1994, **32**, 2099-2110.
  23. I. Barakat, P. Dubois, C. Grandfils and R. Jérôme, *J. Polym. Sci., Part A: Polym. Chem.*, 1999, **37**, 2401-2411.
  24. L. Mespouille, O. Coulembier, D. Paneva, P. Degée, I. Rashkov and P. Dubois, *Chem. - Eur. J.*, 2008, **14**, 6369-6378.
  25. S. Agarwal, *Polym. Chem.*, 2010, **1**, 953-964.
  26. W. J. Bailey, Z. Ni and S.-R. Wu, *J. Polym. Sci., Polym. Chem. Ed.*, 1982, **20**, 3021-3030.
  27. J. Bailey, J. L. Chou, P. Z. Feng, V. Kuruganti and L. L. Zhou, *Acta Polym.*, 1988, **39**, 335-341.
  28. W. J. Bailey, Z. Ni and S. R. Wu, *Macromolecules*, 1982, **15**, 711-714.

29. L. Ren, C. Speyerer and S. Agarwal, *Macromolecules*, 2007, **40**, 7834-7841.
30. H. Wickel, S. Agarwal and A. Greiner, *Macromolecules*, 2003, **36**, 2397-2403.
31. J.-F. Lutz, J. Andrieu, S. Üzgün, C. Rudolph and S. Agarwal, *Macromolecules*, 2007, **40**, 8540-8543.
32. N. Xiao, H. Liang and J. Lu, *Soft Matter*, 2011, **7**, 10834-10840.
33. G. G. Hedir, C. A. Bell, N. S. Jeong, E. Chapman, I. R. Collins, R. K. O'Reilly and A. P. Dove, *Macromolecules*, 2014, **47**, 2847-2852.
34. B. Ochiai and T. Endo, *J. Polym. Sci., Part A: Polym. Chem.*, 2007, **45**, 2827-2834.
35. A. Tardy, V. Delplace, D. Siri, C. Lefay, S. Harrisson, B. de Fatima Albergaria Pereira, L. Charles, D. Gigmes, J. Nicolas and Y. Guillaneuf, *Polym. Chem.*, 2013, **4**, 4776-4787.
36. Y. Zhang, M. Zheng, T. Kissel and S. Agarwal, *Biomacromolecules*, 2011, **13**, 313-322.
37. L. Ren and S. Agarwal, *Macromol. Chem. Phys.*, 2007, **208**, 245-253.
38. F. Sanda, T. Takata and T. Endo, *Macromolecules*, 1993, **26**, 1818-1824.
39. F. Sanda and T. Endo, *J. Polym. Sci., Part A: Polym. Chem.*, 2001, **39**, 265-276.
40. A. de Meijere, V. Bagutski, F. Zeuner, U. K. Fischer, V. Rheinberger and N. Moszner, *Eur. J. Org. Chem.*, 2004, **2004**, 3669-3678.
41. T. Hirano, A. Tabuchi, M. Seno and T. Sato, *Macromolecules*, 2001, **34**, 4737-4741.
42. V. Delplace, S. Harrisson, A. Tardy, D. Gigmes, Y. Guillaneuf and J. Nicolas, *Macromol. Rapid Commun.*, 2014, **35**, 484-491.
43. S. Ata, D. Mal and N. K. Singha, *RSC Adv.*, 2013, **3**, 14486-14494.

44. D. J. Siegwart, J. K. Oh and K. Matyjaszewski, *Prog. Polym. Sci.*, 2012, **37**, 18-37.
45. D. H. Seuyep N, D. Szopinski, G. A. Luinstra and P. Theato, *Polym. Chem.*, 2014, **5**, 5823-5828.
46. D. H. Seuyep N, G. A. Luinstra and P. Theato, *Polym. Chem.*, 2013, **4**, 2724-2730.
47. E. Behraves, S. Jo, K. Zygourakis and A. G. Mikos, *Biomacromolecules*, 2002, **3**, 374-381.
48. L. Krishna and M. Jayabalan, *J. Mater. Sci.: Mater. Med.*, 2009, **20**, 115-122.
49. W. J. Bailey, S.-R. Wu and Z. Ni, *Die Makromolekulare Chemie*, 1982, **183**, 1913-1920.
50. T. Kelen and F. Tüdös, *J. Macromol. Sci., Part A: Chem.*, 1975, **9**, 1-27.

## 4.7 Supporting Information

### 4.7.2 Homopolymerization behavior of VCP

The homopolymerization behavior of the monomer VCP under radical ring-opening polymerization condition at 120 °C was studied. After purification, the polymers were obtained as white solid. The representative  $^1\text{H}$  NMR spectrum of VCP homopolymer is shown in Figure S1. The characteristic proton signals of VCP units after polymerization are marked. According to the previous report of T. Endo *et al.*<sup>1</sup>, the structures of both ring-opened and ring-closed VCP units coexist in the VCP homopolymer. In the  $^1\text{H}$  NMR spectrum, the peak at  $\delta = 5.2$  ppm corresponds to the double bond protons from the VCP ring-opened structure (Structure 1 in Figure 4-S1). The broad signals between 1.5-2.5 ppm can be assigned to the protons from the VCP ring-closed structure (Structure 2 in Figure 4-S1). The peaks at  $\delta = 1.1$  ppm and  $\delta = 4.1$  ppm correspond to the  $\text{CH}_3\text{CH}_2\text{O}$ -group, which exists in both - the ring-opened and ring-closed - structure. Through comparing the total peak areas of double bond protons (peak *c* in Figure 4-S1,  $\delta = 5.2$  ppm) and methyl group (peak *a* in Figure 4-S1,  $\delta = 1.2$  ppm) the fraction of VCP units with ring-opened structure was calculated to be 52 mol%.

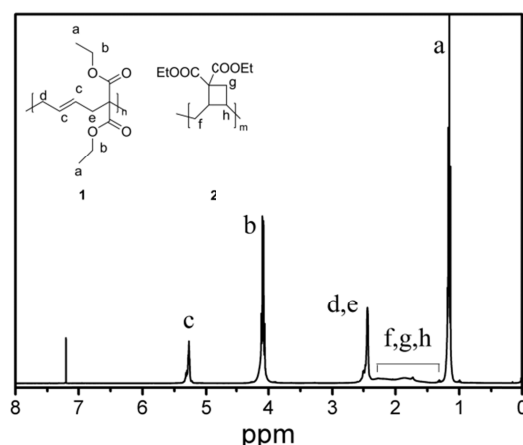


**Figure 4-S1.**  $^1\text{H}$ -NMR spectrum of VCP homopolymer prepared at 120 °C. Structure 1: VCP unit with ring-opened structure in PVCP; structure 2: VCP unit with ring-closed structure in PVCP.

### 4.7.3 Structure characterization of APCNs

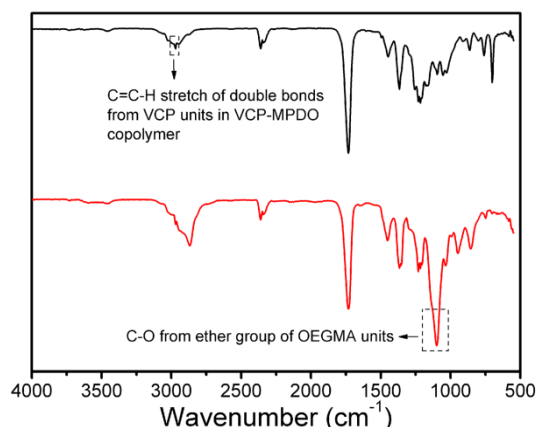


**Figure 4-S2.** IR spectra of original VCP-MPDO copolymers (black) and APCNs after purification (red).

### 4.7.4 Calculation of reactivity ratios for VCP and MPDO copolymerization

The copolymerization of VCP and MPDO was carried out with various monomer feed ratios and low yields (~5%) to determine the reactivity ratios. The feed ratios and compositions of the resulting copolymers are summarized in Table 4-S1.

**Table 4-S1.** VCP-MPDO copolymerization for determining reactivity ratios

entry <sup>a</sup>	VCP:MPDO in feed (mol-%)	Yield (%)	VCP:MPDO in Copolymer (mol-%) <sup>b</sup>
Copolymer I	80:20	5.7	67:33
Copolymer II	59:41	7.8	53:47
Copolymer III	39:61	4.2	46:54
Copolymer IV	28:72	5.1	42:58
Copolymer V	13:87	4.4	34:66

<sup>a</sup> reaction time: 6 h; reaction temperature: 120 °C; initiator: di-*tert*-butyl peroxide (1 wt% of monomer)

<sup>b</sup> Determined using <sup>1</sup>H-NMR of the resulting VCP-MPDO copolymers.

The  $r$ -parameters are determined applying the Kelen-Tüdös method as follows (Table 4-S2).<sup>2</sup>

$$\eta = \left[ r_1 + \frac{r_2}{\alpha} \right] \cdot \xi - \frac{r_2}{\alpha} \quad (1)$$

$$\eta = \frac{G}{\alpha + F} \quad (2)$$

$$\xi = \frac{F}{\alpha + F} \quad (3)$$

$$G = \frac{x(y-1)}{y} \quad (4)$$

$$F = \frac{x^2}{y} \quad (5)$$

$x$  = molar ratio of comonomers in feed =  $m_1/m_2$  ;  $y$  = molar composition of the copolymer =  $M_1/M_2$

$$\alpha = \text{constant} = \sqrt{F_m F_M} \quad (F_m = \text{smallest } F\text{-value}; F_M = \text{biggest } F\text{-value})$$

**Table 4-S2.**  $r$ -parameters calculation using Kelen-Tüdös method

	x	y	G	F	$\eta$	$\xi$
Copolymer I	4.04	2.04	2.06	8.00	0.24	0.93
Copolymer II	1.41	1.12	0.16	1.77	0.07	0.75
Copolymer III	0.65	0.86	-0.10	0.49	-0.10	0.45
Copolymer IV	0.39	0.71	-0.16	0.21	-0.19	0.26
Copolymer V	0.15	0.51	-0.14	0.04	-0.22	0.07

$$\alpha = \sqrt{F_m F_M} = 0.5923$$

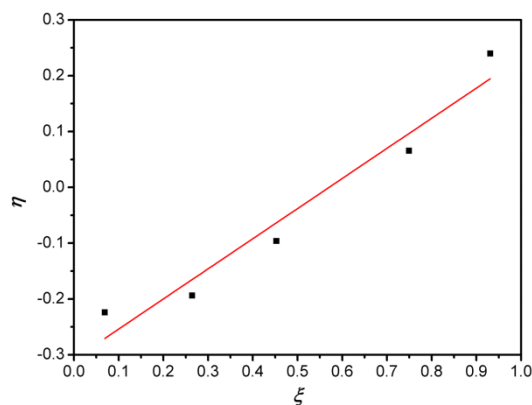


**Figure 4-S3.** Kelen-Tüdös plot for the determination of VCP and MPDO reactivity ratios (linear fit to the experimental data:  $R^2 = 0.953$ ).

The plot of  $\eta$  vs.  $\zeta$  is shown in Figure 4-S3. From the slope and intercept of the linear fit, the monomer reactivity ratios of VCP and MPDO were determined to  $r_{VCP} = 0.23 \pm 0.08$  and  $r_{MPDO} = 0.18 \pm 0.02$ . A comparison of the experimental data from Table 4-S1 with the calculated copolymerization diagram, using the  $r$ -values determined by the Kelen-Tüdös method, shows an excellent agreement.

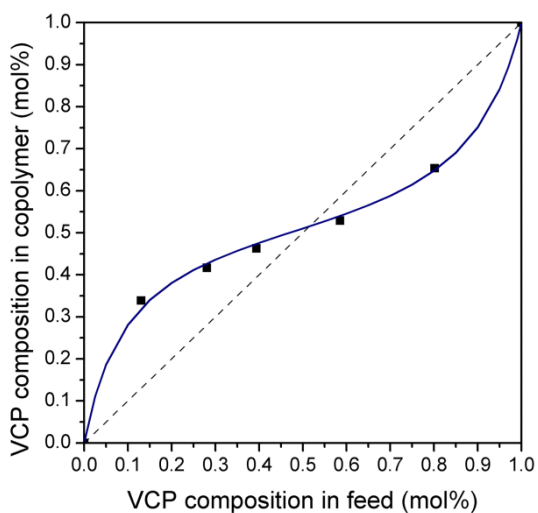


**Figure 4-S4.** Calculated copolymerization diagram (blue curve) and comparison with experimental data (squares) from Table S1.

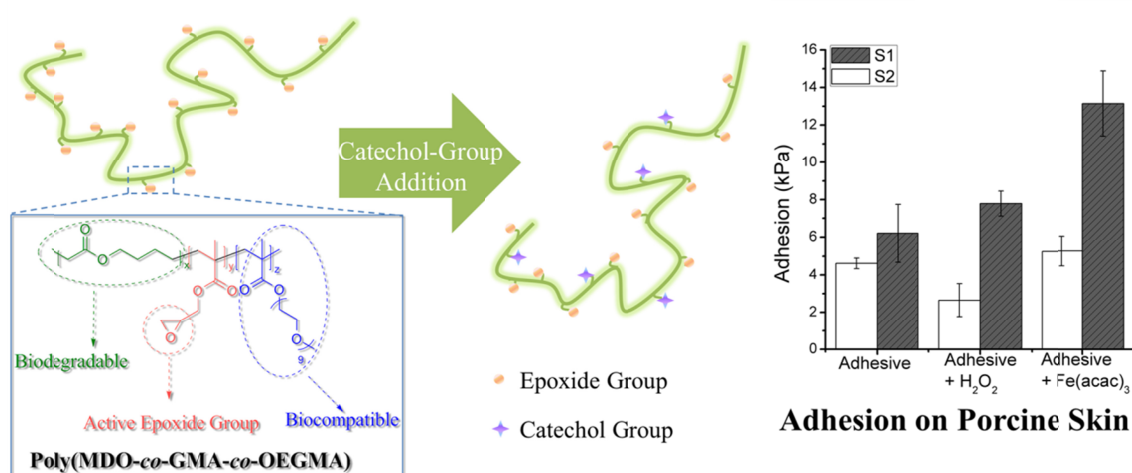
#### 4.7.5 Reference

1. Sanda, F.; Takata, T.; Endo, T. *Macromolecules* **1993**, *26*, 1818-1824.
2. Kelen, T.; Tüdös, F. *J. Macromol. Sci., Part A: Chem.* **1975**, *9*, 1-27.



## Chapter 5

### Enzymatically Degradable DOPA-containing Polyester Based Adhesives by Radical Polymerization



The results of this chapter have been submitted to *Macromolecules* as:

“Enzymatically Degradable DOPA-containing Polyester Based Adhesives by Radical Polymerization”

by Yinfeng Shi, Peiran Zhou, Valérie Jérôme, Ruth Freitag, and Seema Agarwal\*



## 5.1 Abstract

A designed 3,4-dihydroxyphenylalanine (DOPA) containing enzymatic degradable non-toxic synthetic adhesive with good adhesion to soft tissue and metals made by a simple two-step reaction is presented in this article. The adhesive had degradable polycaprolactone-type of repeat units together with glycidyl methacrylate (GMA) and oligo(ethylene glycol) methacrylate (OEGMA) in the polymer backbone. Radical initiated copolymerization of 2-methylene-1,3-dioxepane (MDO), glycidyl methacrylate (GMA) and OEGMA followed by immobilization of DOPA on epoxy rings of GMA provided the adhesive material.  $\text{Fe}(\text{acac})_3$  was proved to be the most effective cross-linking agent with lap shear strength of  $13.13 \pm 1.74$  kPa and  $218.4 \pm 16.0$  kPa on soft tissue (porcine skin) and metal (aluminum), respectively. The cross-linked adhesive showed good adhesion stability in pH 7 PBS buffer at 37 °C for at least one week. Due to the high adhesive strength, enzymatic degradability and low toxicity, the material is a promising candidate for future studies as medical glue.



## 5.2 Introduction

Adhesives are widely used in various industrial and medical fields in everyday life.<sup>1</sup> The medical polymeric adhesives in the applications like surgical operation, damage repairing *etc.* were very attractive and widely researched in the recent years.<sup>2-7</sup> One of the highly studied biomimetic adhesive systems is based on 3,4-dihydroxyphenylalanine (DOPA) and/or DOPA-mimetic catechol.<sup>8-11</sup> The DOPA group can be introduced onto polymer chains in various ways such as vinyl polymerization of DOPA containing monomers, polymer analogous reactions, chain-end ligation *etc.* as described in a recent review article.<sup>12</sup> DOPA can interact strongly with various substrates such as soft tissues (porcine dermal tissue)<sup>13, 14</sup>, hard mineralised tissues (cortical bone)<sup>15</sup>, metals (titanium, aluminium)<sup>16, 17</sup>, bovine submaxillary mucin<sup>18</sup> *etc.* leading to adhesion even in the presence of water. Also, many different cross-linking agents with DOPA containing polymers were tried in order to optimize the adhesive strength and speed of adhesion. Some of the commonly used cross-linking methods and agents were: oxidation in presence of oxygen, enzymes (such as tyrosinase, horseradish peroxidase), H<sub>2</sub>O<sub>2</sub>, silver oxide, periodate and cross-linking by coordination to metal ions such as Fe<sup>3+</sup> and other transition metal ions.<sup>19</sup>

In many of the literature known examples of DOPA containing polymeric adhesives, the C-C backbone hinders biodegradability and hence limits their use. Poly(amino acid) and polyester backbone could provide additional functionality such as biodegradability to DOPA based adhesives. For instance, synthetic analogs of DOPA containing natural peptides were prepared by ring-opening polymerization of *R*-amino acid and *N*-carboxyanhydride (NCA) by Deming *et al.*<sup>20</sup> Catechol functionalised amino acid-based poly(ester urea) (PEU) was produced using multi-step reaction sequence by Becker *et al.* The effect of substrate, molar mass, polymer concentration and type of curing agent on adhesive strength was studied. The lap-shear adhesive strength on porcine skin was comparable to commercial fibrin glue.<sup>21</sup> Poly(ethylene glycol) (PEG) block

copolymers with biodegradable polylactide and polycaprolactone were also reported for immobilization of DOPA containing peptides.<sup>16,22</sup> Messersmith *et al.* reported a branched poly(ethylene glycol) (PEG) end-functionalized with DOPA through alanine-alanine (Ala-Ala) dipeptide linker, which was susceptible to degradation by neutrophil elastase, for biodegradable adhesive application.<sup>23</sup> Most of the literature known methods of producing degradable DOPA containing adhesives used multistep reaction strategies requiring protection-deprotection chemistry.

In this work, we present a simple two-step method of making DOPA containing enzymatically degradable, biocompatible polymeric adhesive. In the first step, a terpolymer of oligo(ethylene glycol) methacrylate (OEGMA), glycidyl methacrylate (GMA) and 2-methylene-1,3-dioxepane (MDO) was produced using radical polymerization. MDO is a very well-studied cyclic ketene acetal that undergoes radical ring-opening polymerization for the formation of polycaprolactone (PCL) i.e. provides ester linkages in the polymer backbone.<sup>24-27</sup> Its copolymers with many other vinyl monomers such as methyl methacrylate, styrene, vinyl acetate, glycidyl methacrylate etc. are very well studied by us and others with an aim to provide degradability to otherwise non-degradable C-C backbone containing vinyl polymers.<sup>28-32</sup> Poly(ethylene glycol) (PEG) is widely used to reduce the *in vivo* body foreign reactions.<sup>33-35</sup> OEGMA is one of the vinyl polymerizable monomers for introducing PEG in a polymer.

The epoxide ring of GMA in terpolymer was used for immobilisation of 3-(3,4-dihydroxyphenyl)propionic acid, DOPA-mimetic catechol group in the second step. The amount of DOPA can easily be varied in the polymers by changing the amount of GMA in feed. The terpolymers were characterized for structure, adhesive properties, enzymatic degradability and biocompatibility.

## 5.3 Experimental Section

### 5.3.1 Materials

Glycidyl methacrylate (GMA, Aldrich) and oligo(ethylene glycol) methacrylate (OEGMA,  $M_n \sim 500$ , Aldrich) was passed through a basic alumina column to remove the inhibitor. Azobisisobutyronitrile (AIBN) was obtained from Sigma-Aldrich and recrystallized from methanol before use. 3-(3,4-dihydrophenyl)propionic acid (Alfa Aesar), phosphate-buffered saline (PBS, pH = 7, VWR Chemicals), Fe(acac)<sub>3</sub> (Aldrich), H<sub>2</sub>O<sub>2</sub> (30%, VWR Chemicals) and Lipase (from *Pseudomonas cepacia*,  $\geq 30$  U/mg, Aldrich) were used as received. 2-Methylene-1,3-dioxepane (MDO) was synthesized with our published procedure.<sup>28</sup> All solvents were distilled before use. Porcine skins were purchased from a local grocery store. 3-(4, 5-Dimethylthiazolyl-2)-2,5-diphenyl tetrazolium bromide (MTT), was purchased from Sigma-Aldrich. For cell culture materials were from Greiner, media and solutions were from Biochrome AG, Berlin, Germany.

### 5.3.2 Materials

<sup>1</sup>H (300 MHz), <sup>13</sup>C (75 MHz) NMR spectra were recorded on a Bruker Ultrashield-300 spectrometer in CDCl<sub>3</sub>, using tetramethylsilane (TMS) as an internal standard. UV-Vis measurement was carried out on a Hitachi U-3000 spectrometer. Gel permeation chromatography (GPC) was used for the measurement of molecular weights and polydispersity indexes (PDI). The instrument was equipped with 4 PSS-SDV gel columns (particle size = 5  $\mu$ m) with porosity ranges from 10<sup>2</sup> to 10<sup>5</sup> Å (PSS, Mainz, Germany) together with a differential refractive index detector (RI-101 from Shodex). THF (HPLC grade) was used as a solvent (for dissolving polymer and as eluting solvent) with flow rate of 1.0 mL/min.

### 5.3.3 Copolymerization of MDO, GMA and OEGMA under free radical condition

The details of the experimental procedure used for making the terpolymer (entry 1, Table 5-1) were described here. The mixture of MDO (0.26 g, 4.0 e.q.), GMA (0.42 g, 5.0 e.q.), OEGMA (0.29 g, 1.0 e.q.) and AIBN (1 mol% of monomers) was dissolved in 3.5 mL toluene and added into a 10-mL Schlenk tube equipped with a magnetic stirring bar under argon. The systems were degassed by freeze-vacuum-thaw cycle three times and sealed under argon. The sealed tubes were placed in a preheated oil bath at 60 °C for 2 h while stirring. After this time the reaction mixture was precipitated in hexane. Finally the polymer was dried in vacuum at 60 °C for 48 h. Different polymers were made by changing the feed ratio of the comonomers (Table 5-1) using similar procedure.

### 5.3.4 Coupling of catechol group

The details of the experimental procedure for preparing the adhesive S1 (entry 1, Table 2) were described here as an example. 3-(3,4-dihydrophenyl)propionic acid (0.34 g, 2.0 e.q. of GMA units in OEGMA-*co*-GMA-*co*-MDO copolymer) was dissolved in degassed poly(OEGMA-*co*-GMA-*co*-MDO) (0.4 g) THF solution (15 mL) under argon. The molar ratio of 3-(3,4-dihydrophenyl)propionic acid and the GMA units in poly(OEGMA-*co*-GMA-*co*-MDO) was 2:1. The reaction proceeded at 65 °C for 20 h under argon. The solvent was then distilled off and the degassed chloroform was added into the resulting reaction mixture. The unreacted 3-(3,4-dihydrophenyl)propionic acid was precipitated and filtered off. Finally the solvent was distilled out and the purified polymer was stored under argon.

### 5.3.5 Adhesion study on porcine skin

Adhesion property study was carried out by lap shear strength test on porcine skin. The porcine skins were cut to 1 × 4.5 cm size. 10±1 mg catechol groups coupled polyester

was spread over a  $1 \times 1$  cm area on one of porcine skin. The polymer was cross-linked by air,  $\text{H}_2\text{O}_2$  (30%, 15  $\mu\text{L}$ ) or  $\text{Fe}(\text{acac})_3$  solution in water (10 wt%, 15  $\mu\text{L}$ ) for 5 min. Another porcine skin was overlapped on the adhesive applied part and compressed for 30 sec. The lap shear strength was measured at room temperature with a Zwick/Roell testing machine (model 2008) equipped with 1 kN load cell. The maximum bonding force was recorded and divided by the overlapping contact area of porcine skins to calculate the lap adhesion strength as described in literature<sup>14</sup>.

### 5.3.6 Effect of PBS on adhesion property

Effect of PBS buffer on adhesion property was carried out by lap shear strength test on aluminum sheets coated with adhesive before and after dipping in buffer. The aluminum sheets were cut to  $1 \times 4.5$  cm size and overlapped at a  $1 \times 1$  cm area with adhesives (cross-linked by air,  $\text{H}_2\text{O}_2$  or  $\text{Fe}(\text{acac})_3$  solutions in water, same as adhesion study on porcine skins). The adherends were placed in pH = 7 PBS for different time intervals. After drying at 50 °C under vacuum overnight, the shear strength of adhesive was carried out with Zwick/Roell testing machine (model 2008) at a pull-rate of 2 mm/min.

### 5.3.7 *In vitro* enzymatic degradation

*In vitro* enzymatic degradation studies were carried out on  $\text{Fe}(\text{acac})_3$  cross-linked samples. 100 mg cross-linked sample was placed in pH = 7 PBS buffer solution with 0.2 mg/mL  $\text{NaN}_3$  and Lipase from *Pseudomonas cepacia* enzyme (5 U/mL) at 37 °C. The degradation medium was replaced every 24 hours. After definite time intervals, the sample were filtered, freeze dried and weighed.

### 5.3.8 MTT assay

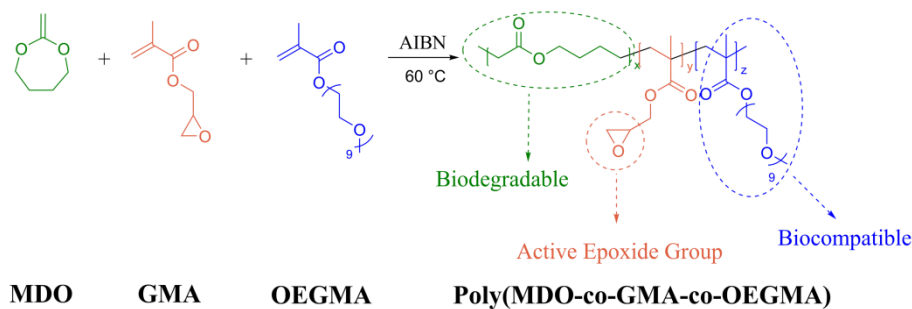
The cytotoxicity of the adhesive S1 (produced using copolymer OEGMA:GMA:MDO = 23:51:26, S1 in Table 5-2) and adhesive S2 (produced using copolymer OEGMA:GMA:MDO = 36:38:26, S2 in Table 5-2) was tested using L929 murine

fibroblasts (CCL-1, ATCC) according to the norm ISO 10993-5 using 1 mg/mL MTT-stock solution. The L929 cells were maintained in MEM cell culture medium supplemented with 10 % fetal calf serum (FCS), 100 mg/mL streptomycin, 100 IU/mL penicillin, and 4 mM L-glutamine. Cells were cultivated at 37° C in a humidified 5% CO<sub>2</sub> atmosphere. The polymers were solubilized at the highest possible concentrations in DMSO – due to the limit of solubility of these polymers in DMSO, stock solutions at concentrations  $\leq 20$  mg/mL were prepared. The polymers were tested in a concentration range from 0 to 0.4 mg/mL (corresponding to up to 2 vol. % DMSO per well, i.e., a concentration already slightly toxic for the cells) in 96-well plates. The solvent alone was included as control. The cells were seeded at a density of  $1 \times 10^4$  cells per well 24 hours prior to the experiment. As 100% viability control, untreated cells were used. For each dilution step, eight replicates were used. After dissolving the metabolically formed formazan crystals in isopropanol, the absorbance was measured using a plate reader (Genios Pro, Tecan) at a wavelength of 580 nm.

## 5.4 Results and Discussion

### 5.4.1 Synthesis of Poly(OEGMA-co-GMA-co-MDO) via RROP

The synthetic route to poly(OEGMA-co-GMA-co-MDO), the aliphatic polyester with enzymatic degradability and biocompatibility, was shown in the Scheme 5-1. The radical ring-opening copolymerization of OEGMA, GMA and MDO was carried out at 60 °C using AIBN as initiator. A series of poly(OEGMA-co-GMA-co-MDO) was prepared with various monomer ratios in feed (Table 5-1). The chemical structure of the resulting copolymers was determined by NMR spectroscopy (Figure 5-1). The characteristic signals of PMDO<sup>25</sup>, PGMA<sup>36</sup> and POEGMA<sup>29</sup> were observed in NMR spectra. In <sup>1</sup>H-NMR spectrum, all peaks could be well assigned by their chemical structures. The copolymer composition was calculated by comparing the integral ratios of -COO-CH<sub>2</sub>-CH<sub>2</sub>- of MDO units ( $\delta = 4.13$  ppm, peak *b* in Figure 1A), -OCH<sub>2</sub>CH<sub>2</sub>- of OEGMA units ( $\delta = 3.59$  ppm, peak *i* in Figure 5-1A) and epoxy group of GMA units ( $\delta = 3.21$  ppm). It is well-known that, MDO could be polymerized either as a ring-opened (formation of ester units) or ring-retained structure (formation of acetal rings).<sup>26</sup> In <sup>13</sup>C-NMR spectrum of resulting polymer, no peak was obvious around  $\delta = 100$  ppm (Figure 5-1B), which proved in combination with peaks observed in <sup>1</sup>H-NMR spectrum that all MDO units were polymerized as ring-opened structure providing caprolactone-type of repeat units in the polymer backbone.



**Scheme 5-1.** Schematic illustration of the synthesis of poly(OEGMA-co-GMA-co-MDO).

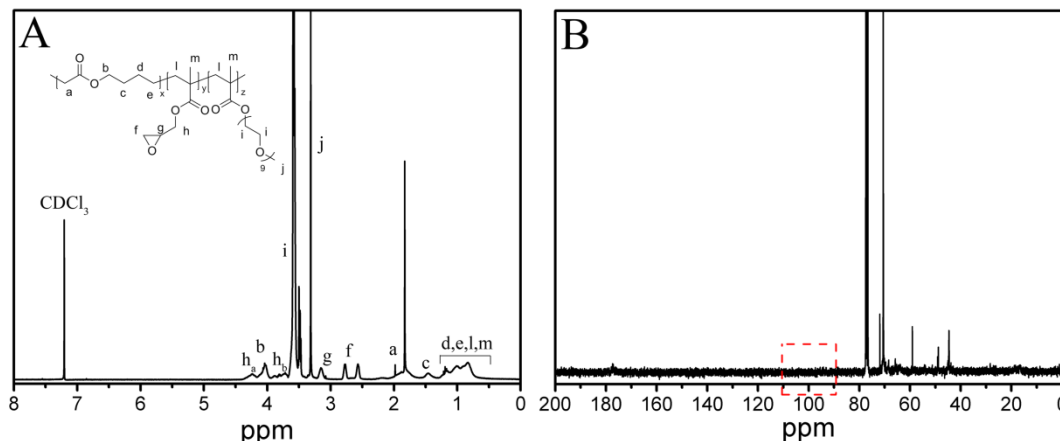


**Figure 5-1.** NMR spectra of poly(OEGMA-*co*-GMA-*co*-MDO), entry 2 in Table 1 as an example: A: <sup>1</sup>H-NMR spectrum; B: <sup>13</sup>C-NMR-spectrum. Absence of signal at  $\delta = 100$  ppm confirms formation of only ring-opened ester units from MDO.

The copolymers showed very high molar mass ( $1.0 - 1.4 \times 10^5$  g/mol) with unimodal GPC curves (Figure 5-2). The copolymer with the composition of OEGMA:GMA:MDO = 11:67:22 (entry 1 in Table 5-1) was obtained as white solid, while other copolymers (comonomer ratio in copolymer: OEGMA:GMA:MDO = 23:51:26 and 35:39:26, entries 2 and 3 in Table 5-1) were transparent viscous liquids (Figure 5-3). The viscous liquids (entries 2 and 3, Table 5-1) were used for adhesive application in this work.

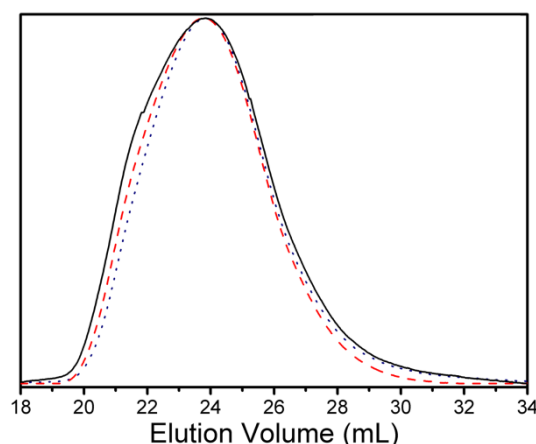


**Figure 5-2.** GPC traces of poly(OEGMA-*co*-GMA-*co*-MDO) with different copolymer compositions. Black: entry 1 in Table 5-1; red: entry 2 in Table 5-1; navy: entry 3 in Table 5-1.

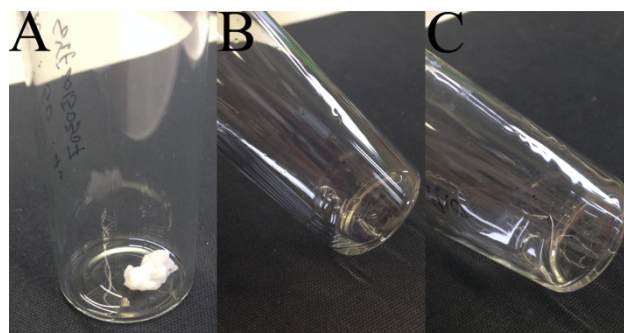


**Figure 5-3.** Photograph of poly(OEGMA-*co*-GMA-*co*-MDO) with different composition. A: copolymer of entry 1 in Table 5-1 (white solid); B: copolymer of entry 2 in Table 5-1 (transparent viscous liquid); C: copolymer of entry 3 in Table 5-1 (transparent viscous liquid).

**Table 5-1.** Copolymerization data and reaction conditions for OEGMA-GMA-MDO copolymers with various compositions.

Entry <sup>a</sup>	Feed composition (molar ratio) OEGMA:GMA:MDO	Yield (%)	$M_n^b$	PDI <sup>b</sup>	Polymer composition (molar ratio) OEGMA:GMA:MDO <sup>c</sup>
1	10:50:40	41.6	$1.37 \times 10^5$	2.2	11:67:22
2	25:35:40	35.3	$1.16 \times 10^5$	2.0	23:51:26
3	35:25:40	30.5	$1.02 \times 10^5$	2.3	35:39:26

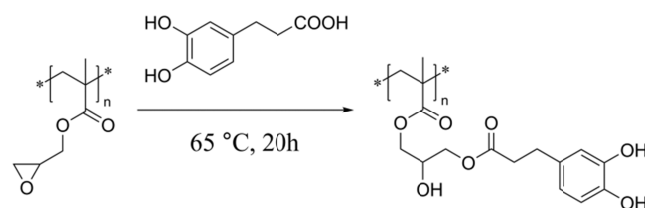
<sup>a</sup>: Reaction conditions: initiator: AIBN (1 mol% of monomers); temperature: 60 °C; reactions time: 2 h; solvent: toluene (1.9 mmol/mL of total monomers)

<sup>b</sup>: Determined by THF-GPC with RI detector; PMMA-standard was used for calibration (Figure 5-1).

<sup>c</sup>: Determined by <sup>1</sup>H-NMR spectra of resulting OEGMA-GMA-MDO copolymers (Figure 5-2).

#### 5.4.2 Covalent Immobilization of Catechol Group onto Poly(OEGMA-*co*-GMA-*co*-MDO)

Based on the high reactivity<sup>31</sup>, the epoxy group of GMA in poly(OEGMA-*co*-GMA-*co*-MDO) was used for covalent immobilization of catechol group by reaction with 3-(3,4-dihydroxyphenyl)propionic acid at 65 °C for 20 hours (Scheme 5-2).



**Scheme 5-2.** Ring-opening reaction of epoxy group on poly(OEGMA-co-GMA-co-MDO) chains with 3-(3,4-dihydroxyphenyl)propionic acid.

To determine the structure of resulting polymer after catechol immobilization, the functionalized polymer was dissolved in degassed THF (HPLC grade) under argon and then analyzed by UV/Vis spectroscopy. By comparing the UV/Vis spectra of resulting polymer and 3-(3,4-dihydroxyphenyl)propionic acid, it was obvious that the catechol group was immobilized on polymer as its characteristic peak was not changed (Figure 5-4).  $^1\text{H-NMR}$  spectroscopy was used to determine the amount of catechol grafted onto poly(OEGMA-co-GMA-co-MDO) (Figure 5-5). The integration ratio of catechol peaks at  $\delta = 6.4\text{--}6.6$  and the unreacted well-defined epoxy peak at  $\delta = 3.2$  ppm was used for determining grafting efficiency and amount of catechol immobilized on polymer backbone (Table 5-2).

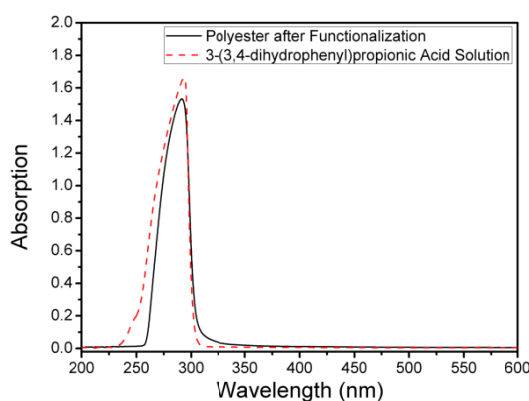


**Figure 5-4.** Comparison of UV/Vis spectra of catechol functionalized poly(OEGMA-co-GMA-co-MDO) (black) and 3-(3,4-dihydroxyphenyl)propionic acid (red) in THF (HPLC grade); concentration of functionalized terpolymer: 6.0 mg/mL, concentration of 3-(3,4-dihydroxyphenyl)propionic acid: 0.8 mg/mL.

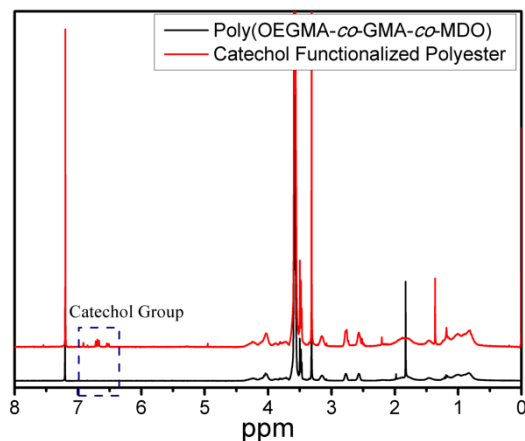


**Figure 5-5.**  $^1\text{H-NMR}$  spectra of poly(OEGMA-*co*-GMA-*co*-MDO) (bottom) and the catechol functionalized polyester (poly(OEGMA-*co*-GMA-*co*-MDO) (top).

**Table 5-2.** Characterization of catechol functionalized polyester.

Sample	Polymer composition OEGMA:GMA:MDO	Reacted GMA units in copolymer (mol%)	Content of catechol group on functionalized polyester (mol%)
S1	23:51:26	30.3	15.5
S2	35:39:26	23.9	9.3

### 5.4.3 Adhesion Property Characterization of Adhesives with and without cross-linking

For adhesive application, medical grade hydrogen peroxide (30% in water) or  $\text{Fe}(\text{acac})_3$  (10 wt% in water) were used as cross-linking agents. Fresh porcine skin was used as representative soft tissue for studying the adhesion property as determined by lap shear strength test measurement (Figure 5-6A). The adhesion properties with/without cross-linkers were shown in Figure 5-6B. Due to the higher content of catechol groups (catechol group content of S1: 15.5 mol%, catechol group content of S2: 9.3 mol%), pure catechol functionalized terpolyester S1 had the lap adhesion strength of  $6.21 \pm 1.53$  kPa, which was slightly higher than that of adhesive S2 ( $4.62 \pm 0.28$  kPa). The adhesive S1 cross-linked by  $\text{Fe}(\text{acac})_3$  exhibited the best adhesive property (lap adhesion strength

$13.13 \pm 1.74$  kPa), which was increased by 150 % compared with the catechol functionalized polyester without cross-linking. Because of the differences in methodology and types of adherends, it is difficult to directly make a comparison of our result and other reported studies in the literature. However, the adhesive property of  $\text{Fe}(\text{acac})_3$  cross-linked adhesive S1 is similar to the literature adhesive system with C-C non-degradable backbone, which was based on the terpolymer of acrylic acid (AA), acrylic acid *N*-hydroxysuccinimide ester (AANHS) and *N*-methacryloyl-3,4-dihydroxyl-*L*-phenylalanine (MDOPA), and cross-linked by thiol-terminated 3-armed poly(ethylene glycol)<sup>14</sup>. The lap adhesion strength value of our system was much greater than the existing medical adhesive CoSeal ( $\sim 0.6$  kPa, Baxter, Inc.)<sup>37</sup> and fibrin glue ( $\sim 5$  kPa)<sup>38</sup> obtained in the previous studies. Compared with the reported catechol-based biodegradable PEU copolymers (lap shear measurement value  $\sim 9$  kPa on porcine skin)<sup>21</sup>, the present adhesive showed a higher adhesion on porcine skin.

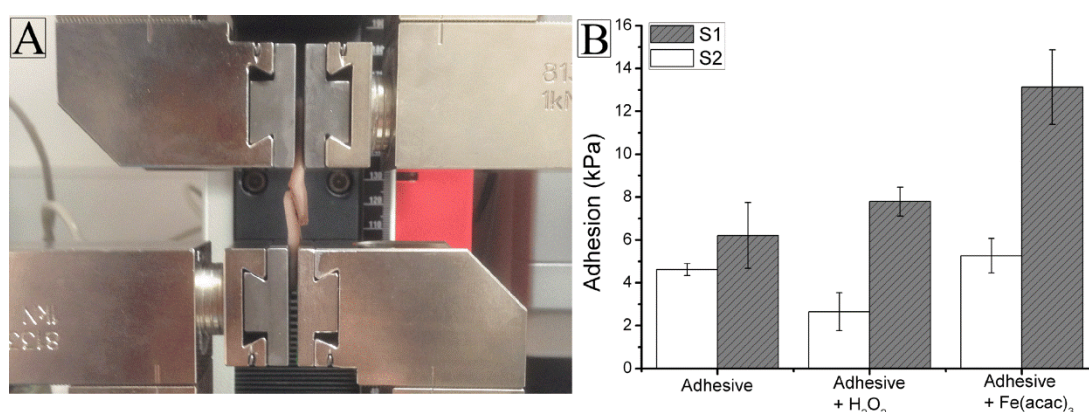


**Figure 5-6.** Adhesion test on porcine skin. A: photograph of lap shear strength test on fresh porcine skin. B: Adhesion properties of prepared adhesives with different cross-linking agents.

It was interesting to check the effect of PBS buffer on adhesion strength as these materials could be interesting as medical glue. Unfortunately, the test could not be carried out using porcine skin as it started deteriorating under our experimental conditions with time, therefore aluminium sheets were used. The aluminium sheets were cut to  $1 \times 4.5$  cm size and overlapped at a  $1 \times 1$  cm area with adhesives. After cross-linking with  $\text{H}_2\text{O}_2$  or

$\text{Fe}(\text{acac})_3$  at 37 °C for 1 hour, the adherends were placed in pH = 7 PBS buffer solution at 37 °C for different time intervals and tested for lap shear test before and after putting in buffer solution (Figure 5-7). Due to the substrate influences on the DOPA containing biomimetic adhesives,<sup>17</sup> the adhesion strength on aluminum sheets was much higher than on porcine and the sample S1 cross-linked with  $\text{Fe}(\text{acac})_3$  exhibited the highest adhesive strength around  $218.4 \pm 16.0$  kPa (Figure 5-7A) and the least drop in strength after putting in PBS buffer for 7 days ( $143.3 \pm 37.4$  kPa) and could be highly promising candidate as medical glue.

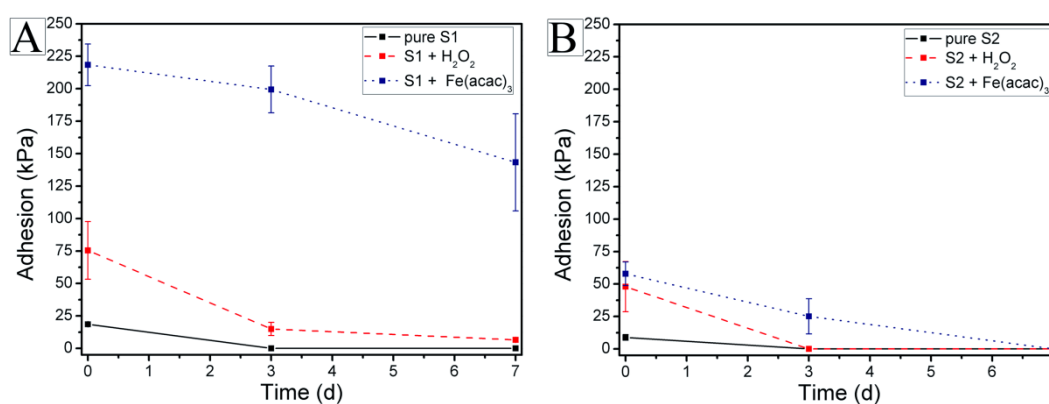


**Figure 5-7.** Lap shear strength of adhesives after placing in pH = 7 PBS buffer solution for different time. A: adhesion property of adhesive S1 against PBS buffer solution; B: adhesion property of adhesive S2 against PBS buffer solution.

The intended use of MDO in terpolymers was to provide enzymatically degradable ester linkages in the polymer backbone. Therefore, further enzymatic degradation studies were carried out using  $\text{Fe}(\text{acac})_3$  cross-linked S1 sample by putting 100 mg in PBS buffer (pH = 7) in presence of lipase from *Pseudomonas cepacia* (5 U/mL) and 0.2 mg/mL  $\text{NaN}_3$ . This mixture was then placed at 37 °C with shaking for different time. After freeze drying, the remaining weight of the adhesive was recorded and described in Figure 8. It's obvious that the prepared adhesive could be degraded in the presence of lipase from *Pseudomonas cepacia*. Due to the amorphous structure and hydrophilic groups (PEG group) on the functionalized terpolyester, the adhesive showed a fast degradation rate (compared with pure catechol functionalized PCL polymers<sup>22</sup>).

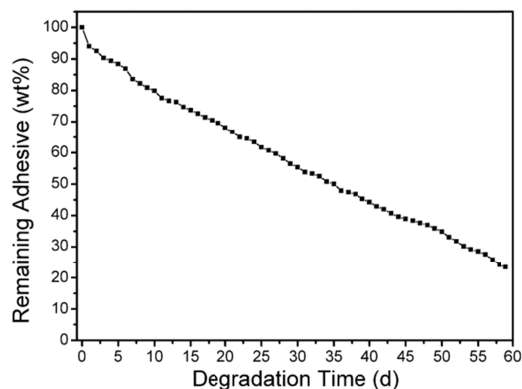


**Figure 5-8.** Mass loss profiles of adhesive S1 cross-linked by Fe(acac)<sub>3</sub>.

#### 5.4.4 Biocompatibility

The copolymers of adhesive S1 and adhesive S2 showing adhesive properties could be interesting as medical glues. In order to obtain an initial idea of their cytotoxicity towards mammalian cells, the standard MTT assay was performed. Therefore, the L929 cells were exposed to both polymers for 24 hours. Within the analyzed range of concentrations, none of the adhesive polymers were toxic enough to reduce the viability of cell population by 50%. Both adhesives did not show higher cytotoxicity than the solvent (DMSO) for concentration  $\leq 0.4$  mg/mL (Figure 5-9).

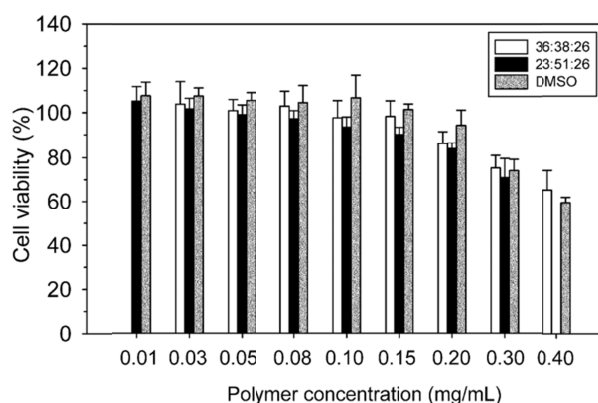


**Figure 5-9.** Cytotoxicity of the catechol functionalized OEGMA-GMA-MDO copolymers in L929 cells. Incubation period was 24 hours and cell seeding density  $1 \times 10^4$  cells per well. The data represent mean  $\pm$  s.d. from three independent experiments: black: adhesive S1; white adhesive S2.

## 5.5 Conclusion

In this report, we designed a novel biomimetic adhesive with good adhesion property, biodegradability and biocompatibility. The bio-adhesive could be successfully produced via a simple two-step reaction. The chemical structure of the resulting DOPA mimetic adhesive was confirmed by NMR and UV/Vis spectroscopy. The synthetic adhesive could be rapidly and effectively cross-linked using  $\text{Fe}(\text{acac})_3$  as cross-linking agent. After cross-linking, the adhesive showed a good adhesion property on porcine skin and the lap adhesion strength value is much greater than the existing medical adhesive CoSeal ( $\sim 0.6$  kPa, Baxter, Inc.)<sup>37</sup> and fibrin glue ( $\sim 5$  kPa)<sup>38</sup> obtained in the previous studies. Under the condition of body temperature ( $37\text{ }^\circ\text{C}$ ), the cross-linked adhesive showed good adhesion stability against pH = 7 PBS solution in at least 7 days. Due to the unique property, enzymatically degradability and low toxicity, the adhesive showed a potential to be used in the medical application field.

**Acknowledgment:** Julia Müller (Chair for Process Biotechnology, University of Bayreuth) assisted with the MTT experiments.

## 5.6 References

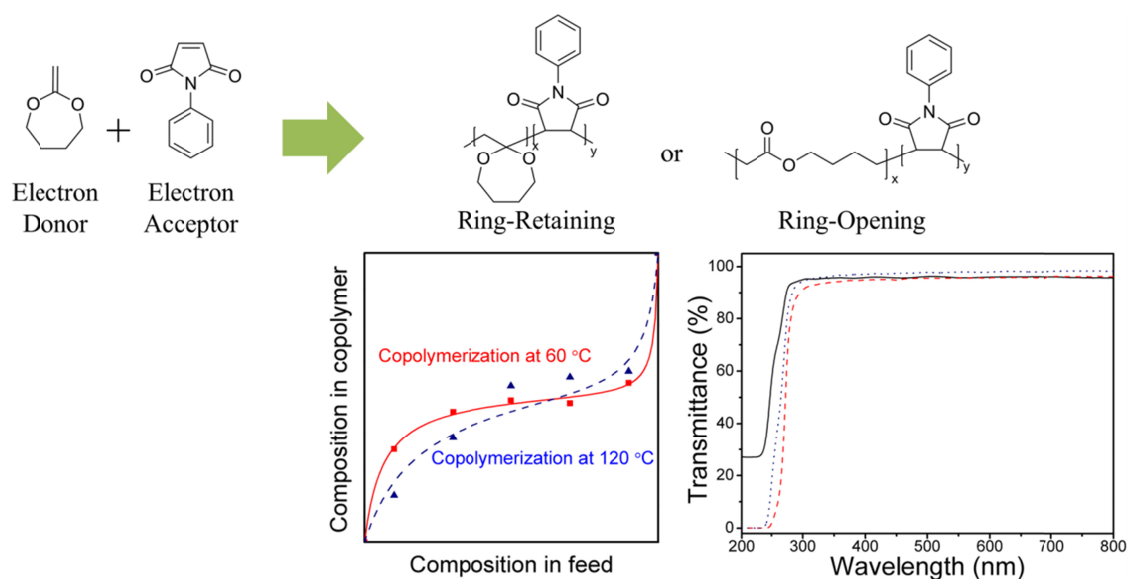
1. P. Cognard, in *Handbook of Adhesives and Sealants*, ed. C. Philippe, Elsevier Science Ltd, 2006, vol. Volume 2, pp. 51-195.
2. J. H. Waite, *Integrative and Comparative Biology*, 2002, **42**, 1172-1180.
3. T. E. Lipatova, in *Biopolymers/Non-Exclusion HPLC*, Springer Berlin Heidelberg, 1986, vol. 79, pp. 65-93.
4. L. Moroni and J. H. Elisseeff, *Mater. Today*, 2008, **11**, 44-51.
5. W. D. Spotnitz and S. Burks, *Transfusion*, 2008, **48**, 1502-1516.
6. Y. Liu, K. Ai and L. Lu, *Chem. Rev.*, 2014, **114**, 5057-5115.
7. M. Cencer, M. Murley, Y. Liu and B. P. Lee, *Biomacromolecules*, 2015, **16**, 404-410.
8. J. H. Waite and M. L. Tanzer, *Science*, 1981, **212**, 1038-1040.
9. T. J. Deming, *Curr. Opin. Chem. Biol.*, 1999, **3**, 100-105.
10. N. Holten-Andersen, M. J. Harrington, H. Birkedal, B. P. Lee, P. B. Messersmith, K. Y. C. Lee and J. H. Waite, *Proceedings of the National Academy of Sciences*, 2011, **108**, 2651-2655.
11. M. J. Harrington, A. Masic, N. Holten-Andersen, J. H. Waite and P. Fratzl, *Science*, 2010, **328**, 216-220.
12. E. Faure, C. Falentin-Daudré, C. Jérôme, J. Lyskawa, D. Fournier, P. Woisel and C. Detrembleur, *Prog. Polym. Sci.*, 2013, **38**, 236-270.
13. A. B. Sean, R.-J. Marsha, P. L. Bruce and B. M. Phillip, *Biomedical Materials*, 2007, **2**, 203.

14. H. Chung and R. H. Grubbs, *Macromolecules*, 2012, **45**, 9666-9673.
15. H. Shao, K. N. Bachus and R. J. Stewart, *Macromolecular Bioscience*, 2009, **9**, 464-471.
16. B. P. Lee, C.-Y. Chao, F. N. Nunalee, E. Motan, K. R. Shull and P. B. Messersmith, *Macromolecules*, 2006, **39**, 1740-1748.
17. C. R. Matos-Pérez, J. D. White and J. J. Wilker, *J. Am. Chem. Soc.*, 2012, **134**, 9498-9505.
18. K. Huang, B. P. Lee, D. R. Ingram and P. B. Messersmith, *Biomacromolecules*, 2002, **3**, 397-406.
19. J. Yang, M. A. Cohen Stuart and M. Kamperman, *Chem. Soc. Rev.*, 2014, **43**, 8271-8298.
20. M. Yu and T. J. Deming, *Macromolecules*, 1998, **31**, 4739-4745.
21. J. Zhou, A. P. Defante, F. Lin, Y. Xu, J. Yu, Y. Gao, E. Childers, A. Dhinojwala and M. L. Becker, *Biomacromolecules*, 2015, **16**, 266-274.
22. J. L. Murphy, L. Vollenweider, F. Xu and B. P. Lee, *Biomacromolecules*, 2010, **11**, 2976-2984.
23. C. E. Brubaker and P. B. Messersmith, *Biomacromolecules*, 2011, **12**, 4326-4334.
24. S. Jin and K. E. Gonsalves, *Macromolecules*, 1998, **31**, 1010-1015.
25. W. J. Bailey, Z. Ni and S.-R. Wu, *J. Polym. Sci., Polym. Chem. Ed.*, 1982, **20**, 3021-3030.
26. S. Agarwal, *Polym. Chem.*, 2010, **1**, 953-964.
27. S. Agarwal, N. Naumann and X. Xie, *Macromolecules*, 2002, **35**, 7713-7717.
28. S. Agarwal and L. Ren, *Macromolecules*, 2009, **42**, 1574-1579.

29. Q. Jin, S. Maji and S. Agarwal, *Polym. Chem.*, 2012, **3**, 2785-2793.
30. T. Cai, Y. Chen, Y. Wang, H. Wang, X. Liu, Q. Jin, S. Agarwal and J. Ji, *Polym. Chem.*, 2014, **5**, 4061-4068.
31. J. Undin, A. Finne-Wistrand and A.-C. Albertsson, *Biomacromolecules*, 2013, **14**, 2095-2102.
32. J. Undin, A. Finne-Wistrand and A.-C. Albertsson, *Biomacromolecules*, 2014, **15**, 2800-2807.
33. L. van Vlerken, T. Vyas and M. Amiji, *Pharm. Res.*, 2007, **24**, 1405-1414.
34. G. Liu, Q. Jin, X. Liu, L. Lv, C. Chen and J. Ji, *Soft Matter*, 2011, **7**, 662-669.
35. P. Gasteier, A. Reska, P. Schulte, J. Salber, A. Offenhäusser, M. Moeller and J. Groll, *Macromolecular Bioscience*, 2007, **7**, 1010-1023.
36. M. H. Espinosa, P. J. O. del Toro and D. Z. Silva, *Polymer*, 2001, **42**, 3393-3397.
37. Y. Liu, H. Meng, S. Konst, R. Sarmiento, R. Rajachar and B. P. Lee, *ACS Applied Materials & Interfaces*, 2014, **6**, 16982-16992.
38. I. Strehin, Z. Nahas, K. Arora, T. Nguyen and J. Elisseeff, *Biomaterials*, 2010, **31**, 2788-2797.

## Chapter 6

### Thermally stable optically transparent copolymers with degradable ester linkages



The results of this chapter have been submitted to *e-polymers* as:

“Thermally stable optically transparent copolymers of 2-methylene-1,3-dioxepane and *N*-phenyl maleimide with degradable ester linkages”

by Yinfeng Shi and Seema Agarwal\*



## 6.1 Abstract

The copolymers of 2-methylene-1,3-dioxepane (MDO) and *N*-phenyl maleimide (NPM) prepared by radical polymerization with high thermal stability, glass transition temperature and optical transparency are presented. The polymers made under specific reaction conditions i.e. 120°C and high amounts of MDO had degradable ester units, which were formed via radical ring-opening polymerization of MDO. Formation of charge-transfer complex between MDO and NPM also led to the formation of high molar mass copolymers by simple mixing and heating of monomers without use of any initiator. The structural characterization of the copolymers including mechanistic studies was carried out using NMR and thermal properties were studied using DSC and TGA.



## 6.2 Introduction

*N*-substituted maleimides are interesting monomers for making transparent thermally stable polymeric materials.<sup>1-8</sup> Under radical polymerization condition, *N*-substituted maleimides make either AB-alternating or sequence controlled 2:1 AAB-polymers with vinyl monomers having electron rich double bond such as styrene, vinyl ether, alpha-substituted propylene.<sup>3</sup> The alternating polymers were formed via a charge transfer complex between electron rich and electron poor monomers.<sup>9-12</sup> The maleimide ring structure in every repeat unit provides very high thermal stability and glass transition temperature to the resulting polymers.<sup>1-4</sup>

Cyclic ketene acetals (CKAs) are interesting monomers with an electron rich double bond due to the presence of two electron donating oxygen atoms. They undergo radical and cationic ring-opening polymerization and provide polyesters, polyacetals or a combination of two depending upon the structure of CKA and reaction conditions.<sup>13</sup> 2-methylene-1,3-dioxepane (MDO) is one of the very well-studied CKA in terms of homo- and copolymerization with large number of vinyl monomers such as methyl methacrylate (MMA)<sup>14</sup>, styrene (St)<sup>15</sup>, vinyl acetate (VAc)<sup>16,17</sup>, propargyl acrylate (PA)<sup>18</sup>, glycidyl methacrylate (GMA)<sup>19, 20</sup> etc. Homopolymerization of MDO leads to the aliphatic biodegradable polyester with polycaprolactone (PCL) like structure<sup>21</sup>, whereas cationic polymerization of MDO provides mainly ring-retained acetal units in the polymer backbone<sup>22</sup>. Due to the big difference between the reactivity ratios, quantitative ring-opening leading to block-type statistical copolymers with ester units coming from MDO together with vinyl comonomer units is possible.<sup>23</sup>

Interestingly, MDO provided hydrolytically degradable polymers with high glass transition temperature ( $T_g$ ) by simple mixing and heating with electron deficient  $\alpha$ -methylene- $\gamma$ -butyrolactone, which is a bio-based monomer derived from white tulips, in our previous work.<sup>24</sup> With an aim to provide highly thermal-stable (bio)degradable transparent cost-effective polymer, the copolymerization behavior of MDO and *N*-phenyl

maleimide (NPM) was studied in this work. After radical ring-opening copolymerization, MDO was expected to provide degradable ester units on the polymer backbone and NPM was expected to introduce high thermal stability and glass transition temperature. We studied the copolymerization behavior of NPM and MDO using different reaction conditions such as monomer feeds, reaction temperatures, with and without radical initiators. The mechanistic aspects, the structure and thermal properties of the resulting copolymers were studied using NMR, DSC and TGA analysis. The hydrolytically degradable copolymers of 2-methylene-1,3-dioxepane (MDO) and *N*-phenyl maleimide (NPM) with high thermal stability, glass transition temperatures and optical transparency could be obtained under specific reaction conditions.

## 6.3 Experimental Section

### 6.3.1 Materials

The monomer (2-Methylene-1,3-dioxepane (MDO)) was made according to published literature.<sup>25</sup> 2,2'-Azobis(isobutyronitrile) (AIBN, Aldrich) and *N*-phenylmaleimide (NPM, Aldrich) were used after recrystallization from methanol. Di-*tert*-butyl peroxide (DTBP, Aldrich) was used as received. All solvents were distilled before use.

### 6.3.2 Instrumentation

<sup>1</sup>H (300 MHz), <sup>13</sup>C (75 MHz) NMR spectra were recorded on a Bruker Ultrashield-300 spectrometer in CDCl<sub>3</sub>, using tetramethylsilane (TMS) as an internal standard. Deconvolution technology was used for NMR-spectra analysis. UV-Vis measurement was carried out on a Hitachi U-3000 spectrometer. Molecular weights ( $M_{n, GPC}$  and  $M_{w, GPC}$ ) and polydispersity indexes (PDI) of the polymers were determined by gel permeation chromatography (GPC). The columns and detector used were two PSS-SDV gel columns (PSS, Mainz, Germany) and differential refractive index detector, respectively. DMF (HPLC grade) with LiBr (5 g/L in DMF) was used as an eluting solvent with flow rate of 0.5 mL/min. A PMMA calibration was employed for molar mass analysis. Mettler thermal analyser with 851 TG and 821 DSC modules were used for determination of thermal stability and glass transition temperatures, respectively in nitrogen. A heating rate of 10 K/min was used. The amount of sample used for measurements was 10±1 mg for both DSC and TGA analysis.

### 6.3.3 General procedure for the copolymerization of MDO and NPM

The reactions were carried out under argon in a Schlenk tube. The mixture of MDO and NPM with different mole ratios (MDO:NPM = 1:9, 3:7, 5:5, 7:3 and 9:1) and radical initiator (AIBN or DTBP) (1 wt% of monomer) were dissolved in anisole and degassed

by three freeze-vacuum-thaw cycles. The reaction was started by putting the tube in a preheated oil bath at different temperatures (60 °C, using AIBN as initiator, or 120 °C, using DTBP as initiator) for 2 h while stirring. After this, the reaction mixture was precipitated into methanol, filtered and dried at 40 °C for 48 h.

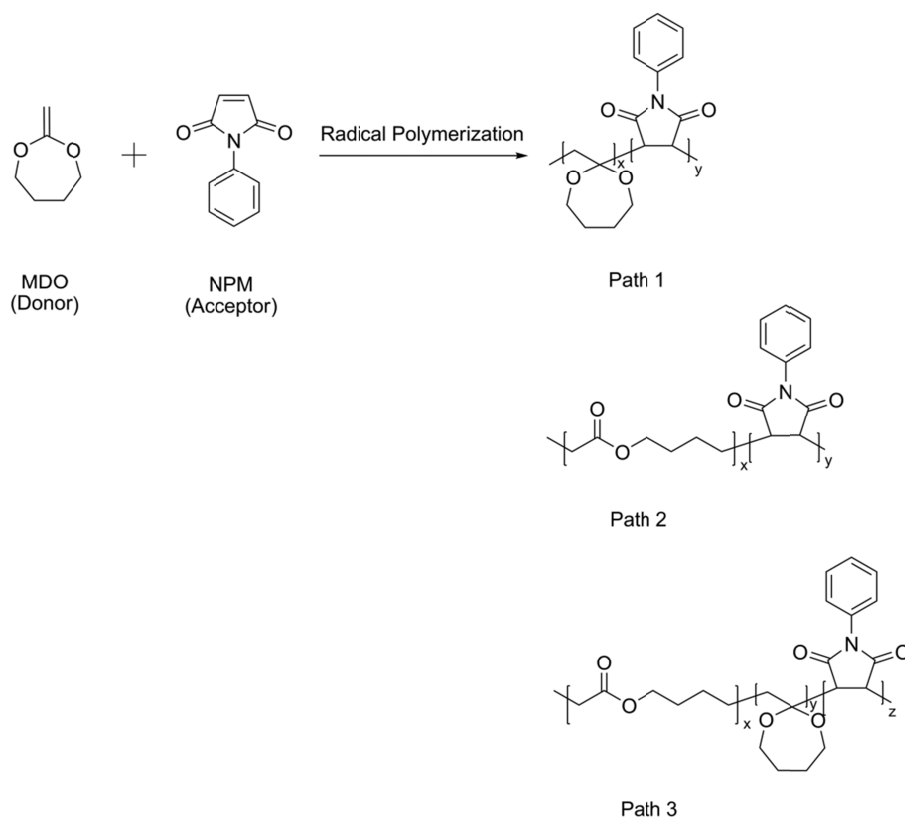
#### **6.3.4 Methanolysis of copolymers (MDO-NPM)**

The copolymer prepared at 120°C with MDO:NPM = 5:5 in feed was used for hydrolysis experiment. 0.30 g of copolymer was dissolved in a mixture of dioxane (15 mL) and methanolic KOH (25 mL, 5 wt%) and heated to reflux for 24h. After this time, the solution was neutralized with 3 ml of concentrated hydrochloric acid and then extracted with chloroform followed by washing with water. The solvent was evaporated under reduced pressure to get a yellow solid which was dried under vacuum at 50 °C for two days.

## 6.4 Results and Discussion

### 6.4.1 Copolymerization of MDO and NPM at 60 °C

Initially, various reactions for the copolymerization of MDO with NPM were carried out by changing the molar ratio of two monomers in feed (MDO:NPM = 1:9, 3:7, 5:5, 7:3 and 9:1) at 60 °C using AIBN as initiator. The GPC traces for the reaction product were unimodal (Figure 6-1) with molar mass ranged from  $6.38 \times 10^4$  to  $2.08 \times 10^5$  and polydispersity index (PDI) from 1.7 to 2.0. During copolymerization, MDO could undergo either ring-opening polymerization giving ester units, vinyl polymerization producing acetal rings or a combination of two (Scheme 6-1).<sup>13</sup>



**Scheme 6-1.** Different possibilities during MDO-NPM copolymerization. Path 1: MDO copolymerized with ring-retained structure; Path 2: MDO copolymerized with ring-opened structure; Path 3: MDO copolymerized with ring-opened and ring-retained structure.

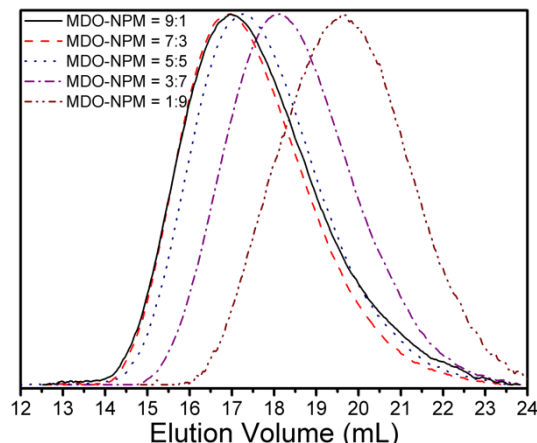


**Figure 6-1.** GPC curves of copolymers made by radical polymerization of MDO and NPM with different monomer ratios in feed at 60 °C.

In previous studies it showed formation of quantitative ester units during copolymerization with vinyl monomers using radical initiators at reactions temperatures between 60-120 °C,<sup>13, 25-27</sup> whereas cationic polymerization of MDO provided mainly ring-retained acetal units.<sup>22</sup> Therefore, the resulting copolymer structure was characterized by <sup>1</sup>H-NMR and <sup>13</sup>C-NMR spectroscopy (Figure 6-2). In <sup>13</sup>C-NMR spectra, a very strong peak at  $\delta = 100$  ppm was observed. This showed the presence of ring-retained acetal rings formed by vinyl polymerization of MDO as the major structure (Figure 6-2B). The characteristic proton signals of both ring-retained MDO and NPM units were also present and marked in the <sup>1</sup>H-NMR spectrum (Figure 6-2A). The peak integration at  $\delta = 6.5-7.5$  ppm (aromatic protons of NPM) and  $\delta = 2.5$  ppm (methylene group (*a*) of MDO unit) was used for the determination of copolymer composition as listed in Table 6-1. The comonomer ratio of MDO and NPM in resulting copolymers was almost 1:1 for different feed ratios. The copolymer with very large amount of NPM in feed (MDO:NPM = 1:9) showed deviation from copolymer composition of MDO:NPM = 1:1 and the ratio of comonomers in copolymer was calculated as MDO:NPM = 1:3. On using very large amounts of MDO in the feed (MDO:NPM = 9:1), a small peak appeared at  $\delta = 4.0$  ppm in <sup>1</sup>H-NMR spectrum originating from -C(O)OCH<sub>2</sub>- protons of ring-opened ester MDO units (supporting information, Figure 6-S1). This showed the

formation of a mixed structure with both ester (formed by ring-opening) and ring-acetal units (formed by ring-retained vinyl polymerization) in copolymers on using large amounts of MDO monomer in feed (Path 3 in Scheme 6-1). The ratio of ring-opened and ring-retained units of MDO was determined by deconvolution of overlapping  $^1\text{H-NMR}$  peaks between  $\delta = 4.1\text{-}3.9$  ppm. Approximately, only 4 mol% of the total MDO units were ring-opened and present as ester units in the MDO-NPM copolymer prepared with the feed monomer ratio of MDO:NPM = 9:1. The results confirmed that the MDO units showed a high potential to undergo simple vinyl polymerization with ring-retained units at 60 °C (Path 1 in Scheme 6-1). The MDO units with ring-opened ester structure only existed in the MDO-NPM copolymer prepared with the monomer ratio of MDO:NPM = 9:1 in feed.

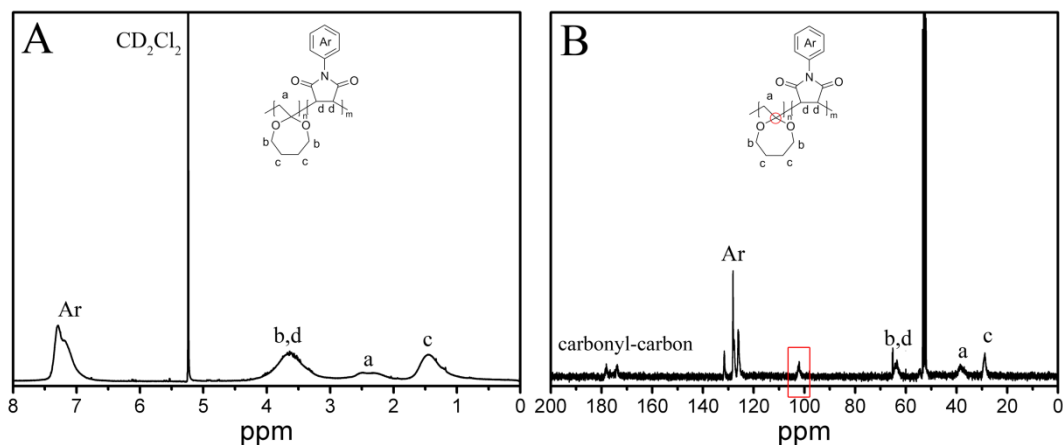


**Figure 6-2.**  $^1\text{H-NMR}$  (A) and  $^{13}\text{C-NMR}$  (B) spectra of MDO-NPM copolymer (MDO:NPM = 5:5 in feed) prepared at 60°C.

**Table 6-1.** Copolymerization of MDO and NPM at 60 °C.

Entry	Feed ratio (molar ratio)		Yield %	$M_n^b$	PDI <sup>b</sup>	Copolymer composition (molar ratio) <sup>c</sup>		MDO with ring-opened structure (mol %) <sup>c</sup>
	MDO	NPM				MDO <sup>d</sup>	NPM	
	1 <sup>a</sup>	90				10	26.3	
2 <sup>a</sup>	70	30	61.3	$2.08 \times 10^5$	1.8	53	47	- <sup>e</sup>
3 <sup>a</sup>	50	50	52.4	$1.81 \times 10^5$	1.8	49	51	- <sup>e</sup>
4 <sup>a</sup>	30	70	51.0	$1.28 \times 10^5$	1.7	45	55	- <sup>e</sup>
5 <sup>a</sup>	10	90	37.9	$6.38 \times 10^4$	1.9	25	75	- <sup>e</sup>

<sup>a</sup>: Initiator: AIBN, 0.5 mol % of monomer; reaction temperature: 60 °C; reaction time: 2 h; solvent: anisole.

<sup>b</sup>: Characterized by GPC with RI detector, calibration with PMMA standard (Figure 6-1).

<sup>c</sup>: Characterized by <sup>1</sup>H-NMR spectra of MDO-NPM copolymers with deconvolution method (Figure 6-2A).

<sup>d</sup>: Ring-opened and ring-retained MDO.

<sup>e</sup>: The content of MDO units with ring-opened structure was very low (lower than 1 mol% of all MDO units in copolymer) and could not be calculated due to the strong overlapping.

## 6.4.2 Copolymerization of MDO and NPM at 120 °C

In an effort to produce MDO-NPM copolymers with higher content of MDO units with ring-opened structure, a series of MDO-NPM copolymers were prepared at 120 °C with various monomer ratios in feed. The GPC traces for the copolymers (MDO:NPM = 9:1, 7:3, 5:5 and 3:7 in feed) were unimodal (Figure 6-3). The copolymer made with very high amount of NPM in feed (MDO:NPM = 1:9) showed bimodality (Figure 6-3).

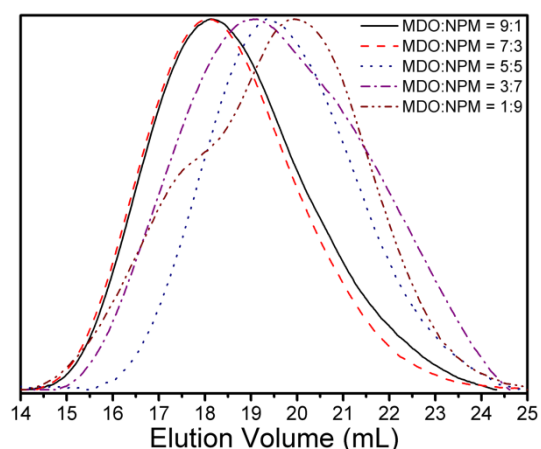


**Figure 6-3.** GPC traces of polymers made by radical polymerization of NPM and MDO with different monomer ratios in feed at 120 °C.

The microscopic structure of MDO-NPM copolymers was characterized by  $^1\text{H-NMR}$  (Figure 6-4A) and  $^{13}\text{C-NMR}$  (Figure 6-4B) with full assignments. All copolymers in  $^{13}\text{C-NMR}$  spectra showed the presence of ketal carbon at  $\delta = 100$  ppm due to ring-retained acetal units from MDO. Compared with the  $^{13}\text{C-NMR}$  spectra of copolymers prepared at 60 °C (Figure 6-4B, black curve), an extra peak at  $\delta = 170$  ppm in  $^{13}\text{C-NMR}$  spectrum of MDO-NPM prepared at 120 °C (Figure 6-4B, red curve) was obvious, which was corresponding to the carbonyl-carbon ( $k$ ) of ring-opened MDO units (ester units, Structure 3). Compared with the  $^1\text{H-NMR}$  spectrum of resulting copolymers prepared at 60 °C (Figure 6-4A, black curve), the peak at  $\delta = 4.0$  ppm in  $^1\text{H-NMR}$  spectrum due to the  $-\text{OCH}_2-$  protons of ester units formed by ring-opening of MDO during copolymerization at 120 °C was obvious (Figure 6-4A, red curve). Other

characteristic peaks observed in  $^1\text{H-NMR}$  were:  $\delta = 6.5\text{-}7.5$  ppm (aromatic protons of NPM) and  $\delta = 2.4\text{-}3.1$  ppm (methylene protons (*a*) of MDO with ring-retained Structure **1** and  $-\text{CH}_2\text{C}(\text{O})\text{O}-$  protons (*f*) of MDO with ring-opened ester units (Structure **3**). Using deconvolution of overlapping peaks between  $\delta = 2.4\text{-}3.1$  (Figure 6-S2 in Support Information), the ratio of ester units in comparison to the ring-retained acetal units were determined (Table 6-2). The deconvolution was carried out using automatic program of MestReNova. The copolymers prepared at  $120\text{ }^\circ\text{C}$  showed enhanced tendency to undergo ring-opening polymerization with the formation of ester units in comparison to the polymers prepared at  $60\text{ }^\circ\text{C}$ . An increase in the amount of ester units in copolymers was obtained with increase in MDO in feed. The copolymer, which was prepared at  $120\text{ }^\circ\text{C}$  with MDO:NPM = 9:1 in feed, had 54 mol% of the total MDO units as ring-opened esters. Whereas the copolymer with MDO:NPM = 5:5 in feed showed 39 mol% of ring-opened structures. On reducing the amount of MDO below 50 mol % in the initial feed, the amount of ring-opened MDO was strongly decreased and could not be determined with accuracy.

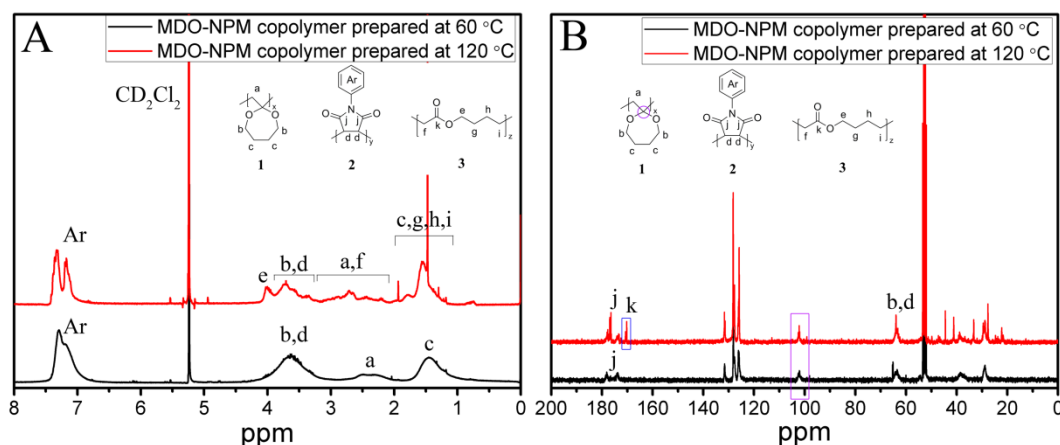


**Figure 6-4.**  $^1\text{H-NMR}$  and  $^{13}\text{C-NMR}$  spectra of MDO-NPM copolymer, monomer ratio of MDO:NPM = 7:3 in feed as an example. A:  $^1\text{H-NMR}$  and B:  $^{13}\text{C-NMR}$ , black curve: copolymerization at  $60\text{ }^\circ\text{C}$ , red curve: copolymerization at  $120\text{ }^\circ\text{C}$ .

**Table 6-2.** Copolymerization of MDO and NPM at 120 °C.

Entry	Feed ratio (molar ratio)		Yield %	$M_n^b$	PDI <sup>b</sup>	Copolymer composition (molar ratio) <sup>c</sup>		MDO with ring-opened structure (mol %) <sup>c</sup>
	MDO	NPM				MDO <sup>d</sup>	NPM	
6 <sup>a</sup>	90	10	22.6	$1.03 \times 10^5$	2.1	59	41	54
7 <sup>a</sup>	70	30	55.3	$1.13 \times 10^5$	2.1	57	43	45
8 <sup>a</sup>	50	50	85.1	$6.03 \times 10^4$	2.1	54	46	39
9 <sup>a</sup>	30	70	82.4	$5.46 \times 10^4$	2.7	36	64	- <sup>e</sup>
10 <sup>a</sup>	10	90	81.9	$6.59 \times 10^4$	bimodal	16	84	- <sup>e</sup>

<sup>a</sup>: Initiator: DTBP, 0.5 mol % of monomer; reaction temperature: 120 °C; reaction time: 2 h; solvent: anisole.

<sup>b</sup>: Characterized by GPC with RI detector, calibration with PMMA standard.

<sup>c</sup>: Characterized by <sup>1</sup>H-NMR spectra of MDO-NPM copolymers with deconvolution method.

<sup>d</sup>: Ring-opened and ring-retained MDO.

<sup>e</sup>: The content of MDO units with ring-opened structure was very low and could not be calculated due to the strong overlapping.

### 6.4.3 Copolymerization mechanism

The comonomer-copolymer composition curves for copolymerization at 60 and 120 °C were shown in Figure 6-5. The monomer reactivity ratios at different temperatures could be determined on the basis of comonomer-copolymer composition curves for the MDO and NPM copolymerization at 60°C and 120°C. The  $r_{MDO}$  and  $r_{NPM}$  values were 0.0241 and 0.1202 respectively for the copolymerization at 60 °C, which were much lower than the monomer reactivity ratios for the copolymerization at 120 °C ( $r_{MDO} = 0.0839$  and  $r_{NPM} = 0.3208$ ). These results also suggested the alternating copolymerization tendency of MDO and NPM at 60 °C.

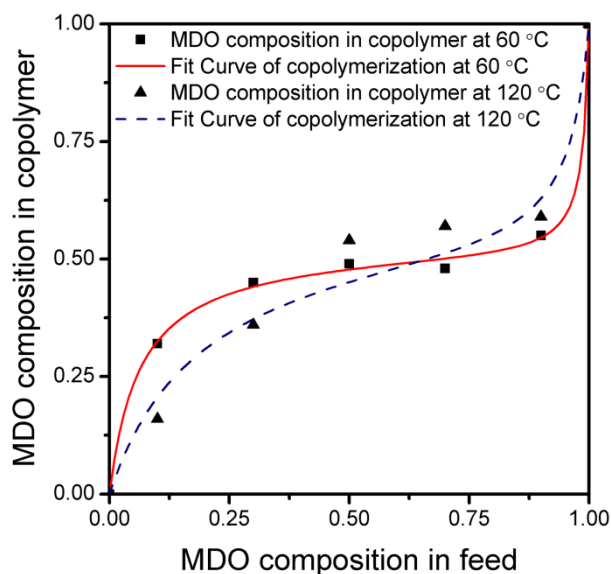


**Figure 6-5.** Comonomer-copolymer composition curves for the MDO and NPM copolymerization at different temperatures (entry 1-5 in Table 6-1 and entry 6-10 in Table 6-2).

Using nonlinear least-squares curve fitting method, the curve was drawn. Red curve: Fit curve of copolymerization at 60 °C; Navy curve: Fit curve of copolymerization at 120 °C. Fitting equation:

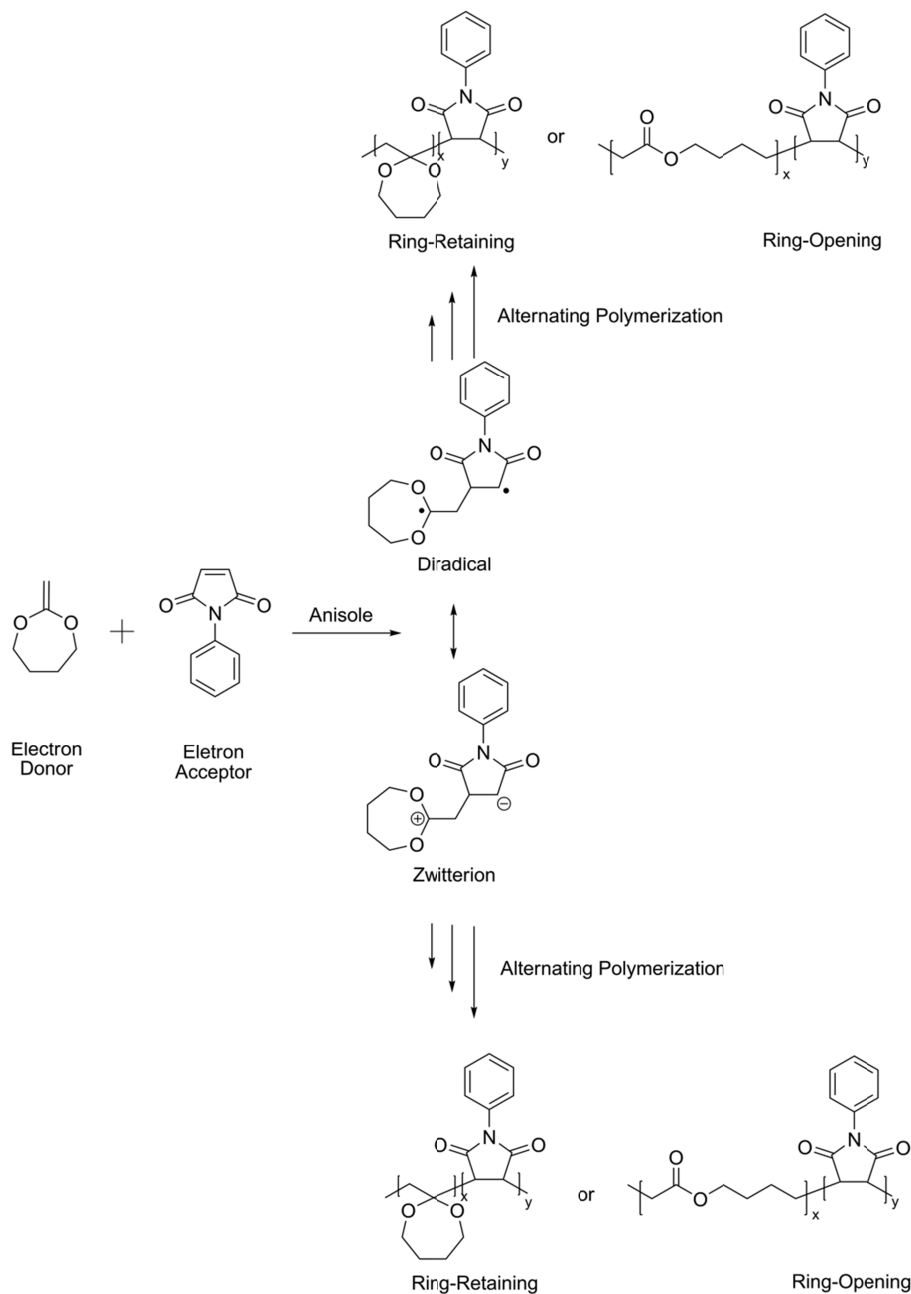
$$F_1 = \frac{r_1 f_1^2 + f_1 f_2}{r_1 f_1^2 + 2f_1 f_2 + r_2 f_2^2} \quad (f_1, f_2: \text{mole fractions of monomers in the feed}; F_1, F_2: \text{mole fractions in the copolymer}).$$

Copolymerization at 60 °C:  $r_{MDO} = 0.0241$ ,  $r_{NPM} = 0.1202$ ,  $R^2 = 0.998$ ;

Copolymerization at 120 °C:  $r_{MDO} = 0.0839$ ,  $r_{NPM} = 0.3208$ ,  $R^2 = 0.972$ .

NPM has electron deficient double bond whereas MDO double bond is electron rich due to neighboring electron donating oxygen atoms. The simple mixing of the two monomers could lead to the formation of charge transfer complex and spontaneous polymerization without any initiator. In fact, heating a mixture of NPM and MDO (1:1 molar ratio) without any initiator at 60 and 120 °C led to high molar mass polymers in 22h with unimodal GPC curves but with low yield (entry 11 and entry 14 in Table 6-3). The yield was around 10% at 60 °C whereas it was around 32 % at 120 °C. The copolymer composition (MDO:NPM) was almost 1:1 in both cases. With the polymerization at 120 °C, 37% of the total MDO units were ring-opened in the form of esters (entry 14 in Table 6-3), whereas the MDO polymerized in the form of ring-acetals at 60 °C (entry 11 in Table 6-3).

The alternating copolymerization of electron-rich vinyl monomers (styrene, acrylates *etc.*) with electron-deficient vinyl monomers like 2,3,4,5,6-pentafluorostyrene, maleic anhydride, *N*-phenyl maleimide *etc.* was widely researched by Seagusa<sup>10</sup> and Hall<sup>11</sup>. Based on their work, the alternating copolymerization could be preceded by diradical or zwitterion mechanism (Scheme 6-2).



**Scheme 6-2.** Mechanism of MDO-NPM copolymerization

To get insight into the mechanism of polymerization, a blank reaction was carried out. Equimolar amounts, 2.12 mmol each of MDO and NPM were dissolved in 1 mL  $\text{CDCl}_3$  and stirred under argon for 1 h. The resulting complex was directly analyzed by  $^1\text{H-NMR}$  spectroscopy. TMS was used as internal standard. The  $^1\text{H-NMR}$  spectra (Figure 6-6) showed that the peak *a* corresponding to the protons from  $\text{CH}=\text{CH}$  group of monomer NPM was shifted from  $\delta = 6.78$  to  $\delta = 6.56$  (peak *a'*) and the peak *b* corresponding to the protons from  $\text{CH}_2=\text{C}$  group of monomer MDO was shifted from  $\delta = 3.41$  to  $\delta = 3.30$  (peak *b'*). This result strongly suggested the interaction between the double bonds of MDO and NPM. Due to formation of the MDO-NPM complex, the other proton signals of the MDO and NPM monomer also showed a small shift in the peaks in  $^1\text{H-NMR}$  spectrum.

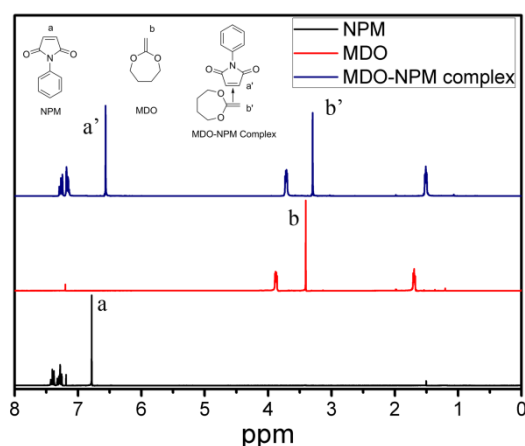


**Figure 6-6.** Comparison of  $^1\text{H-NMR}$  spectra of MDO-NPM complex with the monomer MDO and NPM.

To learn the mechanism of this reaction, MDO-NPM copolymerization was carried out in presence of radical inhibitor such as hydroquinone. Although polymer yields were less, the presence of hydroquinone did not completely inhibit the polymerization and the copolymer composition was MDO:NPM = 1:1. The MDO was present predominately as acetal-ring at 60 °C, whereas 21 % of total MDO units were ring-opened to ester units at 120 °C, which was much less in comparison to the product obtained either via simple

mixing of two monomers or made by radical polymerization (Table 6-3). The occurrence of polymerization even in the presence of hydroquinone indicated the mixed mechanism occurring during NMP-MDO copolymerization. The similar behavior was observed during copolymerization of MDO with tulipalin-A based vinyl monomer in our previous study.<sup>24</sup> The addition of hydroquinone led to ionic polymerization overweighing the radical one thereby providing more ring-retained MDO units. MDO cationic polymerization provided ring-retained structures in majority as shown previously in the literature.<sup>22</sup>

**Table 3.** Comparison of MDO-NPM copolymerization with different reaction conditions in anisole (monomer ratio in feed MDO:NPM = 1:1).

Entry	Inhibitor / Initiator	Reaction Temp. °C	Yield %	$M_n^d$	PDI <sup>d</sup>	copolymer composition (molar ratio) <sup>e</sup>		MDO with ring-opened structure (mol %) <sup>e</sup>
						MDO <sup>f</sup>	NPM	
11 <sup>a</sup>	-	60	9.4	$2.66 \times 10^5$	1.9	48	52	- <sup>g</sup>
12 <sup>b</sup>	hydroquinone	60	6.6	$2.57 \times 10^4$	1.6	47	53	- <sup>g</sup>
13 <sup>c</sup>	AIBN	60	52.4	$1.81 \times 10^5$	1.8	49	51	- <sup>g</sup>
14 <sup>a</sup>	-	120	31.7	$5.36 \times 10^4$	2.6	53	47	37
15 <sup>b</sup>	hydroquinone	120	10.3	$4.14 \times 10^4$	2.9	54	46	21
16 <sup>c</sup>	DTBP	120	85.1	$6.03 \times 10^4$	2.1	54	46	39

<sup>a</sup>: Spontaneous copolymerization, reaction time: 22 h.

<sup>b</sup>: Copolymerization with inhibitor,  $c_{\text{inhibitor}} = 1$  wt% of monomer, reaction time: 22 h.

<sup>c</sup>: Copolymerization with initiator,  $c_{\text{initiator}} = 0.5$  wt% of monomer, reaction time: 2 h.

<sup>d</sup>: Characterized by GPC with RI detector, calibration with PS standard.

<sup>e</sup>: Characterized by <sup>1</sup>H-NMR spectra of MDO-NPM copolymers with deconvolution technology.

<sup>f</sup>: ring-opened and ring-retained MDO.

<sup>g</sup>: The content of MDO units with ring-opened structure was very low and could not be calculated due to the strong overlapping.

#### 6.4.4 Thermal, optical and hydrolytic degradability studies

The thermal stability of the MDO-NPM copolymers made by radical polymerization was performed by TGA analysis (Figure 6-S3 in Supporting Information). All polymers were highly thermally stable (decomposition temperature was higher than 300°C). Due to the presence of ester units formed by ring-opening of MDO during copolymerization, the MDO-NPM copolymers with the monomer ratio of MDO:NPM = 9:1, 7:3 and 5:5 in feed at 120 °C showed a two-step thermal decomposition (initial decompositions at 320 °C and 410 °C). Whereas on reducing the amount of MDO below 50 mol % in the initial feed, the amount of ring-opened MDO in MDO-NPM copolymer was strongly decreased and it showed one-step decomposition (decomposed at 410 °C).

The glass transition temperatures for the copolymers prepared at 120°C were determined using DSC-technique. The copolymers showed two glass transition temperatures except for the sample with MDO:NPM = 9:1 in the feed. Homo-poly(NPM) showed very high glass transition temperature (more than 300 °C) due to rigid ring-structure.<sup>1</sup> The glass transition temperature of poly(MDO) is dependent upon the mode of polymerization. The poly(MDO) with 100% ring-opened ester units showed  $T_g$  of -60 °C<sup>28</sup>. Due to the ring structure, the poly(MDO) with 100% ring-retained units would have a higher glass transition temperature than poly(MDO) with 100% ring-opened ester units. A hypothetical  $T_g$  of NPM-MDO copolymer, which had an assuming composition of NPM and 100% ring-opened MDO units with 1:1, could be calculated as 73 °C using Fox equation ( $W$ : weight ratio of monomers in NPM-MDO copolymer):

$$\frac{1}{T_g} = \frac{W_{(MDO)}}{T_{g(MDO)}} + \frac{W_{(NPM)}}{T_{g(NPM)}}$$

The copolymers prepared at 120 °C in the present work showed a mixed structure with ring-retained acetal and ring-opened ester units from MDO besides NPM rings in the polymer backbone. Due to this immiscible random structure of the resulting copolymer (*i.e.* block of ring-retained MDO-*co*-NPM and block of ring-opened MDO-*co*-NPM),

two glass transition temperatures between the  $T_g$  of homopoly(NPM) and poly(MDO) with fully ring-opened structure were observed in the DSC curves (Figure 6-7). Because the amount of ring-opened MDO was strongly decreased, the MDO-NPM copolymer prepared at 120 °C with reducing the amount of MDO below 50 mol % (i.e. ring retained structure predominating) in the initial feed had a similar  $T_g$  with the copolymer prepared at 60 °C (only ring-retained structure). As an example, the copolymer of entry 9 in Table 6-2 had the glass transition temperature at 94 °C and 222 °C, which were similar to the  $T_g$  of copolymer of entry 4 in Table 6-1 ( $T_{g1} = 90$  °C,  $T_{g2} = 225$  °C). With increasing the amount of MDO units with ring-opened structure, the difference between these two glass transition temperatures was reduced (Table 6-4).

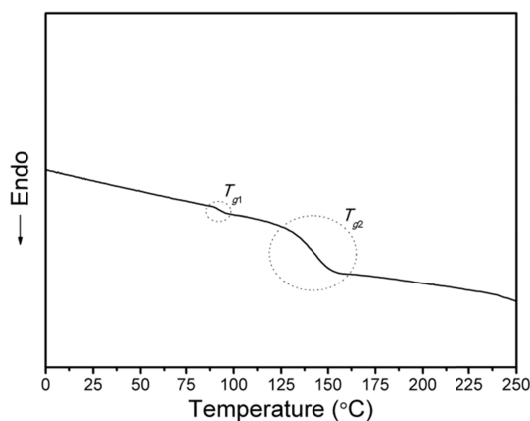


**Figure 6-7.** DSC trace of MDO-NPM copolymer (monomer ratio in feed: MDO:NPM = 5:5, entry 8 in Table 6-2).

**Table 6-4.** Thermal characterization of MDO-NPM copolymers prepared at different temperatures.

Entry	Copolymer composition (molar ratio) <sup>b</sup>		MDO with ring-opened structure (mol %) <sup>b</sup>	<i>dec. T</i> (°C) <sup>d</sup>	<i>T<sub>g</sub></i> (°C) <sup>e</sup>
	MDO <sup>c</sup>	NPM			
6 <sup>a</sup>	59	41	54	330, 416	106
7 <sup>a</sup>	57	43	45	322, 409	104, 142
8 <sup>a</sup>	54	46	39	326, 405	97, 142
9 <sup>a</sup>	36	64	<sup>f</sup>	409	94, 222
10 <sup>a</sup>	16	84	<sup>f</sup>	425	93, 272

<sup>a</sup>: Initiator: DTBP, 0.5 mol % of monomer; reaction temperature: 120 °C; reaction time: 2 h; solvent: anisole, same as entry 6-10 in Table 6-2.

<sup>b</sup>: Characterized by <sup>1</sup>H-NMR spectra of MDO-NPM copolymers with deconvolution method.

<sup>c</sup>: ring-opened and ring-retained MDO.

<sup>d</sup>: Characterized by TGA technology.

<sup>e</sup>: Characterized by DSC technology.

<sup>f</sup>: The content of MDO units with ring-opened structure was very low and could not be calculated due to the strong overlapping.

The films of MDO-NPM copolymers with higher ester content (entry 6-8 in Table 6-2) were prepared using spin coating. The optical transparency of the films was characterized by UV-Vis spectroscopy (Figure 6-8). All the MDO-NPM copolymer films showed a high transmittance (higher than 90 %) in the range of 300-800 nm. Due to the phenyl group on the polymer chains, the transmittance was strongly decreased in the range of 200-300 nm.

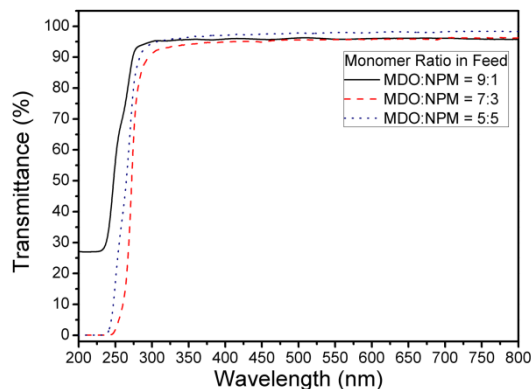


**Figure 6-8.** UV-Vis transmittance spectra of MDO-NPM copolymer films prepared using spin coating: black curve: entry 6 in Table 6-2; red curve: entry 7 in Table 6-2; navy curve: entry 8 in Table 6-2.

Because of the hydrolytically unstable linkage of ester group from the ring-opened MDO units on the NPM-MDO copolymer chains, the copolymers prepared with higher MDO monomer ratio in feed at 120 °C (entry 6-8 in Table 6-2) are degradable under basic condition. The alkaline hydrolysis was carried out to study the hydrolytic degradable tendency of the NPM-MDO copolymers (entry 8 in Table 6-2 was used as an example). After 24 hours degradation with KOH in methanol/dioxane cosolvent, the NPM-MDO copolymer was completely degraded. The remaining solid was less than 5 wt% of the original NPM-MDO copolymer and showed as fragments of degraded polymer from the  $^1\text{H-NMR}$  spectrum (Figure 6-S4).

## 6.5 Conclusion

The copolymers of 2-methylene-1,3-dioxepane (MDO) and *N*-phenyl maleimide (NPM) with high thermal stability, glass transition temperatures and optical transparency could be obtained under specific reaction conditions. The mixed copolymer structure with ester, ring-acetal and NPM-ring units in the backbone were observed using NMR spectroscopy. The relative amounts of these three units in the polymer backbone were dependent upon the reaction temperature and the amount of MDO in the feed. Increased temperature (120°C) and higher amounts of MDO in feed led to polymers with more ester units. The high molar mass polymers were generated by simple mixing of the two monomers MDO and NMP at 60 and 120 °C due to charge transfer complex formation. The resulting polymers could be highly interesting as degradable high glass transition temperature transparent polymers for applications in packaging industry and therefore requires in future further properties characterization including mechanical properties.

## 6.6 References

1. T. Doi, A. Akimoto, A. Matsumoto, Y. Oki and T. Otsu, *J. Polym. Sci., Part A: Polym. Chem.*, 1996, **34**, 2499-2505.
2. M. Hisano, K. Takeda, T. Takashima, Z. Jin, A. Shiibashi and A. Matsumoto, *Macromolecules*, 2013, **46**, 3314-3323.
3. M. Hisano, K. Takeda, T. Takashima, Z. Jin, A. Shiibashi and A. Matsumoto, *Macromolecules*, 2013, **46**, 7733-7744.
4. D. R. Suwier, P. A. M. Steeman, M. N. Teerenstra, M. A. J. Schellekens, B. Vanhaecht, M. J. Monteiro and C. E. Koning, *Macromolecules*, 2002, **35**, 6210-6216.
5. A. Matsumoto, T. Kubota and T. Otsu, *Macromolecules*, 1990, **23**, 4508-4513.
6. K.-D. Ahn, Y.-H. Lee and D. Koo, II, *Polymer*, 1992, **33**, 4851-4856.
7. D. J. T. Hill, L. Y. Shao, P. J. Pomery and A. K. Whittaker, *Polymer*, 2001, **42**, 4791-4802.
8. B. Gacal, L. Cianga, T. Agag, T. Takeichi and Y. Yagci, *J. Polym. Sci., Part A: Polym. Chem.*, 2007, **45**, 2774-2786.
9. Z. M. O. Rzaev, H. Milli and G. Akovali, *Polym. Int.*, 1996, **41**, 259-265.
10. T. Saegusa, *Angew. Chem. Int. Ed. Engl.*, 1977, **16**, 826-835.
11. H. K. Hall, *Angew. Chem. Int. Ed. Engl.*, 1983, **22**, 440-455.
12. S.-i. Yamamoto, F. Sanda and T. Endo, *Macromolecules*, 1999, **32**, 5501-5506.
13. S. Agarwal, *Polym. Chem.*, 2010, **1**, 953-964.

14. G. E. Roberts, M. L. Coote, J. P. A. Heuts, L. M. Morris and T. P. Davis, *Macromolecules*, 1999, **32**, 1332-1340.
15. L. M. Morris, T. P. Davis and R. P. Chaplin, *Polymer*, 2001, **42**, 495-500.
16. J. Undin, T. Illanes, A. Finne-Wistrand and A.-C. Albertsson, *Polym. Chem.*, 2012, **3**, 1260-1266.
17. G. G. Hedir, C. A. Bell, N. S. Jeong, E. Chapman, I. R. Collins, R. K. O'Reilly and A. P. Dove, *Macromolecules*, 2014, **47**, 2847-2852.
18. S. Maji, F. Mitschang, L. Chen, Q. Jin, Y. Wang and S. Agarwal, *Macromol. Chem. Phys.*, 2012, **213**, 1643-1654.
19. J. Undin, A. Finne-Wistrand and A.-C. Albertsson, *Biomacromolecules*, 2013, **14**, 2095-2102.
20. J. Undin, A. Finne-Wistrand and A.-C. Albertsson, *Biomacromolecules*, 2014, **15**, 2800-2807.
21. W. J. Bailey, Z. Ni and S.-R. Wu, *J. Polym. Sci., Polym. Chem. Ed.*, 1982, **20**, 3021-3030.
22. P. C. Zhu, Z. Wu and C. U. Pittman, *J. Polym. Sci., Part A: Polym. Chem.*, 1997, **35**, 485-491.
23. S. Agarwal, *Polym. J.*, 2006, **39**, 163-174.
24. S. Agarwal and R. Kumar, *Macromol. Chem. Phys.*, 2011, **212**, 603-612.
25. S. Agarwal and L. Ren, *Macromolecules*, 2009, **42**, 1574-1579.
26. Q. Jin, S. Maji and S. Agarwal, *Polym. Chem.*, 2012, **3**, 2785-2793.
27. S. Agarwal, N. Naumann and X. Xie, *Macromolecules*, 2002, **35**, 7713-7717.
28. S. Agarwal and C. Speyerer, *Polymer*, 2010, **51**, 1024-1032.

## 6.7 Supporting Information

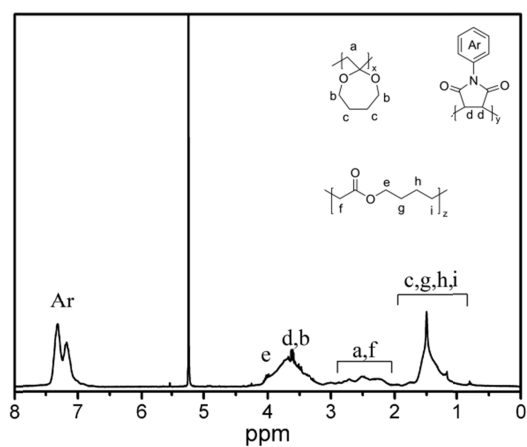


**Figure 6-S1.**  $^1\text{H-NMR}$  spectrum of MDO-NPM copolymer prepared at 60 °C with the monomer ratio of MDO:NPM = 9:1 in feed (entry 1 in Table 6-1).

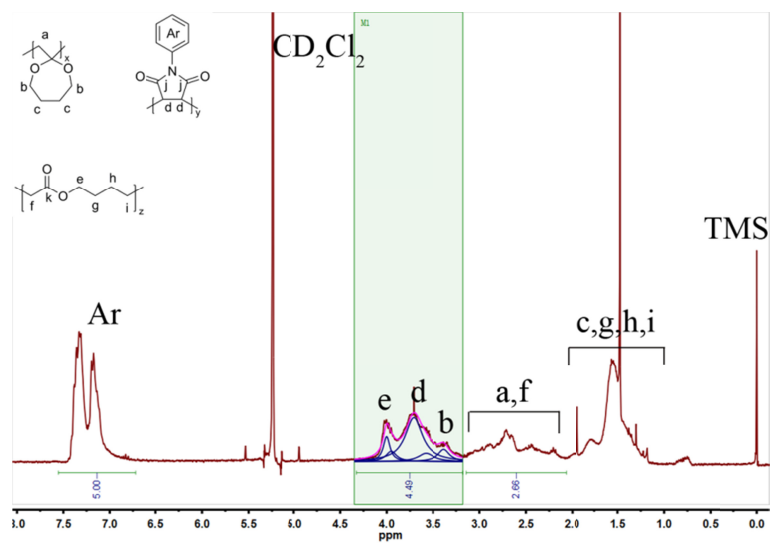


**Figure 6-S2.**  $^1\text{H-NMR}$  analysis using deconvolution technology (entry 9 in Table 6-1 as example); red curve: original  $^1\text{H-NMR}$  spectrum; blue curve: deconvolution curve; magenta curve: sum curve after deconvolution.

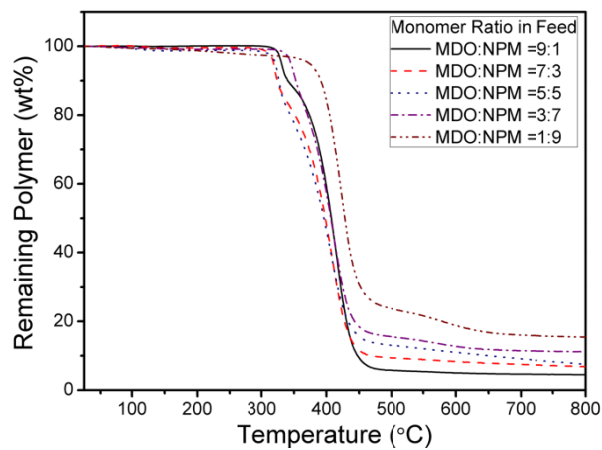


**Figure S3.** TGA traces of MDO-NPM copolymers prepared at 120 °C.

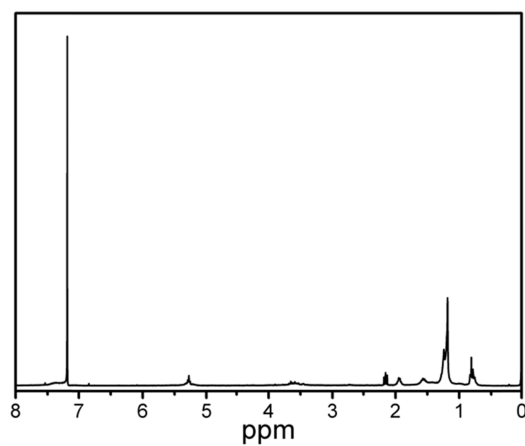


**Figure 6-S4.** NMR spectrum of remaining organic component after 24 hours alkaline hydrolysis of MDO-NPM copolymer prepared at 120 °C (entry 8 in Table 6-2) in methanol/dioxane cosolvent.

## List of Publications

1. **Y. Shi**, Z. Zheng, and S. Agarwal, A Rare Example of the Formation of Polystyrene-Grafted Aliphatic Polyester in One-Pot by Radical Polymerization, *Chem. Eur. J.*, **2014**, *20*, 7419-7428.
2. **Y. Shi**, H. Schmalz, and S. Agarwal, Designed Enzymatically Degradable Amphiphilic Conetworks by Radical Ring-Opening Polymerization, **2015**, submitted to *Macromolecules*.
3. **Y. Shi**, P. Zhou, V. Jérôme, R. Freitag, and S. Agarwal, Enzymatically Degradable DOPA-containing Polyester Based Adhesives by Radical Polymerization, **2015**, submitted to *Macromolecules*.
4. Y. Shi and S. Agarwal, Thermally stable optically transparent copolymers of 2-methylene-1,3-dioxepane and *N*-phenyl maleimide with degradable ester linkages, **2015**, submitted to *e-polymers*.



## Conference Presentations

1. Y. Shi, H. Wang, S. Agarwal, “Functional degradable biomaterials with various macromolecular architectures and properties”, *poster presentation at Bayreuth Polymer Symposium*, September 2013, Bayreuth Germany.
2. Y. Shi, Z. Zheng, S. Agarwal, “Rare example of grafting of polyesters onto polystyrene in one-step by radical polymerization”, *oral presentation at 248<sup>th</sup> ACS national meeting*, August 2014, San Francisco, USA.



## Acknowledgements

I would like to thank all the people helped and supported me during my Ph.D. thesis time in Marburg and Bayreuth.

First of all, I would like to thank my supervisor Prof. Seema Agarwal for giving me the opportunity to finish my Ph.D. work in Philipps-Universität Marburg and University of Bayreuth and for this highly interesting topic. I am very thankful for her supervision of my Ph.D. thesis and also during my master study in Marburg. I am grateful for the opportunities to present our research at international conferences.

I thank Prof. Andreas Andreas Greiner for the useful tips and his great supports during my thesis.

I want to thank Dr. Valérie Jérôme for the fruitful cooperation and the help for cytotoxicity test.

I would like to thank my coworkers in Lab 798 for the perfect cooperation. They are Holger Pletsch, Tina Löbling, Pin Hu, Payal Tyagi and Florian Käfer.

I thank our present and former technical assistants Melanie Förtsch, Marietta Böhm and Annette Krökel in MC II for their help with all kinds of analytical issues. In addition, I thank Gaby Oliver for her help in Bayreuth.

Most of all, I would like to thank all the members in MC II for the good working atmosphere and nice working cooperation. They have given me a great memorable time in Marburg and Bayreuth.

Also, I would like to thank my students Minde Jin, Zilin Wang and Peiran Zhou for the assistance work on several projects with me.

Special thanks go to Prof. Jun Ling from Zhejiang University and Dr. Zhicheng Zheng from old MC II group for their discussion. I am also thankful for their everlasting

## Acknowledgements

---

willingness to help and the fun we had in Freiburg and San Francisco.

I thank the Bayreuth graduate school of Mathematical and Natural Science (BayNat) for a membership in the Ph.D. program “Polymer Science”.

At last, I owe my thanks to my parents and my wife Yiqun Ye for their love and unlimited support in these years. Especially thank you Yiqun for everything. Your love gives me encouragement to face the tough times. Thank you so much.

## **Versicherung und Erklärungen**

Hiermit erkläre ich mit damit einverstanden, dass die elektronische Fassung meiner Dissertation unter Wahrung meiner Urheberrechte und des Datenschutzes einer gesonderten Überprüfung hinsichtlich der eigenständigen Anfertigung der Dissertation unterzogen werden kann.

Hiermit erkläre ich eidesstattlich, dass die Dissertation selbständig verfasst und keine anderen als die von mir angegebenen Quellen und Hilfsmittel benutzt habe.

Ich habe die Dissertation nicht bereits zur Erlangung eines akademischen Grades anderweitig eingereicht und habe auch nicht bereits diese oder eine gleichartige Doktorprüfung endgültig nicht bestanden.

Hiermit erkläre ich, dass keine Hilfe von gewerblichen Promotionsberatern bzw. –vermittlern in Anspruch genommen habe und auch künftig nicht nehmen werde.

Yinfeng Shi

Bayreuth, 20.05.2015